BioMed Research International

Mitochondria and Cancer

Guest Editors: Ryan Parr, Andrew Harbottle, John P. Jakupciak, and Gurmit Singh

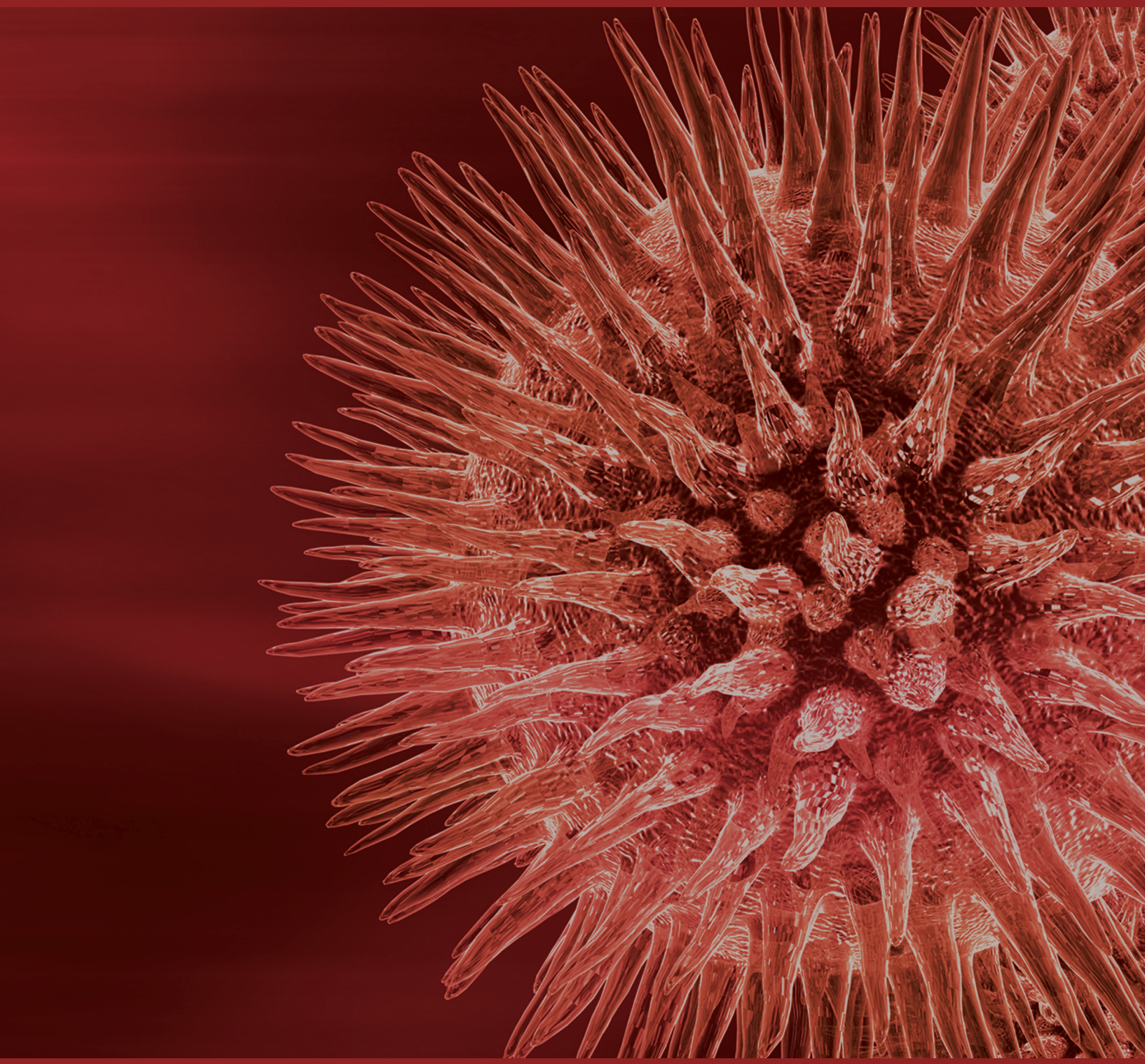

Mitochondria and Cancer

BioMed Research International

Mitochondria and Cancer

Guest Editors: Ryan Parr, Andrew Harbottle,
John P. Jakupciak, and Gurmit Singh

Editorial Board

The editorial board of the journal is organized into sections that correspond to the subject areas covered by the journal.

Agricultural Biotechnology

Ahmad Zuhairi Abdullah, Malaysia
Guihua H. Bai, USA
Christopher P. Chanway, Canada
Ravindra N. Chibbar, Canada
Adriana S. Franca, Brazil
Ian Godwin, Australia
Hari B. Krishnan, USA
Carol A. Mallory-Smith, USA
Xiaoling Miao, China
Dennis P. Murr, Canada
Rodomiro Ortiz, Sweden
Encarnación Ruiz, Spain
B. C. Saha, USA
Abdurrahman Saydut, Turkey
Mariam B. Sticklen, USA
Kok Tat Tan, Malaysia
Chiu-Chung Young, Taiwan

Animal Biotechnology

E. S. Chang, USA
Bhanu P. Chowdhary, USA
Noelle E. Cockett, USA
Peter Dovc, Slovenia
Scott C. Fahrenkrug, USA
Dorian J. Garrick, USA
Thomas A. Hoagland, USA
Tosso Leeb, Switzerland
James D. Murray, USA
Anita M. Oberbauer, USA
Jorge A. Piedrahita, USA
Daniel Pomp, USA
Kent M. Reed, USA
Lawrence Reynolds, USA
Lawrence B. Schook, USA
Mari A. Smits, The Netherlands
Leon Spicer, USA
J. Verstegen, USA
Matthew B. Wheeler, USA
Kenneth L. White, USA

Biochemistry

David Ronald Brown, UK
Saulius Butenas, USA
Vittorio Calabrese, Italy
Miguel Castanho, Portugal
Francis J. Castellino, USA
Roberta Chiaraluce, Italy
D. M. Clarke, Canada
Francesca Cutruzzolà, Italy
Paul W. Doetsch, USA
Hicham Fenniri, Canada
Nick V. Grishin, USA
J. Guy Guillemette, Canada
Paul W. Huber, USA
Chen-Hsiung Hung, Taiwan
Maria Jerzykiewicz, Poland
Michael Kalafatis, USA
B. E. Kemp, Australia
Phillip E. Klebba, USA
Wen-Hwa Lee, USA
George Makhatadze, USA
Leonid Medved, USA
Susan A. Rotenberg, USA
Jason Shearer, USA
Andrei Surguchov, USA
John B. Vincent, USA
Y. George Zheng, USA

Bioinformatics

T. Akutsu, Japan
Miguel A. Andrade, Germany
Mark Y. Borodovsky, USA
Rita Casadio, Italy
David Corne, UK
Sorin Draghici, USA
Eugénio Ferreira, Portugal
Stavros J. Hamodrakas, Greece
Paul Harrison, USA
George Karypis, USA
Guohui Lin, Canada
Satoru Miyano, Japan
Zoran Obradovic, USA
Florencio Pazos, Spain
Zhirong Sun, China
Ying Xu, USA
Alexander Zelikovsky, USA
Albert Zomaya, Australia

Biophysics

Miguel Castanho, Portugal
P. Bryant Chase, USA
Kuo-Chen Chou, USA
Rizwan Khan, India
Ali A. Khraibi, Saudi Arabia
Rumiana Koynova, USA
Serdar Kuyucak, Australia
Jianjie Ma, USA
S. B. Petersen, Denmark
Peter Schuck, USA
Claudio M. Soares, Portugal

Cell Biology

Omar Benzakour, France
Sanford I. Bernstein, USA
Phillip I. Bird, Australia
Eric Bouhassira, USA
Mohamed Boutjdir, USA
Chung-Liang Chien, Taiwan
Richard Gomer, USA
Paul J. Higgins, USA
Pavel Hozak, Czech Republic
Xudong Huang, USA
Anton M. Jetten, USA
Seamus J. Martin, Ireland
Manuela Martins-Green, USA
Shoichiro Ono, USA
George Perry, USA
M. Piacentini, Italy
George E. Plopper, USA
Lawrence Rothblum, USA
Michael Sheetz, USA
James L. Sherley, USA
G. S. Stein, USA
Richard Tucker, USA
Thomas van Groen, USA
Andre Van Wijnen, USA
Steve Winder, UK
Chuanyue Wu, USA
Bin-Xian Zhang, USA

Genetics

Adewale Adeyinka, USA
Claude Bagnis, France
J. Birchler, USA
Susan Blanton, USA
Barry J. Byrne, USA
R. Chakraborty, USA
Domenico Coviello, Italy
Sarah H. Elsea, USA
Celina Janion, Poland
J. Spencer Johnston, USA
M. Ilyas Kamboh, USA
Feige Kaplan, Canada
Manfred Kayser, The Netherlands
Brynn Levy, USA
Xiao Jiang Li, USA
Thomas Liehr, Germany
James M. Mason, USA
Mohammed Rachidi, France
Raj S. Ramesar, South Africa
Elliot D. Rosen, USA
Dharambir K. Sanghera, USA
Michael Schmid, Germany
Markus Schuelke, Germany
Wolfgang Arthur Schulz, Germany
Jorge Sequeiros, Portugal
Mouldy Sioud, Norway
Rongjia Zhou, China

Genomics

Vladimir Bajic, Saudi Arabia
Margit Burmeister, USA
Settara Chandrasekharappa, USA
Yataro Daigo, Japan
J. Spencer Johnston, USA
Vladimir Larionov, USA
Thomas Lufkin, Singapore
John L. McGregor, France
John V. Moran, USA
Yasushi Okazaki, Japan
Gopi K. Podila, USA
Momiao Xiong, USA

Immunology

Hassan Alizadeh, USA
Peter Bretscher, Canada
Robert E. Cone, USA
Terry L. Delovitch, Canada
Anthony L. DeVico, USA
Nick Di Girolamo, Australia
Don Mark Estes, USA
Soldano Ferrone, USA
Jeffrey A. Frelinger, USA
John Robert Gordon, Canada
James D. Gorham, USA
Silvia Gregori, Italy
Thomas Griffith, USA
Young S. Hahn, USA
Dorothy E. Lewis, USA
Bradley W. McIntyre, USA
R. Lee Mosley, USA
Marija Mostarica-Stojković, Serbia
Hans Konrad Muller, Australia
Ali Ouaissi, France
Kanury V. S. Rao, India
Yair Reisner, Israel
Harry W. Schroeder, USA
Wilhelm Schwaeble, UK
Nilabh Shastri, USA
Yufang Shi, China
Piet Stinissen, Belgium
Hannes Stockinger, Austria
Graham R. Wallace, UK

Microbial Biotechnology

Suraini Abd-Aziz, Malaysia
Jozef Anné, Belgium
Nuri Azbar, Turkey
Yoav Bashan, Mexico
Marco Bazzicalupo, Italy
Hakan Bermek, Turkey
Nico Boon, Belgium
José Luis Campos, Spain
Yinguang Chen, China
Luca Simone Cocolin, Italy
Peter Coloe, Australia
Daniele Daffonchio, Italy
Han de Winde, The Netherlands
Raf Dewil, Belgium
Jos Domingos Fontana, Brazil
Petros Gikas, Greece
Tom Granstrom, Finland
Ismail Kiran, Turkey
Hongjuan Liu, China
Yanhe Ma, China
Paula Loureiro Paulo, Brazil
Bernd H A Rehm, New Zealand
Alberto Reis, Portugal
Muthuswamy Sathishkumar, Singapore
Ramkrishna Sen, India
Angela Sessitsch, Austria
Ya-Jie Tang, China
Orhan Yenigun, Turkey
Eileen Hao Yu, UK

Microbiology

D. Beighton, UK
Steven R. Blanke, USA
Stanley Brul, The Netherlands
Isaac K. O. Cann, USA
Stephen K. Farrand, USA
Alain Filloux, UK
Gad Frankel, UK
Roy Gross, Germany
Hans-Peter Klenk, Germany
Tanya Parish, UK
Gopi K. Podila, USA
Frederick D. Quinn, USA
Didier A. Raoult, France
Isabel Sá-Correia, Portugal
P. L. C. Small, USA
Michael Thomm, Germany
H. C. van der Mei, The Netherlands
Schwan William, USA

Molecular Biology

Rudi Beyaert, Belgium
Michael Bustin, USA
Douglas Cyr, USA
K. Iatrou, Greece
Lokesh Joshi, Ireland
David W. Litchfield, Canada
Wuyuan Lu, USA
Patrick Matthias, Switzerland
John L. McGregor, France
S. L. Mowbray, Sweden
Elena Orlova, UK
Yeon-Kyun Shin, USA
William S. Trimble, Canada
Lisa Wiesmuller, Germany
Masamitsu Yamaguchi, Japan

Oncology

Colin Cooper, UK
F. M. J. Debruyne, The Netherlands
Nathan Ames Ellis, USA
Dominic Fan, USA
Gary E. Gallick, USA
Daila S. Gridley, USA
Xin-yuan Guan, Hong Kong
Anne Hamburger, USA
Manoor Prakash Hande, Singapore
Beric Henderson, Australia
Daehee Kang, Republic of Korea
Abdul R. Khokhar, USA
Rakesh Kumar, USA
Macus Tien Kuo, USA
Eric W. Lam, UK
Sue-Hwa Lin, USA
Kapil Mehta, USA
Orhan Nalcioglu, USA
P. J. Oefner, Germany
Allal Ouhtit, Oman
Frank Pajonk, USA
Waldemar Priebe, USA
F. C. Schmitt, Portugal
Sonshin Takao, Japan
Ana Maria Tari, USA
Henk G. Van Der Poel, The Netherlands
Haodong Xu, USA
David J. Yang, USA

Pharmacology

Abdel A. Abdel-Rahman, USA
M. Badr, USA
Stelvio M. Bandiera, Canada
Ronald E. Baynes, USA
R. Keith Campbell, USA
Hak-Kim Chan, Australia
Michael D. Coleman, UK
J. Descotes, France
Dobromir Dobrev, Germany
Ayman El-Kadi, Canada
Jeffrey Hughes, USA
Kazim Husain, USA
Farhad Kamali, UK
Michael Kassiou, Australia
Joseph J. McArdle, USA
Mark J. McKeage, New Zealand
Daniel T. Monaghan, USA
T. Narahashi, USA
Kennerly S. Patrick, USA
Vickram Ramkumar, USA
Michael J. Spinella, USA
Quadiri Timour, France
Todd W. Vanderah, USA
Val J. Watts, USA
David J. Waxman, USA

Plant Biotechnology

Prem L. Bhalla, Australia
J. R. Botella, Australia
Elvira Gonzalez De Mejia, USA
Shi-You Ding, USA
Metin Guru, Turkey
H. M. Häggman, Finland
Liwen Jiang, Hong Kong
P. B. Kirti, India
Yong Pyo Lim, Republic of Korea
Gopi K. Podila, USA
Ralf Reski, Germany
Sudhir Sopory, India

Toxicology

Michael Aschner, USA
Juergen Buenger, Germany
Michael L. Cunningham, USA
Laurence D. Fechter, USA
Hartmut Jaeschke, USA
Y. James Kang, USA
M. Firoze Khan, USA
Pascal Kintz, France
Qaisar Mahmood, Pakistan
R. S. Tjeerdema, USA
Kenneth Turteltaub, USA
Brad Upham, USA

Virology

Contents

Hindawi Publishing Corporation
BioMed Research International
Volume 2013, Article ID 763703, 2 pages
http://dx.doi.org/10.1155/2013/763703

Editorial
Mitochondria and Cancer

Ryan Parr,[1] Andrew Harbottle,[2] John P. Jakupciak,[3] and Gurmit Singh[4,5]

[1] *Mitomics Inc., Suite 1000, 290 Munro Street, Thunder Bay, ON, Canada P7A 7T1*
[2] *Mitomics Inc., and Bioincubator Suite, Medical School, New Castle University, Framlington Place, Newcastle upon Tyne NE2 4HH, UK*
[3] *Cipher Systems, Annapolis, MD 21401, USA*
[4] *Juravinski Cancer Centre, 699 Concession Street, Hamilton, ON, Canada L8V 5C2*
[5] *Department of Pathology and Molecular Medicine, McMaster University, 1280 Main Street W, Hamilton, ON, Canada L8N 3Z5*

Correspondence should be addressed to Ryan Parr; r.parr@mitomicsinc.com

Received 8 January 2013; Accepted 8 January 2013

The future of mitochondrial DNA research has the potential to uncover new insights on genetic diseases and open new opportunities to discover ways to control mitochondria and their influence on the human health and cancer. The outcomes of this work will expand the understanding of cellular respiration and disease risk. In this special issue, we give examples of strategies for the measurement of oxidative stress; a critical factor in tumor progression. While the mitochondrial genome has been well characterized, the associations of the broad spectrum of mitochondrial genotypes remains a relatively rich field of study.

Genetic tools are beginning to be realized which characterize mitochondrial populations and link their associations with normal and malignant cells. There are many large-scale deletions which require further investigation. There are populations of genotypes that rise and fall with tissue field effects. Mutations in the mitochondrial genome can alter the cellular biochemical behavior, changing the conditions for potential tumor growth. In this special issue we also address roles of mitochondrial interactions which are central to the physiological processes involved in malignant transformation. Measurements of DNA damage associated with prostate and other cancers can be normalized by comparative measurements of mitochondrial subpopulations. This can be used to assess DNA damage and somatic mutations under physiological and pathological conditions and can serve as a strategy to measure cell toxicity as a guide for devising innovative cancer preventions and treatments.

On account that mitochondrial DNA is accessible across various tissues, noninvasive collection and analyses are possible. From such investigations, it has been demonstrated that there is a progression of change in mitochondria through the tissues, as a field effect, that is, associated with the tumor tissue progression. Tumorigenic effects related to increasing ROS are well known in prostate and other solid tumor cancers.

Mapping mutations across the entire mitochondrial genome are fundamental to the future work on mitochondrial "omic" investigations. Mitochondrial whole genome sequencing pioneered the concepts of conducting whole genome analyses to understand forensics. This has resulted in efforts to go beyond simple STR typing and to type the entire chromosome. It is because of the increased resolution achieved by sequencing whole metagenomes that, by extension, other fields of diagnostics, personalized medicine, and bacterial and viral forensics have emerged (J. P. Jakupciak unpublished data).

Through the study of mitochondria, mechanisms of cancer are emerging. The influence of mitochondria on the metastatic potential of cancer cell lines points to a promising future and in vivo characterization of populations of mitochondria will function as a "looking-glass" into monitoring the modulation events and even predicting changes in metastatic capabilities. Mitochondrial genomics is poised to enhance the over all field of omics and contribute significantly to the advent of personalized medicine [1].

In this special issue, the authors present some of the latest findings in this exciting and rapidly expanding area of genomic research:

(i) specific heteroplasmic somatic alterations in the mitochondrial genome contribute to the cell proliferation;

(ii) a new paradigm for oxidative stress and cell and DNA damage has important implications for both cancer prevention and treatment;

(iii) an assay for gauging systemic oxidative stress using peripheral blood;

(iv) upregulation of a nuclear gene whose molecular interactions contribute to mitochondrial dysfunction, promoting cell proliferation;

(v) a cancerization field effect described by progressive mitochondrial mutations in noninvasiveand invasive breast cancer.

Ryan Parr
Andrew Harbottle
John P. Jakupciak
Gurmit Singh

References

[1] R. L. Parr and L. H. Martin, "Mitochondrial and nuclear genomics and the emergence of personalized medicine," *Human Genomics*, vol. 6, p. 3, 2012.

Hindawi Publishing Corporation
BioMed Research International
Volume 2013, Article ID 612369, 10 pages
http://dx.doi.org/10.1155/2013/612369

Review Article

Mitochondria and Cancer: Past, Present, and Future

M. L. Verschoor,[1,2] R. Ungard,[1,2] A. Harbottle,[3] J. P. Jakupciak,[4] R. L. Parr,[5] and G. Singh[1,2]

[1] *Juravinski Cancer Centre, 699 Concession Street, Hamilton, ON, Canada L8V 5C2*
[2] *Department of Pathology and Molecular Medicine, McMaster University, 1280 Main Street W, Hamilton, ON, Canada L8N 3Z5*
[3] *Mitomics Inc., Bioincubator Suite, The Medical School, New Castle University, Framlington Place, Newcastle Upon Tyne NE2 4HH, UK*
[4] *Cipher Systems, Annapolis, MD 21401, USA*
[5] *Mitomics Inc., 290 Munro Street, Suite 1000, Thunder Bay, ON, Canada P7A 7T1*

Correspondence should be addressed to R. L. Parr; r.parr@mitomicsinc.com

Received 30 October 2012; Accepted 13 December 2012

Academic Editor: George Perry

The area of mitochondrial genomics has undergone unprecedented growth over the past several years. With the advent of the age of omics, investigations have reached beyond the nucleus to encompass the close biological communication and finely coordinated interactions between mitochondria and their nuclear cell mate. Application of this holistic approach, to all metabolic interactions within the cell, is providing a more complete understanding of the molecular transformation of the cell from normal to malignant behavior, before histopathological indications are evident. In this review the surging momentum in mitochondrial science, as it relates to cancer, is described in three progressive perspectives: (1) Past: the historical contributions to current directions of research; (2) Present: Contemporary findings, results and approaches to mitochondria and cancer, including the role of next generation sequencing and proteomics; (3) Future: Based on the present body of knowledge, the potential assets and benefits of mitochondrial research are projected into the near future.

1. Past

As far back as 1850 scientists identified the existence of structures within cells that today we call mitochondria [1]. However, it was not until 1898 that the these structures were given the term mitochondria by Carl Benda [2]. Cytologists worked hard to identify the function of mitochondria and in 1912 the first reference to a possible link between mitochondria and respiration was made by Kingsbury [2]. This link was made exclusively from morphological observations. What followed was 30–40 years of intense biochemical analyses before the characterization of mitochondria as the "Powerhouse of the Cell" by Siekevitz in 1957 [3]. Leading up to this there were a number of key events. In 1909 Correns and Baur independently identified the first cases of extracellular inheritance. The source and site of this was unknown at the time, though mitochondria were the prime suspect. Ephrussi's laboratory had been working with yeast and their key publication in 1949 [4] used genetic analysis to show that respiration-deficient baker's yeast harboured mutations found in the cytoplasm, and not the nucleus. Soon thereafter Slonimski and Ephrussi investigated this area further and showed the deficiency was due to mitochondrial dysfunction.

On the back of these exciting findings, one of the most important discoveries in mitochondrial research was made in 1963, when the identification of the existence of mitochondrial DNA (mtDNA) was made by M. M. Nass and S. Nass [5]. Using electron microscopy they showed conclusively that chick embryo mitochondria contained DNA. The importance of this discovery cannot be overstated; as it renewed interest in the evolutionary origin of mitochondria. These findings were confirmed biochemically in 1964 when Schatz and Klima [6] showed that baker's yeast mitochondria also contained DNA. This of course led to more questions, specifically does the mtgenome interact with the nuclear genome, and if so how does this occur?

The mtDNA sequence was first published as being 16,569 base pairs long in 1981 by Anderson et al. [7], the sequence was later revised by Andrews et al. in 1999 [8]. Following the publication of the mtDNA sequence there was a focus on mitochondrial genomics that has been sustained till today. This work initially focused on myopathies and neuropathies by Wallace et al. [9, 10]. These so called "mitochondrial diseases" were due to both mitochondrial and nuclear mutations, where a symbiotic relationship exists between the mitochondrial and nuclear genomes. Understanding the complexity of these interactions is the key to detecting dysfunction within the cell.

Mitochondria control various metabolic functions and synthesizes 95% of cellular metabolic energy, while 1,200 nuclear genes drive and participate in mitochondrial function. There are 37 genes coded for by the mtgenome, 24 of which are dedicated to processing 13 genes within the mtgenome (mtgenome) itself which produce the subunits essential to electron transport. These 13 key genes work in conjunction with 93 nuclear proteins. In cancer cells certain mutations in the mtgenome can alter the biochemical behaviour of mitochondrial/nuclear protein complexes, thereby increasing pools of reactive oxygen species (ROS) which in turn enable tumour growth and may provide proliferative advantage to the cell [11]. Thus despite its small size relative to the nuclear genome, somatic mutations that occur in the mtgenome are able to contribute directly to the process of tumourigenesis.

There is now a significant body of literature describing the interactions between mitochondria and the nucleus. It appears that the somatic mutations which can alter these interactions occur early in the disease process, appearing in histologically normal tissues [12]. This leaves us with a key question with regard to mitochondrial mutations, are they causative factors of disease or a simple record of the development of disease? In 1924 Otto Heinrich Warburg postulated that cancer and tumour growth are in part caused by a change in the way the cells generate their energy. In normal healthy cells, ATP is generated mainly by oxidative breakdown of pyruvate following non-oxidative breakdown of glucose during the process of glycolysis. In contrast, malignant cell metabolism stalls after glycolysis a phenomenon that Warburg reported as the fundamental difference between normal and cancerous cells. These observed differences in the ratio of glycolysis to respiration have become known as the Warburg effect [13]. It has since become clear that these metabolic differences adapt cancer cells to the hypoxic conditions inside solid tumours. Thus it may be theorized that rather than causing cancer, perhaps these changes are characteristics produced by key cancer-causing mutations in certain genes involved in the aforementioned symbiotic relationship between nucleus and mitochondria. These findings have led to a new theory known as the Warburg theory of cancer, which suggests that the main driver of tumorigenesis is an insufficient cellular respiration caused by insult to mitochondria [14].

Clearly mitochondria are key to the function of both normal and malignant cells, and there has been much speculation about the origins of mitochondria, with perhaps the most prevalent theory being that of an endosymbiotic origin. Mitochondria have many features in common with prokaryotes, and this theory is generally accepted today. At its very basic level, the endosymbiotic theory hypothesises that mitochondria, chloroplasts and perhaps other organelles of eukaryotic cells, originated as independent organisms which were taken inside what became eukaryotic cells as endosymbionts. It has been suggested that mitochondria as we know them today developed from proteobacteria, specifically the SAR11 lineage [15]. Although the endosymbiotic theory has been around for over one hundred years, it remains a controversial and developing hypothesis with new evidence for and against the theory still appearing today. Although beyond the scope of this publication, this controversy certainly highlights mitochondria as a hot topic for research in many diverse fields of study.

2. Present

Mitochondria play a central role in the regulation of cellular function, metabolism, and cell death in cancer cells. Several important functional changes to cancer cell mitochondrial have been observed that implicate the organelle in tumour formation including increased production of reactive oxygen species (ROS), decreased oxidative phosphorylation, and a corresponding increase in glycolysis [16, 17]. However, the specific role of mitochondria in tumourigenesis remains unclear as these changes could represent either key mechanisms in tumour initiation, promotion, or simply secondary effects of tumourigenesis. In 2011, deregulated cellular energetics was considered as an additional emerging hallmark of cancer [18]. Cancer cell signaling that is regulated by kinases and phosphatases are guided by cellular redox status and may be a key in malignant transformation. This section briefly examines the role that mitochondria play in the cancer cell phenotype by relating the physiological process of the organelle to genomic and proteomic studies.

2.1. Role of Mitochondria in Oncogenesis. Recent studies of mitochondrial involvement in cancer have uncovered a plethora of differences in the structure and function of these organelles upon comparing metastatic mitochondria to those belonging to nontransformed cells. Notably, modern research has largely upheld the metabolic observations of Warburg and his successors, while refining and greatly expanding the breadth of mechanistic knowledge of mitochondrial state and function in tumour development. The comprehensive mechanisms of the Warburg effect have not yet been isolated; however, multiple intertwining causative and responsive mechanisms have recently been characterized. This understanding of the indicative features of cancer cell metabolism has also directly been applied to current clinical care through the increasingly widespread adoption of positron emission tomography (PET) imaging using glucose analogues to identify cancerous lesions that are characterized by high glucose uptake [19].

Study of the mechanisms of the Warburg effect has revealed that the characteristic metabolic shift towards aerobic glycolysis and increased glucose uptake imparts several

functional advantages to the cancer cell. These advantages permit rapid growth and survival in conditions that would be potentially lethal to noncancerous cells. Perhaps the most significant shift in the understanding of the Warburg effect in recent years has been the abandonment of the view that aerobic glycolysis is a metabolic defect of cancer cells, in favor of the theory that cancer cell metabolism is maintained through regulatory control, and better fits the metabolic profile of rapidly dividing cells [20]. The most recognized of these adaptations is the utilization of abundant glycolytic pathway intermediates in multiple anabolic reactions critical to the survival and growth of rapidly dividing cells. The demand for glucose-derived carbon skeletons for macromolecule synthesis of molecules such as glycogen, phospholipids, triglycerides, and malate, exceeds the demand for efficient ATP production [21]. Glucose is also alternatively metabolized in cancer cells through an enhanced pentose phosphate pathway that results in the synthesis of nucleotides and antioxidant nicotinamide adenine dinucleotide phosphate (NADPH) [20].

The cancer cell's lack of reliance on oxidative phosphorylation for ATP generation also permits cellular survival in conditions of inconsistent oxygen supply, an environment that is typical for rapidly expanding tumours which can, at times, experience inadequate angiogenesis [22]. Local acidification of the tumour microenvironment is also induced through the glycolytic generation of excess bicarbonic and lactic acids. The resultant pH change is recognized to favour tumour growth and invasion through the activation of cancer cell-derived cathepsins and metalloproteinases [23], and the inhibition of the subsequent host immune responses [24]. Additionally, the ensuing excessive production of lactate can be converted to pyruvate in cancer-associated stromal cells to fuel oxidative phosphorylation within these cells [25].

It is also well established that the enhanced production of mitochondrial ROS, most notably superoxide, hydroxyl radicals, and hydrogen peroxide, is a prominent byproduct of cancer cell metabolism. Increased oxidative phosphorylation in pre-metastatic cells therefore increases the production of mitochondrial ROS, which may be an initiative factor in carcinogenesis [26]. The mechanisms of ROS production and their significant downstream effects have become important topics in current mitochondrial research in cancer. Excess ROS act not only as mutagens and initiators of oxidative stress, but are also significant inter- and intracellular signaling molecules, responsible for a host of nuclear and mitochondrial changes in gene expression, the details of which are reviewed by Verschoor et al. [27].

The well-established addiction to glutamine as an energy source of proliferating cancer cells is yet another key hallmark of cancer cell metabolism. In the cytoplasm, glutamine is converted to glutamate by glutaminase, and transported into the mitochondria where it is converted to the TCA cycle intermediate α-ketoglutarate, and also acts as a source of substrates for macromolecule synthesis [28]. Glutamate is also a key substrate of the glutathione-dependent antioxidant system that is the primary intracellular antioxidant mechanism, and that is critical to cellular protection from ROS. Recent studies have also shown that glutamine is an important component in several signaling pathways involved in cell growth including mTOR and ERK pathways, and glutamine uptake and degradation are controlled via c-myc regulation [29].

The increased mitochondrial ROS production in metastatic cells has also been associated with the corresponding upregulation of cellular antioxidant defense mechanisms [30]. In particular, the synthesis of GSH is significantly increased by the enhanced uptake of rate-limiting cystine through the action of the cystine/glutamate antiporter system x_C^-, which is frequently upregulated in cancer cells [31]. This increased antioxidant capacity has been implicated in cellular resistance to chemotherapy and radiation therapy that induce cancer cell death by initiating oxidative stress [32]. In addition, it was recently found that the abundant glutamate excreted as a byproduct of cystine uptake by system x_C^- in cancer cells may also initiate several significant pathologies of metastatic tumours including excitotoxic cell death in tumours of the CNS, and disruption of bone cell signaling in metastatic tumours in the bone [33, 34].

2.2. Genomics of Mitochondrial DNA: Mutations and Polymorphisms. The circular mtgenome encodes 37 genes including several components of the electron transport chain (ETC), tRNAs, and rRNAs. Additionally, mtDNA contains a non-coding region comprised of two hypervariable regions within a displacement loop (D-loop), which is the location of the origin of replication and transcriptional promoters. Mutations in mtDNA are frequently observed in cancer, likely due to the lack of introns, lack of histone protection, and close proximity to damaging ROS. Each cell contains multiple copies of mitochondrial genes, giving rise to mitochondrial homoplasmy, where all the mitochondria of a cell have the same genomic composition, or heteroplasmy, where wild-type and mutant mtDNA coexist [35]. Thus is it possible for a mutation that confers a distinct advantage for cancer cells, such as accelerated growth or enhanced survival, to be clonally expanded to become a homoplasmic mutant and to predominate within a population of cancer cells. Alternatively, Coller and colleagues [36] used a mathematical model to show that random segregation of mtgenomes during rapid tumour development could result in a mutant homoplasmic population without the need for a selective advantage. Regardless of the existence of background homoplasmic mutations that confer no functional consequence, there are numerous mtDNA mutations that result in significant alterations in mitochondrial function that affect tumour development and progression.

In certain cancer tissues mtDNA mutations were more readily detectable and abundant than mutated nuclear p53 DNA, suggesting that mtDNA mutations could serve as excellent cancer biomarkers, particularly for early detection [35]. The most commonly mutated or deleted region of mtDNA in cancer is within the D-loop at the D310 tract, which is a mononucleotide cytidine repeat at position 310 [37]. As the D-loop is involved in mitochondrial replication, mutations in this region could also affect mtDNA copy number, though this theory has yet to be proven empirically.

In one study, colorectal cancer patients with D-loop mutations were found to have significantly lower overall survival rates and increased chemotherapeutic resistance compared to patients who's mtDNA did not harbour such mutations [38]. The high frequency of D-loop deletion or insertion somatic mutations in cancer render these mutations unlikely to confer any functional impairment to mitochondria, and so the uncertain functional consequences of these mutations should remain an important area for mitochondrial research in cancer.

The importance of mitochondrial polymorphisms in cancer development and risk is intimately related to evolutionary haplogroups, and has recently been a contentious area of research. Haplogroups are characterized by a specific mutation that occurs widely within individuals of a particular population, and are further divided into haplotypes generally based on restriction fragment length polymorphisms [39]. Among the main European haplotypes, the A12308G mutation in $tRNA^{Leu2}$ common to haplotype U was associated with increased risk of both renal and prostate cancers [40]. The NADH-ubiquinone oxioreductase chain 3 (ND3) substitution mutation at G10398A has been associated with increased breast cancer risk in both African American and Indian women [41–45]. In European-American women the A10398G ND3 substitution conferred increased risk of breast cancer, as did the T16519C D-loop polymorphism [46]. A comprehensive study of pancreatic cancer risk revealed associations with the A331T substitution in mitochondrial ND2 [47]. Despite these promising findings, and because the majority of mtDNA polymorphisms are functionally inconsequential, associations with specific polymorphisms and cancer risk have been subject to heated debate. Several older studies involving association of specific polymorphisms with cancer risk have been heavily scrutinized due to erroneous experimental design, interpretation, and poor data quality [35]. However, due to the potential usefulness of somatic mtDNA mutational profiling as a diagnostic tool, the study of mitochondrial somatic mutations and associations with cancer should remain an important focus of cancer biomarker research pending proper study design, population stratification, and independent replication of results. Interestingly, one study reports that one well characterized pathological mtgenome alteration, A3243G, drives mtDNA depletion [48].

Mitochondrial depletion, a hallmark of cancer initiation and malignant development, is characterized by a wide range of mtDNA deletions [49, 50]. In prostate cancer, a cascade of both large and small-scale deletions reduce cellular mtDNA. This reduction is associated with androgen independence which facilitates disease progression [51]. Consistent with these findings, a 3.4kb mtgenome deletion is currently being used by many urologists to identify the presence and/or absence of prostate cancer in patients with an initial benign biopsy [52, 53]. Contrary to a negative outcome these patients remain highly suspicious for disease by other clinical parameters.

2.3. Mithondrial Genome Sequencing. Homoplasmic and heteroplasmic mutations have been reported in the mtgenomes of patient tumors [54], and improved patient outcomes have been demonstrated using mtDNA mutation identification for early detection of solid tumours [55]. Clinically, the detection of mtDNA mutations could be reliably used to compare differences in healthy and cancerous tissues, used to monitor mutations in high-risk, asymptomatic patients, or to monitor cancer patients for recurrence of the disease. Although mtDNA mutations have been reported in a wide variety of human cancers extending early detection to cancer prevention has proved problematic with regards to linking homoplasmic or heterplasmic variations with the etiology of cancer. Thus the characterization of populations of mtDNA variation would facilitate broad acceptance of mtDNA analysis.

Initial studies on whole mtgenome analysis established protocols for directly sequencing entire mtgenomes to detect sequence changes. For example, age-matched individuals with lung cancer had strikingly different mtgenome signatures, suggesting that these variants could be cancer-associated changes [56]. To evaluate progression of mtDNA mutation load associated with tumor stage progression, mtDNA mutation type and location across the entire mtgenome were evaluated between individuals with different stages and different types of cancer. Sequence variants were identified in stage I to stage IV tumor samples, and these mutations were distributed across the entire mtgenome with no indication of a hotspot or specific site of mutation associated with specific cancer types or stages. Analysis across larger genome regions indicated a significant clustering of mtDNA mutations in the ND gene complex, while 10% of mitochondrial mutations were found in the D-loop region.

The importance of whole genome analysis can be recognized in analogous measurements of entire mtgenomes. In human forensics, sequencing entire mtgenome is more effective because polymorphisms in mtgenomes can be useful for resolving individuals who have the identical hypervariable (HV) HV1 and HV2 control region sequences [57]. Using the whole genome as a potential source of mutations improves the discrimination power of forensic assays [58], and by extension cancer diagnostics, prognostics and tumor profiling. Figure 1 illustrates the advantage of whole genome analysis. All ten samples have identical D-loop mutation patterns and types, thus these samples are not distinguishable with only partial mtgenome analysis. As whole mtgenome sequencing is ubiquitous, easy to perform, and high-throughput for even small genomes, whole mtgenome sequencing should be the standard.

2.4. Considerations for Mitochondrial DNA Analysis. Proper analysis of mtgenome mutations is required for accurate correlation of homoplasmic mutations with tumor tissue and stage (Figure 2). Mutations are detected by comparing DNA sequence of tumor tissue to that of normal tissue or blood from the same individual [59]. It is important to use blood as control tissue measurements because it is necessary to subtract out mtDNA variation that arises from accumulation of damage over the lifespan, for example, due to aging. Direct analysis of haplogroups associated with

Fragment position	2850	3009	4500	4791	5458	6213	6270	6345	6774	7011	7709	8082	8616	9492	9946	10392	10533	11250	11885	12068	12395	14146	14867	15041	15815		
Caucasian 01	*	*	*	*	*	*	*	*	*	*	*	*	*	*	*	4	*	*	1	*	*	*	*	1	*	*****	*****	4**1* ***1*
Caucasian 02	*	*	2	*	*	*	*	*	*	*	*	*	*	*	1	*	*	3	*	*	*	*	*	*	*	**2**	*****	****1 **3** *****
Caucasian 03	*	*	*	3	*	*	*	*	2	*	*	4	*	*	*	*	*	*	*	*	*	*	*	*	*	*****	***2* *4*** ***** *****
Caucasian 04	*	*	*	*	*	*	*	*	*	*	*	*	*	*	*	*	*	*	*	*	*	*	*	*	*	***3*	*****	***** ***** *****
Caucasian 05	*	1	*	*	1	*	*	*	*	2	*	*	*	*	*	*	*	*	*	1	*	*	*	3	*	*1**1	*****	2***** ****1 ****3
Caucasian 06	*	1	*	*	*	*	*	*	*	1	*	*	*	*	*	*	*	*	*	*	*	3	*	*	*	31***	****1 ***** ***** ***3***
Caucasian 07	*	*	*	*	*	*	*	4	*	*	*	*	*	*	*	*	*	*	*	*	3	*	*	*	*	*****	***4* ***** ***** 3****
Caucasian 08	*	*	*	*	*	1	*	*	*	*	*	*	2	3	*	*	*	*	*	*	*	*	*	*	*	****1	**23*	***** *****
Caucasian 09	*	*	*	*	*	*	*	*	2	*	*	*	*	*	*	*	2	*	*	*	*	*	*	*	*	*****	**2**	***** *****
Caucasian 10	*	1	*	*	*	*	3	*	*	*	*	*	*	*	*	*	*	*	*	*	*	*	1	*	*	*1***	3***	***** ***** **1**

Figure 1: Numbered position of location of mutations in the mtgenome is listed across the top. Transformation of sequence information to a number enables a bar-code description of the samples. The HV regions do contain mutations, but they are identical and hence of no informative value and are not shown. On the contrary, mutations across the entire mtgenome demonstrates that whole genome analysis has clear utility.

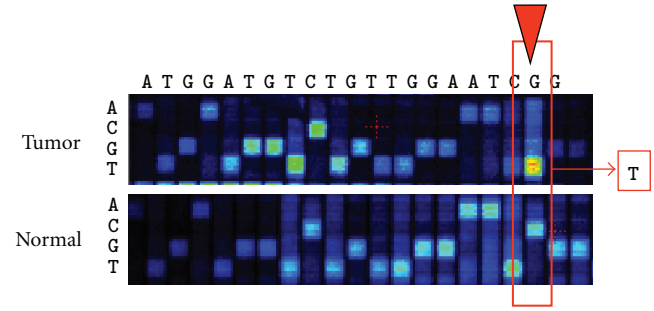

Figure 2: Samples were analyzed by whole genome sequence comparison of (1) tumour tissue and (2) matched patient blood. The sequence of a small region of the mtgenome is indicated across the top of the figure. The red box indicates position and type of mutation observed in the tumour specimen.

cancer does not establish a correlation with variation of mtgenomes metastasis [60]. Comparison of control tissue to tumor tissue must be conducted with such samples collected from the same individual. Accurate detection of mtDNA mutations must account for other sources of errors, for example nuclear mitochondrial pseudogenes (numts) are sources of contamination during PCR amplification. This warrants careful experimental design and cautious interpretation of heteroplasmic results. Hence, mtgenome disease-associated biomarkers must be authenticated to preclude false-positive detection of paralogous nuclear pseudogenes [61].

2.5. Cancer Field Effect. Another important reason to characterize entire mtgenomes is because of occurrence of mtDNA mutations that could be part of a cancer field effect within tissue. These mutations could be biomarkers for progressive mutation patterns in lesions. However, correlation between single mutation sites and specific gradings remains loosely associated. Instead of attempting to define hotspots for mutations, the gradual accumulation of mutation(s) distributed across entire genomes could be considered as an "individualized" marker of progression. Studies have reported no correlation of tumor-associated mtDNA mutations with respect to patient age. The mutation load or population are uniquely attributed to each starting point, and thereafter constrained by risk and rate based on initial populations. While mutation load is individualized, DNA damage may not be compartmentalized to one site. Although low sensitivity assays and limited sampling have plagued the majority of mtgenome comparative studies, not every tumor possessed sequence variants, while some samples contained a number of variants [58, 62].

Analysis for identical damage in different tissues (cancer versus control) could be more apparent with analysis of populations of mtgenomes that indicate tissue predisposed to cancer. Absence of a 1 : 1 correlation between the mutation patterns of tumor progression is likely a result of tissue sampling. Hence, population analyses would facilitate characterization of specific locations and surrounding tissues. In summary, there are salient considerations for mtDNA mutation identification comparative studies between potential

cancer tissue, different types and stages of tumors, as well as non-invasive collected samples and experimental controls. It is imperative to incorporate analysis of the entire mtgenome and accurate identification of heteroplasmic mitochondrial populations. Additionally, the sampling of bodily fluids and tissues surrounding cancerous tissue will facilitate defining the extent of the cancer field effect.

The derivation of sequence changes in the mtgenome in cancer remains unclear. Should these changes prove to be clonal expansions of a heteroplasmy already present in the tissue rather than tumour-associated *in situ* mutations, early detection of cancer may thus rely on the ability to differentiate levels of heteroplasmy. In general, studies of mtDNA mutations in cancer indicate the presence of sequence variants spanning the entire mtgenome, and therefore full genome sequencing will provides the cancer diagnostic community with a useful biomarker discovery approach. Such characterization of populations would be useful to define PCR panels for inexpensive triage and screening of human populations. The sensitivity of mutation detection, rates as little as 2% contribution to the admixture of normal and tumor DNA, indicate heterogeneous biological samples such as bodily fluids, lavage specimens, fine-needle aspirates, or biopsies can potentially be analyzed for cancer-associated mitochondrial DNA mutations. The identified heteroplasmic and homoplasmic sequence variants from tumors and blood (control) and urine (for matched bladder cancer) and bronchoalveolar lavage (for matched lung cancer) were measured from the same individual. It is a reasonable assumption that heteroplasmies should comprise multiple subpopulations of mutated mtDNA molecules. Research that incorporated whole mtgenome analysis using sensitive methods describes sequence variant identification of both heteroplasmic and homoplasmic sequence variants in clinical samples distributed across the mtgenome. Hence, small cohort studies that use incomplete mtgenome sequencing or methods designed to scan discrete portions of the genome, miss important sequence variants associated with cancer or other diseases. It is now possible to screen populations to understand specific frequencies and distributions, and to compare sequences of entire mtgenomes in order to have a comprehensive characterization of sample material. Finally, on account mtDNA mutations are well validated, mitochondrial research is beginning to concentrate on understanding the link between mitochondrial function and pathological states. There are a few studies that have begun to address the association of mitochondrial function with change in homeostasis [63, 64], as well as mitochondrial redox state [65]. As technology improves to allow the accurate assessment of cellular interaction and hemodynamics, monitoring the effects of mitochondrial dysfunction in combination with using mtgenome mutation diagnostics on the pathophysiology of cancer cells will begin to support medical decision-making.

2.6. Mitochondrial Proteomics. The majority of mitochondrial proteins are encoded by the nuclear genome and imported to the mitochondria to perform their specific functions. Thus the mitochondrial proteome is the result of complex crosstalk between both nuclear and mitochondrial programs, and is greatly influenced by pathological conditions including cancer. In the past decade, the mitochondrial proteome has been characterized from highly purified mitochondria resulting in a comprehensive list of over 1,000 mitochondrial proteins (as reviewed in [66]). Using the wealth of knowledge from such studies, numerous databases have been created such as MitoInteractome [67], MitoP2 [68], HMPDb, and MitoMiner [69]. The MitoInteractome database contains 6,549 protein sequences derived from mutltiple databases (SwissProt, MitoP, MitoProteome, HPRD, GO) from several different species creating a comprehensive protein-protein interaction network. Certainly one of the most extensive databases, MitoP2 contains data from a wide breadth of mitochondrial proteomic studies spanning from single protein studies to extensive proteome-wide mapping and expression studies. The HMPDb (Human Mitochondrial Protein Database) provides consolidated information on mitochondrial DNA sequences, polymorphisms, disease-related proteins, and 3-D mitochondrial protein structures. Collectively these databases serve as wonderful utilities for the discovery and characterization of novel mitochondrial biomarkers for diagnosis and molecular targets for drug treatments.

Extensive protein expression differences have been found in mitochondrial glycolytic enzymes, heat-shock proteins, cytoskeleton proteins, and antioxidant enzymes through comparative proteomic analysis. In regards to metabolism, proteins of the glycolytic and pentose phosphate pathways tend to be induced, along with reductions in oxidative phosphorylation pathways [66, 70]. Recently, Chen et al. (2011) performed 2D-DIGE and MALDI-TOF mass spectrometry to compare the proteomic profile of purified mitochondria from normal breast cells (MCF10A), non-invasive breast cancer cells (MCF7), and invasive breast cancer cells (MDA-MB-231) [71]. The most differentially expressed mitochondrial proteins between normal and cancerous cells included cytochrome oxidase subunit 5B, malate dehydrogenase, and elongation factor Tu. Several proteomic studies have shown a significant correlation between high levels of heat-shock protein 70 (HSP-70) in a variety of cancers including gastric adenocarcinoma, hepatocarcinoma, and oesophageal cancer [66]. HSP-70 functions as a mediator of cell proliferation, cellular senescence, and cellular immortalization, and when concentrated in to cytoplasm sequesters p53 and activates Ras-Raf signaling which controls cell proliferation [72, 73].

Recent observations and interest in mitochondrial research has generated a lot of enthusiasm and hope that novel therapeutic agents will be identified that are effective for cancer therapy. In a general sense a dynamic and bidirectional exchange between the metabolic status of the cell generated by mitochondria and genetic profile of a cell will provide a better understanding of metabolites and unexplored signaling mechanisms. Hence a complete understanding of the mitochondrial proteome and its regulation by metabolites, including ROS, will provide a better understanding of the symbiotic relationship that has evolved in eukaryotic cells. Additionally, recent advances in high-throughput technologies, such as next-gen sequencing

and Mitochip [74], have allowed for the rapid and accurate detection of mtDNA mutations, polymorphisms, or copy number variations in a variety of tissues and bodily fluids [55, 75–79].

3. Future

The mitochondrion, as the biochemical nexus of the cell, is a critical consideration in the genomics era of the new millennium. Although much of the current funding is aligned to continuing to further understand the functional details of the nuclear genome, the mitochondrion and its modest complement of DNA and protein is emerging as a crucial component of the biological networking of nuclear pathways. In addition to generating 95% of the chemical fuel firing cellular metabolism through carbohydrate breakdown, mitochondrial perform and mediate a number of events including ROS generation, retrograde calcium signaling and intrinsic apoptosis. Most of these pathways are fundamentally altered during malignant transformation. For example, the apoptotic pathway is severed and carbohydrate metabolism is preempted for anaerobic respiration. Mitochondria shroud a multitude of unidentified proteins, suggesting yet to be understood, deeper biological functions [80]. This important information is not yet fully detailed; however, it is rich with promise. It is likely that these discoveries will provide new approaches to cancer treatment, diagnosis and prognosis. For example, the accelerated mutation rate of the mtgenome offers early identification of malignant transformation by identification of a field effect in normal appearing tissue [81]. This molecular conditioning is well attested particularly in prostate cancer [52, 82, 83]. In addition, the mtgenome has a high copy number and an increased somatic mutation rate in comparison to its nuclear counterpart, providing multiple target copies with target markers. This threesome of characteristics (field effect, copy number, mutation rate) will enable monitoring of vulnerable epithelium in organs such as the lungs, colon, breasts, prostate, and ovaries. Resection of both tumors and the surrounding field may have important implications for recurrence [79]. Since malignant transformation is a 20 to 30 year process, in most cases a shift to a field effect could allow prediction of the development of intraepithelial neoplasia (IEN). Specific markers may indicate which IEN lesions and molecular renovations may progress towards a malignant phenotype. The American Association for Cancer Research (AACR) Task Force on the Treatment and Prevention of IEN published the following statement in 2002:

> *"The AACR IEN Task Force recommends focusing on established precancers as the target for new agent development because of the close association between dysplasia and invasive cancer and because a convincing reduction in IEN burden provides patient benefit by reducing cancer and because a convincing reduction in IEN burden provides patient benefit by reducing cancer risk and/or by decreasing the need for invasive interventions [84]."*

In addition, the traits of mtDNA have successfully led to identification of mitochondrial mutations in low cellular biofluids such as nipple aspirate fluid [85]. Significant resolution between bladder cancer stages Ta, T1 and T2 was obtained using the SNP counts in whole mtgenome sequencing of urine cell pellets in 20 of 31 patients [86]. Notably, circulating cell-free mitochondrial DNA in peripheral blood has diagnostic utility for breast cancer, urological malignancies, and predicting prostate cancer recurrence. [87–89].

Due to its central role in cell physiology, specific alterations in the mtgenome may indicate the status of specific pathways or impact biological outcomes. For example, mutations in mitochondrial respiratory complexes may influence the induction of apoptosis [90] and promote metastatic behavior in both prostate and breast cancers [49]. These studies suggest that the sequence of bases in the mtgenome are finely ordered to the point that even some sequence specific haplogroups may be more susceptible to malignancies [50]. This concept should not be surprising since "natural selection mediated by climate has contributed to shape the current distribution of mtDNA" [91]. Hence mitochondria are dynamic, adaptable molecules able to mitigate biological compromise given metabolic parameters. Disease susceptibility may be tolerated due to imposed climatic constraints.

The cellular ganglion of mitochondria, plethora of pathways and high volume molecular trafficking have been recognized as ideal chemotherapeutic targets [52]; however, this approach draws the proverbial "double-edged sword." For instance, the adjuvant treatment of estrogen receptor positive breast cancer with tamoxifen requires intact and fully operational mitochondria [92]. Importantly, mitochondrial toxicity is a major implication in the failure of chemotherapeutic agents in the late stages of drug development [93]. Careful consideration of mitochondrial and compound interactions is imperative to both target mitochondria for therapeutic indications, while avoiding off-target effects of other therapeutic molecules. Disruption of key mitochondrial molecular transport molecules, such as SCaMC-1, or SLC25A1, in proliferating cells has been suggested as a mitochondrial specific approach to tumor treatment [89, 90].

4. Conclusion

Mitochondria have a critical role to play in the successful conquest of cancer. Further and deeper investigations of this organelle assure profound insights into the missing molecular mechanisms of malignancy. The often referred to "powerhouse of the cell" is beginning to look more like a well ordered neighborhood of sprawling metabolic mansions. Some areas contain décor dating from the earliest of antiquities, while others have yet to be opened and thoroughly explored for the elusive, but ultimate answers to cancer biology; however, many have hurried through the biological lobby of this complex like tourists on a bus schedule. We must now committee to taking the grand tour; more magnificent biological vistas await. Mitochondria may yet be found to be the master of the cellular orchestra.

References

[1] A. L. Lehninger, *The Mitochondrion- Molecular Basis of Structure and Function*, 1965.

[2] L. Ernster and G. Schatz, "Mitochondria: a historical review," *Journal of Cell Biology*, vol. 91, no. 3, part 2, pp. 227s–255s, 1981.

[3] P. Siekevitz, "Powerhouse of the cell," *Scientific American*, no. 1, pp. 131–140, 1957.

[4] P. P. Slonimski and B. Ephrussi, "Action de l'acriflavine sur les levures. V. Le systeme des cytochromes des mutants 'petite colonie'," *Annales de l'Institut Pasteur*, vol. 77, pp. 47–63, 1949.

[5] M. M. Nass and S. Nass, "Intramitochondrial fibers with DNA characteristics. I. Fixation and electron staining reactions," *Journal of Cell Biology*, vol. 19, pp. 593–629, 1963.

[6] G. Schatz and J. Klima, "Triphosphopyridine nucleotide: cytochrome C reductase of Saccharomyces Cerevisiae a 'microsomal' enzyme," *Biochimica et Biophysica Acta*, vol. 81, no. 3, pp. 448–461, 1964.

[7] S. Anderson, A. T. Bankier, B. G. Barrell et al., "Sequence and organization of the human mitochondrial genome," *Nature*, vol. 290, no. 5806, pp. 457–465, 1981.

[8] R. M. Andrews, I. Kubacka, P. F. Chinnery, R. N. Lightowlers, D. M. Turnbull, and N. Howell, "Reanalysis and revision of the cambridge reference sequence for human mitochondrial DNA," *Nature Genetics*, vol. 23, no. 2, p. 147, 1999.

[9] D. C. Wallace, G. Singh, M. T. Lott et al., "Mitochondrial DNA mutation associated with Leber's hereditary optic neuropathy," *Science*, vol. 242, no. 4884, pp. 1427–1430, 1988.

[10] I. J. Holt, A. E. Harding, and J. A. Morgan-Hughes, "Deletions of muscle mitochondrial DNA in patients with mitochondrial myopathies," *Nature*, vol. 331, no. 6158, pp. 717–719, 1988.

[11] L. C. Greaves, A. K. Reeve, R. W. Taylor, and D. M. Turnbull, "Mitochondrial DNA and disease," *The Journal of Pathology*, vol. 226, no. 2, pp. 274–286, 2012.

[12] S. E. Durham, K. J. Krishnan, J. Betts, and M. A. Birch-Machin, "Mitochondrial DNA damage in non-melanoma skin cancer," *British Journal of Cancer*, vol. 88, no. 1, pp. 90–95, 2003.

[13] O. Warburg, K. Posener, and E. Negelein, "Ueber den Stoffwechsel der Tumoren," *Biochemische Zeitschrift*, vol. 152, pp. 319–344, 1924.

[14] O. Warburg, "On the origin of cancer cells," *Science*, vol. 123, no. 3191, pp. 309–314, 1956.

[15] J. C. Thrash, A. Boyd, M. J. Huggett et al., "Phylogenomic evidence for a common ancestor of mitochondria and the SAR11 clade," *Scientific Reports*, vol. 1, article 13, 2011.

[16] Y. Chen, R. Cairns, I. Papandreou, A. Koong, and N. C. Denko, "Oxygen consumption can regulate the growth of tumors, a new perspective on the Warburg effect," *PLoS One*, vol. 4, no. 9, Article ID e7033, 2009.

[17] F. Weinberg, R. Hamanaka, W. W. Wheaton et al., "Mitochondrial metabolism and ROS generation are essential for Kras-mediated tumorigenicity," *Proceedings of the National Academy of Sciences of the United States of America*, vol. 107, no. 19, pp. 8788–8793, 2010.

[18] D. Hanahan and R. A. Weinberg, "Hallmarks of cancer: the next generation," *Cell*, vol. 144, no. 5, pp. 646–674, 2011.

[19] S. S. Gambhir, "Molecular imaging of cancer with positron emission tomography," *Nature Reviews Cancer*, vol. 2, no. 9, pp. 683–693, 2002.

[20] P. S. Ward and C. B. Thompson, "Metabolic reprogramming: a cancer hallmark even warburg did not anticipate," *Cancer Cell*, vol. 21, no. 3, pp. 297–308, 2012.

[21] G. Kroemer and J. Pouyssegur, "Tumor cell metabolism: cancer's Achilles' heel," *Cancer Cell*, vol. 13, no. 6, pp. 472–482, 2008.

[22] J. Pouysségur, F. Dayan, and N. M. Mazure, "Hypoxia signalling in cancer and approaches to enforce tumour regression," *Nature*, vol. 441, no. 7092, pp. 437–443, 2006.

[23] P. Swietach, R. D. Vaughan-Jones, and A. L. Harris, "Regulation of tumor pH and the role of carbonic anhydrase 9," *Cancer and Metastasis Reviews*, vol. 26, no. 2, pp. 299–310, 2007.

[24] K. Fischer, P. Hoffmann, S. Voelkl et al., "Inhibitory effect of tumor cell-derived lactic acid on human T cells," *Blood*, vol. 109, no. 9, pp. 3812–3819, 2007.

[25] M. I. Koukourakis, A. Giatromanolaki, A. L. Harris, and E. Sivridis, "Comparison of metabolic pathways between cancer cells and stromal cells in colorectal carcinomas: a metabolic survival role for tumor-associated stroma," *Cancer Research*, vol. 66, no. 2, pp. 632–637, 2006.

[26] R. A. Zager, A. C. M. Johnson, S. Y. Hanson, and S. Lund, "Acute nephrotoxic and obstructive injury primes the kidney to endotoxin-driven cytokine/chemokine production," *Kidney International*, vol. 69, no. 7, pp. 1181–1188, 2006.

[27] M. L. Verschoor, L. A. Wilson, and G. Singh, "Mechanisms associated with mitochondrialgenerated reactive oxygen species in cancer," *Canadian Journal of Physiology and Pharmacology*, vol. 88, no. 3, pp. 204–219, 2010.

[28] T. Cheng, J. Sudderth, C. Yang et al., "Pyruvate carboxylase is required for glutamine-independent growth of tumor cells," *Proceedings of the National Academy of Sciences of the United States of America*, vol. 108, no. 21, pp. 8674–8679, 2011.

[29] R. J. Deberardinis and T. Cheng, "Q's next: the diverse functions of glutamine in metabolism, cell biology and cancer," *Oncogene*, vol. 29, no. 3, pp. 313–324, 2010.

[30] J. Y. Kim, Y. Kanai, A. Chairoungdua et al., "Human cystine/glutamate transporter: cDNA cloning and upregulation by oxidative stress in glioma cells," *Biochimica et Biophysica Acta*, vol. 1512, no. 2, pp. 335–344, 2001.

[31] W. J. Chung, S. A. Lyons, G. M. Nelson et al., "Inhibition of cystine uptake disrupts the growth of primary brain tumors," *Journal of Neuroscience*, vol. 25, no. 31, pp. 7101–7110, 2005.

[32] Y. Huang, Z. Dai, C. Barbacioru, and W. Sadée, "Cystine-glutamate transporter SLC7A11 in cancer chemosensitivity and chemoresistance," *Cancer Research*, vol. 65, no. 16, pp. 7446–7454, 2005.

[33] J. de Groot and H. Sontheimer, "Glutamate and the biology of gliomas," *GLIA*, vol. 59, no. 8, pp. 1181–1189, 2011.

[34] E. P. Seidlitz, M. K. Sharma, and G. Singh, "A by-product of glutathione production in cancer cells may cause disruption in bone metabolic processes," *Canadian Journal of Physiology and Pharmacology*, vol. 88, no. 3, pp. 197–203, 2010.

[35] A. Chatterjee, S. Dasgupta, and D. Sidransky, "Mitochondrial subversion in cancer," *Cancer Prevention Research*, vol. 4, no. 5, pp. 638–654, 2011.

[36] H. A. Coller, K. Khrapko, N. D. Bodyak, E. Nekhaeva, P. Herrero-Jimenez, and W. G. Thilly, "High frequency of homoplasmic mitochondrial DNA mutations in human tumors can be explained without selection," *Nature Genetics*, vol. 28, no. 2, pp. 147–150, 2001.

[37] M. Sanchez-Cespedes, P. Parrella, S. Nomoto et al., "Identification of a mononucleotide repeat as a major target for mitochondrial DNA alterations in human tumors," *Cancer Research*, vol. 61, no. 19, pp. 7015–7019, 2001.

[38] A. Lièvre, C. Chapusot, A. M. Bouvier et al., "Clinical value of mitochondrial mutations in colorectal cancer," *Journal of Clinical Oncology*, vol. 23, no. 15, pp. 3517–3525, 2005.

[39] K. K. Singh and M. Kulawiec, "Mitochondrial DNA polymorphism and risk of cancer," *Methods in Molecular Biology*, vol. 471, pp. 291–303, 2009.

[40] L. M. Booker, G. M. Habermacher, B. C. Jessie et al., "North American white mitochondrial haplogroups in prostate and renal cancer," *Journal of Urology*, vol. 175, no. 2, pp. 468–472, 2006.

[41] M. Kulawiec, K. M. Owens, and K. K. Singh, "MtDNA G10398A variant in African-American women with breast cancer provides resistance to apoptosis and promotes metastasis in mice," *Journal of Human Genetics*, vol. 54, no. 11, pp. 647–654, 2009.

[42] V. W. Setiawan, L. H. Chu, E. M. John et al., "Mitochondrial DNA G10398A variant is not associated with breast cancer in African-American women," *Cancer Genetics and Cytogenetics*, vol. 181, no. 1, pp. 16–19, 2008.

[43] K. Darvishi, S. Sharma, A. K. Bhat, E. Rai, and R. N. K. Bamezai, "Mitochondrial DNA G10398A polymorphism imparts maternal Haplogroup N a risk for breast and esophageal cancer," *Cancer Letters*, vol. 249, no. 2, pp. 249–255, 2007.

[44] M. P. Mims, T. G. Hayes, S. Zheng et al., "Mitochondrial DNA G10398A polymorphism and invasive breast cancer in African-American women," *Cancer Research*, vol. 66, no. 3, pp. 1880–1881, 2006.

[45] J. A. Canter, A. R. Kallianpur, F. F. Parl, and R. C. Millikan, "Mitochondrial DNA G10398A polymorphism and invasive breast cancer in African-American women," *Cancer Research*, vol. 65, no. 17, pp. 8028–8033, 2005.

[46] R. K. Bai, S. M. Leal, D. Covarrubias, A. Liu, and L. J. C. Wong, "Mitochondrial genetic background modifies breast cancer risk," *Cancer Research*, vol. 67, no. 10, pp. 4687–4694, 2007.

[47] E. T. Lam, P. M. Bracci, E. A. Holly et al., "Mitochondrial DNA sequence variation and risk of pancreatic cancer," *Cancer Research*, vol. 72, no. 3, pp. 686–695, 2012.

[48] C. J. Turner, C. Granycome, R. Hurst et al., "Systematic segregation to mutant mitochondrial DNA and accompanying loss of mitochondrial DNA in human NT2 teratocarcinoma cybrids," *Genetics*, vol. 170, no. 4, pp. 1879–1885, 2005.

[49] A. K. Rasmussen, A. Chatterjee, L. J. Rasmussen, and K. K. Singh, "Mitochondria-mediated nuclear mutator phenotype in Saccharomyces cerevisiae," *Nucleic Acids Research*, vol. 31, no. 14, pp. 3909–3917, 2003.

[50] G. Amuthan, G. Biswas, S. Y. Zhang, A. Klein-Szanto, C. Vijayasarathy, and N. G. Avadhani, "Mitochondria-to-nucleus stress signaling induces phenotypic changes, tumor progression and cell invasion," *EMBO Journal*, vol. 20, no. 8, pp. 1910–1920, 2001.

[51] M. Higuchi, T. Kudo, S. Suzuki et al., "Mitochondrial DNA determines androgen dependence in prostate cancer cell lines," *Oncogene*, vol. 25, no. 10, pp. 1437–1445, 2006.

[52] J. Maki, K. Robinson, B. Reguly et al., "Mitochondrial genome deletion aids in the identification of false- and true-negative prostate needle core biopsy specimens," *American Journal of Clinical Pathology*, vol. 129, no. 1, pp. 57–66, 2008.

[53] K. Robinson, J. Creed, B. Reguly et al., "Accurate prediction of repeat prostate biopsy outcomes by a mitochondrial DNA deletion assay," *Prostate Cancer and Prostatic Diseases*, vol. 13, no. 2, pp. 126–131, 2010.

[54] K. Polyak, Y. Li, H. Zhu et al., "Somatic mutations of the mitochondrial genome in human colorectal tumours," *Nature Genetics*, vol. 20, no. 3, pp. 291–293, 1998.

[55] M. S. Fliss, H. Usadel, O. L. Caballero et al., "Facile detection of mitochondrial DNA mutations in tumors and bodily fluids," *Science*, vol. 287, no. 5460, pp. 2017–2019, 2000.

[56] J. P. Jakupciak, S. Maragh, M. E. Markowitz et al., "Performance of mitochondrial DNA mutations detecting early stage cancer," *BMC Cancer*, vol. 8, article 285, 2008.

[57] P. M. Vallone, J. P. Jakupciak, and M. D. Coble, "Forensic application of the affymetrix human mitochondrial resequencing array," *Forensic Science International*, vol. 1, no. 2, pp. 196–198, 2007.

[58] E. Zietkiewicz, M. Witt, P. Daca, J. Zebracka-Gala, M. Goniewicz, and B. Jarzab, "Current genetic methodologies in the identification of disaster victims and in forensic analysis," *Journal of Applied Genetics*, vol. 53, no. 1, pp. 41–60, 2012.

[59] B. Reguly, J. P. Jakupciak, and R. L. Parr, "3.4 kb mitochondrial genome deletion serves as a surrogate predictive biomarker for prostate cancer in histopathologically benign biopsy cores," *Journal of the Canadian Urological Association*, vol. 4, no. 5, pp. E118–E122, 2010.

[60] S. Ebner, R. Lang, E. E. Mueller et al., "Mitochondrial haplogroups, control region polymorphisms and malignant melanoma: a study in middle European Caucasians," *PLoS One*, vol. 6, no. 12, Article ID e27192, 2011.

[61] R. L. Parr, J. Maki, B. Reguly et al., "The pseudo-mitochondrial genome influences mistakes in heteroplasmy interpretation," *BMC Genomics*, vol. 7, article 185, 2006.

[62] J. P. Jakupciak, G. D. Dakubo, S. Maragh, and R. L. Parr, "Analysis of potential cancer biomarkers in mitochondrial DNA," *Current Opinion in Molecular Therapeutics*, vol. 8, no. 6, pp. 500–506, 2006.

[63] W. H. Koppenol, P. L. Bounds, and C. V. Dang, "Otto Warburg's contributions to current concepts of cancer metabolism," *Nature Reviews Cancer*, vol. 11, no. 5, pp. 325–337, 2011.

[64] A. Mayevsky and G. G. Rogatsky, "Mitochondrial function in vivo evaluated by NADH fluorescence: from animal models to human studies," *American Journal of Physiology*, vol. 292, no. 2, pp. C615–C640, 2007.

[65] A. Mayevsky, R. Walden, E. Pewzner et al., "Mitochondrial function and tissue vitality: bench-to-bedside real-time optical monitoring system," *Journal of Biomedical Optics*, vol. 16, no. 6, Article ID 067004, 2011.

[66] P. Bottoni, B. Giardina, A. Pontoglio, S. Scara, and R. Scatena, "Mitochondrial proteomic approaches for new potential diagnostic and prognostic biomarkers in cancer," *Advances in Experimental Medicine and Biology*, vol. 942, pp. 423–440, 2012.

[67] R. Reja, A. J. Venkatakrishnan, J. Lee et al., "MitoInteractome: mitochondrial protein interactome database, and its application in 'aging network' analysis," *BMC Genomics*, vol. 10, supplement 3, p. S20, 2009.

[68] M. Elstner, C. Andreoli, T. Klopstock, T. Meitinger, and H. Prokisch, "The mitochondrial proteome database: MitoP2," *Methods in Enzymology*, vol. 457, pp. 3–20, 2009.

[69] A. C. Smith, J. A. Blackshaw, and A. J. Robinson, "MitoMiner: a data warehouse for mitochondrial proteomics data," *Nucleic Acids Research*, vol. 40, pp. 1160–1167, 2012.

[70] R. Scatena, "Mitochondria and cancer: a growing role in apoptosis, cancer cell metabolism and dedifferentiation," *Advances in Experimental Medicine and Biology*, vol. 942, pp. 287–308, 2012.

[71] Y. W. Chen, H. C. Chou, P. C. Lyu et al., "Mitochondrial proteomics analysis of tumorigenic and metastatic breast cancer markers," *Functional and Integrative Genomics*, vol. 11, no. 2, pp. 225–239, 2011.

[72] R. Wadhwa, T. Yaguchi, M. K. Hasan, Y. Mitsui, R. R. Reddel, and S. C. Kaul, "Hsp70 family member, mot-2/mthsp70/GRP75, binds to the cytoplasmic sequestration domain of the p53 protein," *Experimental Cell Research*, vol. 274, no. 2, pp. 246–253, 2002.

[73] R. Wadhwa, T. Yaguchi, M. K. Hasan, K. Taira, and S. C. Kaul, "Mortalin-MPD (mevalonate pyrophosphate decarboxylase) interactions and their role in control of cellular proliferation," *Biochemical and Biophysical Research Communications*, vol. 302, no. 4, pp. 735–742, 2003.

[74] A. Maitra, Y. Cohen, S. E. D. Gillespie et al., "The human MitoChip: a high-throughput sequencing microarray for mitochondrial mutation detection," *Genome Research*, vol. 14, no. 5, pp. 812–819, 2004.

[75] J. C. Castle, M. Biery, H. Bouzek et al., "DNA copy number, including telomeres and mitochondria, assayed using next-generation sequencing," *BMC Genomics*, vol. 11, no. 1, article 244, 2010.

[76] L. Fendt, H. Niederstätter, G. Huber et al., "Accumulation of mutations over the entire mitochondrial genome of breast cancer cells obtained by tissue microdissection," *Breast Cancer Research and Treatment*, vol. 128, no. 2, pp. 327–336, 2011.

[77] H. D. Hosgood III, C. S. Liu, N. Rothman et al., "Mitochondrial DNA copy number and lung cancer risk in a prospective cohort study," *Carcinogenesis*, vol. 31, no. 5, pp. 847–849, 2010.

[78] S. Nomoto, K. Yamashita, K. Koshikawa, A. Nakao, and D. Sidransky, "Mitochondrial D-loop mutations as clonal markers in multicentric hepatocellular carcinoma and plasma," *Clinical Cancer Research*, vol. 8, no. 2, pp. 481–487, 2002.

[79] S. Dasgupta, R. Koch, W. H. Westra et al., "Mitochondrial DNA mutation in normal margins and tumors of recurrent head and neck squamous cell carcinoma patients," *Cancer Prevention Research*, vol. 3, no. 9, pp. 1205–1211, 2010.

[80] Y. Jiang and X. Wang, "Comparative mitochondrial proteomics: perspective in human diseases," *Journal of Hematology & Oncology*, vol. 5, article 11, 2012.

[81] G. D. Dakubo, J. P. Jakupciak, M. A. Birch-Machin, and R. L. Parr, "Clinical implications and utility of field cancerization," *Cancer Cell International*, vol. 7, article 2, 2007.

[82] R. L. Parr, G. D. Dakubo, K. A. Crandall et al., "Somatic mitochondrial DNA mutations in prostate cancer and normal appearing adjacent glands in comparison to age-matched prostate samples without malignant histology," *Journal of Molecular Diagnostics*, vol. 8, no. 3, pp. 312–319, 2006.

[83] K. A. Trujillo, A. C. Jones, J. K. Griffith, and M. Bisoffi, "Markers of field cancerization: proposed clinical applications in prostate biopsies," *Prostate Cancer*, vol. 2012, Article ID 302894, 2012.

[84] J. A. O'Shaughnessy, G. J. Kelloff, G. B. Gordon et al., "Treatment and prevention of intraepithelial neoplasia: an important target for accelerated new agent development: recommendations of the American association for cancer research Task force on the Treatment and Prevention of intraepithelial neoplasia," *Clinical Cancer Research*, vol. 8, no. 2, pp. 314–346, 2002.

[85] J. P. Jakupciak, A. Maggrah, S. Maragh et al., "Facile whole mitochondrial genome resequencing from nipple aspirate fluid using MitoChip v2.0," *BMC Cancer*, vol. 8, article 95, 2008.

[86] S. Dasgupta, C. Shao, T. E. Keane et al., "Detection of mitochondrial deoxyribonucleic acid alterations in urine from urothelial cell carcinoma patients," *International Journal of Cancer*, vol. 131, no. 1, pp. 158–164, 2012.

[87] J. Ellinger, D. C. Muller, S. C. Muller et al., "Circulating mitochondrial DNA in serum: a universal diagnostic biomarker for patients with urological malignancies," *Urologic Oncology*, vol. 30, no. 4, pp. 509–515, 2012.

[88] J. Ellinger, S. C. Müller, N. Wernert, A. von Ruecker, and P. J. Bastian, "Mitochondrial DNA in serum of patients with prostate cancer: a predictor of biochemical recurrence after prostatectomy," *British Journal of Urology International*, vol. 102, no. 5, pp. 628–632, 2008.

[89] J. Traba, A. Del Arco, M. R. Duchen, G. Szabadkai, and J. Satrustegui, "SCaMC-1 promotes cancer cell survival by desensitizing mitochondrial permeability transition via ATP/ADP-mediated matrix Ca(2+) buffering," *Cell Death & Differentiation*, vol. 19, no. 4, pp. 650–660, 2012.

[90] O. Catalina-Rodriguez, V. K. Kolukula, Y. Tomita et al., "The mitochondrial citrate transporter, CIC, is essential for mitochondrial homeostasis," *Oncotarget*, vol. 3, no. 10, pp. 1220–1235, 2012.

[91] F. Balloux, L. J. Handley, T. Jombart, H. Liu, and A. Manica, "Climate shaped the worldwide distribution of human mitochondrial DNA sequence variation," *Proceedings of the Royal Society B*, vol. 276, no. 1672, pp. 3447–3455, 2009.

[92] A. Naito, J. Carcel-Trullols, C. H. Xie, T. T. Evans, T. Mizumachi, and M. Higuchi, "Induction of acquired resistance to antiestrogen by reversible mitochondrial DNA depletion in breast cancer cell line," *International Journal of Cancer*, vol. 122, no. 7, pp. 1506–1511, 2008.

[93] J. A. Dykens, L. D. Marroquin, and Y. Will, "Strategies to reduce late-stage drug attrition due to mitochondrial toxicity," *Expert Review of Molecular Diagnostics*, vol. 7, no. 2, pp. 161–175, 2007.

Hindawi Publishing Corporation
BioMed Research International
Volume 2013, Article ID 157547, 10 pages
http://dx.doi.org/10.1155/2013/157547

Research Article

Simultaneous Quantification of Mitochondrial DNA Damage and Copy Number in Circulating Blood: A Sensitive Approach to Systemic Oxidative Stress

Sam W. Chan, Simone Chevalier, Armen Aprikian, and Junjian Z. Chen

Department of Surgery/Division of Urology, The Research Institute of McGill University Health Center, 1650 Cedar Avenue, Room R1.107, Montreal, QC, Canada H3G 1A4

Correspondence should be addressed to Junjian Z. Chen; junjian.chen@mcgill.ca

Received 2 September 2012; Revised 12 November 2012; Accepted 13 November 2012

Academic Editor: Gurmit Singh

Systemic oxidative stress is associated with a wide range of pathological conditions. Oxidative DNA damage is frequently measured in circulating lymphocytes. Mitochondrial DNA (mtDNA) is known to be more sensitive to oxidative damage than nuclear DNA but is rarely used for direct measurement of DNA damage in clinical studies. Based on the supercoiling-sensitive real-time PCR method, we propose a new approach for the noninvasive monitoring of systemic oxidative stress by quantifying the mtDNA structural damage and copy number change in isolated lymphocytes in a single test. We show that lymphocytes have significantly less mtDNA content and relatively lower baseline levels of damage than cancer cell lines. In an *ex vivo* challenge experiment, we demonstrate, for the first time, that exogenous H_2O_2 induces a significant increase in mtDNA damage in lymphocytes from healthy individuals, but no repair activity is observed after 1 h recovery. We further demonstrate that whole blood may serve as a convenient alternative to the isolated lymphocytes in mtDNA analysis. Thus, the blood analysis with the multiple mtDNA end-points proposed in the current study may provide a simple and sensitive test to interrogate the nature and extent of systemic oxidative stress for a broad spectrum of clinical investigations.

1. Introduction

Oxidative stress is a state of physiological imbalance between oxidant production and antioxidant defence at different biological levels. It is implicated in the development of many pathological conditions such as aging, neurodegenerative diseases, and cancer initiation and progression [1–6]. Many diseases are suspected to be linked to oxidative stress, but procurement of disease tissues may be difficult due to its invasive nature and the scarcity of available tissues. However, researchers have mitigated this problem by using the systemic oxidative stress in peripheral tissues, such as circulating blood, as a noninvasive surrogate. Extrinsic factors such as inflammation, nutrient imbalance, and hypoxic environment could affect inter and intracellular redox homeostasis, therefore altering systemic oxidative stress levels; new efforts are made to investigate the interactions between systemic oxidative stress and pathogenesis of many disease conditions [7–13]. For example, several recent studies suggest a correlation between increased systemic oxidative stress and prostate cancer risk and progression [14–16]. Similar results are reported in lung cancer [17], head and neck cancer [18], and other human cancers [19, 20]. Thus, enhanced oxidative stress is not only a common property of the diseased cells, but may also be reflected in the peripheral tissues.

Systemic oxidative stress has been analyzed in serum and blood cells using different biomarkers and assay systems. Genomic DNA in circulating lymphocytes is a widely used target in measuring different end-points of oxidative DNA damage, such as 8-oxoguanine (8-oxo-G) base lesions or DNA strand breaks detected with the comet assay [14–18]. The mitochondrial DNA (mtDNA) in lymphocytes is an attractive alternative target to determine systemic oxidative stress. MtDNA is a circular, multicopy cytoplasmic DNA,

semiautonomously maintained in mitochondria. It is known to be more sensitive to oxidative damage than nuclear DNA [21–23] and has been increasingly used for evaluating systemic oxidative stress with various assays. Similarly to nuclear DNA, 8-oxo-G base lesions can be assessed in purified mtDNA from lymphocytes [24]. Extracellular circulating mtDNA in serum is another marker recently used for evaluating genetic integrity and cancer risk. Elevated levels of free floating mtDNA detected in the plasma or serum are found to be associated with poor prognoses for prostate and testicular germ cell cancers [25–27]. However, the source and nature of this circulating mtDNA are not fully elucidated. Oxidative stress can also affect the total mtDNA content in lymphocytes under various diseased conditions [28]. For example, significant alterations in mtDNA content were detected in lymphocytes from patients with renal cell carcinoma, hyperlipidemia, and Huntington's disease when compared to control populations [19, 29, 30]. However, the relationship between different mtDNA end-points reported in lymphocytes is not clear and the direct measurement of mtDNA strand breaks in lymphocytes has not been reported. We previously developed a sensitive *in vitro* assay to quantify mtDNA structural damage induced by strand breaks, repair and copy number change in prostate cancer cell lines using a supercoiling-sensitive real-time PCR (ss-qPCR) [6, 31]. We showed that oxidative damage can induce single- or double-strand breaks (SSB or DSB), which lead to the disruption of the supercoiled conformation, and that the resulting relaxed conformation is a better qPCR substrate for significantly increased amplification than the supercoiled conformation, even if the starting mtDNA molecules remain the same [31]. Additionally, we observed that prolonged exposure to 95°C heat also introduced strand breaks in the mtDNA. This particular property was advantageously used to disrupt all structural features of mtDNA for precise quantification of the total mtDNA content [31].

The objectives of this current study were to test if the ss-qPCR method could be applied to the lymphocytes and to explore a quantitative strategy to measure multiple mtDNA end-points in circulating blood cells for the study of systemic oxidative stress. We developed an absolute quantification method for precise measurement of mtDNA structural damage, copy number change, and repair activity in blood cells. We demonstrated that mtDNA has low levels of both copy number and baseline damage in lymphocytes as compared to cancer cell lines, and that exogenous H_2O_2 led to a significant increase in mtDNA damage but with little repair activity in inactivated lymphocytes in *ex vivo* experiments.

2. Materials and Methods

2.1. Chemicals, Reagents, and Cell Culture. All chemicals were purchased from Sigma-Aldrich (Oakville, ON, Canada) unless otherwise specified. Prostate cancer cell line LNCaP was purchased from ATCC (Manassas, VA). C4-2, a gift from Dr. L.W.K. Chung, is an isogenic clone of the LNCaP cell line with increased invasive potential [32]. LNCaP and C4-2 prostate cancer cells were cultured in RPMI 1640 complete medium (Invitrogen, Burlington, Ontario, Canada) supplemented with 10% fetal bovine serum (FBS) (Invitrogen) and 1% penicillin-streptomycin (Invitrogen). LNCaP cells were cultured in Poly-L-Lysine (1%) coated dishes. The cells were collected with a Trypsin/EDTA solution, (0.05% trypsin + 0.02% EDTA) then washed down with PBS and stored at −80°C.

2.2. Blood Collection and Lymphocyte Preparation. Healthy male volunteers ranging from 28 to 45 years old were recruited for this pilot study through an institutional review board (REB) approved protocol at the McGill University Health Center. Blood (10 to 15 mL) was collected into 9 mL collection tubes coated with EDTA (Vacu K3EDTA PULL LAV) (Fisher, Monroe, NC). For experiments with whole blood, the samples were immediately stored at −80°C in 10% dimethyl sulfoxide (DMSO) prior to analysis. For experiments with isolated lymphocytes, blood was submitted to Ficoll-Paque Plus (GE Healthcare, Buckinghamshire, England) to recover the lymphocytes [33], then stored at −80°C in 40% RPMI media 1640 supplemented with 50% FBS and 10% DMSO prior to analysis. As per manufacturer's specifications, the extracted sample is composed in majority of lymphocytes (75–93%), with a remaining fraction of monocytes (7–25%) and minimal contaminants from granulocytes, erythrocytes, and platelets (3 ± 2%, 5 ± 2%, and < 0.5%, resp.).

2.3. H_2O_2 Challenge Experiments with Lymphocytes and Whole Blood. Frozen lymphocytes were thawed in a 37°C water bath for 1-2 min and washed with 5 volumes of ice-cold wash medium (50% FBS and 50% RPMI 1640). The lymphocytes were counted and cell viability was assessed under microscope using the trypan blue dye (average of over 90% viability). A total of ~3×10^6 lymphocytes were incubated in 50 mL conical tubes with RPMI-1640 complete medium for 30 min prior to the experiment. The cell suspension was split into three groups of ~1×10^6 cells each, treated with 0 (control) or 120 μM H_2O_2 for 15 min for exposure or allowed to recover in fresh medium for 60 min. The concentration of 120 μM H_2O_2 was chosen to be in the lower-middle range of concentrations used in similar treatments in the literature (50 to 500 μM) [14, 34]. Afterwards, the lymphocyte samples were washed with PBS, spun down to a pellet, and then stored at −80°C before DNA preparation.

Frozen whole blood was thawed in a 37°C water bath for 1-2 min and washed with 5 volumes of ice-cold PBS wash medium. The whole blood cells were counted with trypan blue dye prior to incubation (average of over 90% viability). A total of ~15×10^6 whole blood cells were incubated in RPMI-1640 complete medium in 50 mL conical tubes for 30 min prior to the experiment. Whole blood samples were separated into three groups with ~5×10^6 cells each and treated with 0 or 120 μM H_2O_2 as in the lymphocyte experiment. Whole blood samples were collected after treatment and stored at −80°C before DNA preparation.

2.4. DNA Preparation for the ss-qPCR Analysis. DNA was extracted with the QIAGEN Blood & Cell Culture DNA

Table 1: Primer sequences.

Primers	Forward 5′–3′	Reverse 5′–3
CO2 3285 bp long fragment	CCTAGGGTTTATCGTGTGAG	CTAGTTAATTGGAAGTTAACGG
D-loop 2467 bp long fragment	CGCACGGACTACAACCACGAC	CTGTGGGGGGTGTCTTTGGGG
Calicin 2658 bp long fragment	ATTCCAGAAGCCTTTAACTAG	ACAAATGAGACACAAACTACCG
CO2 (for real-time PCR)	CCCCACATTAGGCTTAAAAACAGAT	TATACCCCCGGTCGTGTAGCGGT
D-loop (for real-time PCR)	TATCTTTTGGCGGTATGCACTTTTAACAGT	TGATGAGATTAGTAGTATGGGAGTGG
Calicin (for real-time PCR)	CTGGTCGCTACATCTACATCTC	CAGGTCAGGCAACTTGGTC

Kit according to the manufacturer's instructions with minor modifications to ensure that both mtDNA and nuclear DNA were collected together [31, 35]. Total DNA was quantified with a NanoDrop spectrophotometer. DNA template solutions of 1 ng/μL were prepared for each sample with 1X Tris/EDTA Buffer Solution (pH 8.0). Each template solution was split into two equal parts with half serving as an original template for the measurement of the damaged/relaxed mtDNA fraction and the other half heat-treated (95°C for 6 min on a PCR machine) to quantify total amount of mtDNA [31].

2.5. Nuclear DNA and mtDNA Standards Preparation for Absolute Quantification. MtDNA standards were prepared for absolute quantification. A 3.3 kb mtDNA fragment containing the CO2 gene and a 2.5 kb fragment containing the D-loop region were amplified from the immortalized normal human prostate cell line, RWPE-1, using primers listed in Table 1. PCR reactions were performed using the GeneAmp PCR 9700 system (ABI) with recombinant *Thermus thermophilus* (rTth) DNA polymerase (ABI). The amplification program was performed as follows: preheat samples to reach 75°C; add rTth DNA polymerase and incubate for 2 min; denature at 94°C for 1 min, followed by 30 cycles of 94°C for 15 sec, 60°C for 30 sec., and 72°C for 3.5 min; then 72°C for 5 min and cool down to 10°C. Amplified DNA fragments were purified with the QIAGEN PCR Purification Kit. The purified products were carefully quantified with the Nanodrop spectrophotometer, and the average of three readings was used for calculating precise copy number according to the following equation (Figure 1):

$$\text{copies}/\mu\text{L} = \frac{[\text{ng}/\mu\text{L}]}{\text{m}}. \quad (1)$$

Six or seven serial dilutions were made ranging from 3×10^6 to 30 or 3×10^7 to 30 copies with a dilution factor of 10 depending on the experiment. The 6-point standard was used for the mtDNA quantification in blood samples, while the 7-point standard was used to demonstrate the dynamic range and linearity of the assay. The original stock solutions were made into small aliquots and stored at −80°C to prevent repeated freeze and thaw.

The nuclear DNA standards were similarly prepared. The nuclear primer sequences are listed in Table 1. A 2.7 kb nuclear fragment containing the calicin gene was amplified from RWPE-1. Calicin is a single-copy nuclear gene that encodes for a basic protein of the sperm head cytoskeleton.

2.6. Quantification of mtDNA Damage and Copy Number Using the Absolute ss-qPCR Method. The amount of relaxed/damaged mtDNA and total copy number were measured by quantifying the original and preheated DNA templates, respectively. The nuclear DNA marker calicin was quantified using the original templates. The qPCR was performed using the Applied Biosystems7500 Fast Real-Time PCR System (ABI) with Power SYBR Fast Green PCR MASTER MIX (ABI) [35]. The original DNA templates and preheated DNA templates and standards were analyzed in triplicates on the same plate. The two-step PCR amplification program for both nuclear DNA and mtDNA was 95.0°C for 30 sec, followed by 40 cycles of 95.0°C for 3 sec and 60.0°C for 30 sec. A melt curve analysis was enabled at the end of amplification. The primer sequences are listed in Table 1. The absolute copy numbers of CO2, D-loop, and calicin were calculated based on the standard curves. Since calicin is a single copy nuclear gene, the cell number could be calculated with the following equation with the assumption that the nuclear equivalent is representative of the cell number (Figure 1):

$$\text{Cell number or nuclear equivalent} = \frac{\text{Calicin copy number}}{\text{ploidy of cell}}. \quad (2)$$

The exact copies of damaged and total mtDNA per cell were calculated from:

$$\frac{\text{mtDNAcopies}}{\text{cell}} = \frac{\text{CO2 or D-Loop copy number}}{\text{cell number}^*}, \quad (3)$$

*cell number and nuclear equivalent will be used interchangeably from this point.

2.7. Data Analysis. All statistical analyses were performed with the aid of Graphpad Prism version 4 software. Unless specified otherwise, the data was analyzed with one-way ANOVA with Dunnett post test, and a $P < 0.05$ is considered significant.

3. Results

3.1. A New Strategy for the Absolute Quantification of Total and Damaged mtDNA. We have devised a new approach for the absolute quantification of mtDNA structural damage and total copy number in a single analysis. The protocol, illustrated in Figure 1, was comprised of four main steps.

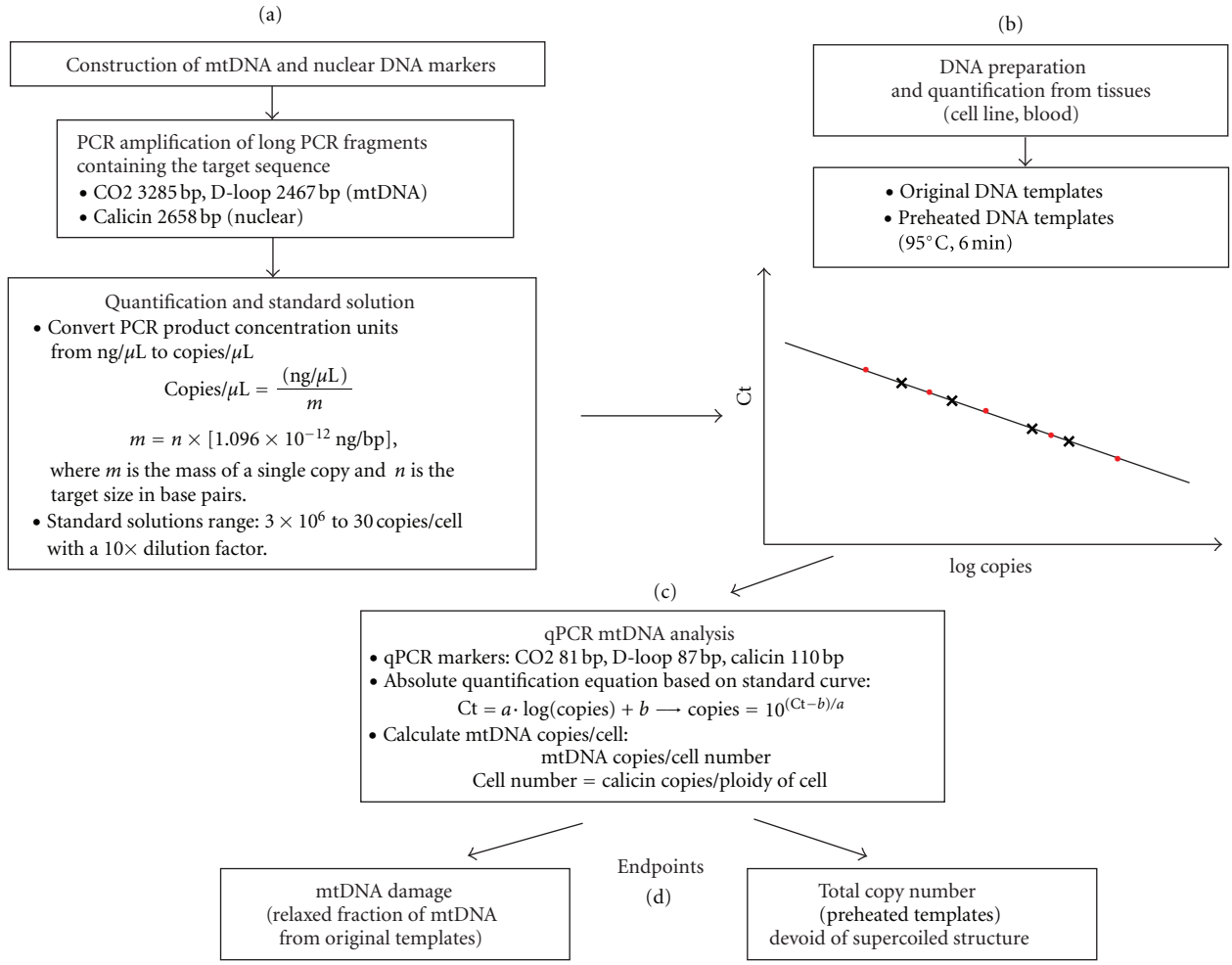

Figure 1: A new strategy for absolute quantification of total and damaged mtDNA. This protocol is separated into four main steps. (a) Construction of the mtDNA and nuclear DNA standards. Long fragments of genes that contained the shorter real-time PCR targets were amplified and a 10X serial dilution was made from 3×10^6 to 30 copies. (b) Preparation of the original and preheated DNA templates from lymphocytes DNA samples for the analysis of mtDNA damage and total mtDNA, respectively. (c) Real-time PCR absolute quantification analysis of mtDNA damage and total content. (d) Interpretation of the data.

The first step consisted in the construction of mtDNA and nuclear DNA standards (Figure 1(a)). Two to three kb DNA fragments containing mtDNA (CO2 or D-loop) and nuclear DNA (calicin) were amplified by PCR from a normal prostate cell line, RWPE-1. The concentration (copies/μL) of these long DNA fragments were quantified and calculated according to (1). The second step was to prepare the DNA templates for qPCR analysis (Figure 1(b)). Each DNA template was split into two equal halves. One half was used for the quantification of relaxed mtDNA and calicin nuclear DNA copies. The other half was pretreated at 95°C for 6 min to unfold any structure and was used for quantifying total mtDNA. The third step consisted in the absolute quantification using qPCR (Figure 1(c)). To obtain mtDNA content per cell, the exact amount of mtDNA and nuclear DNA copies were quantified and calculated from the standard curves according to the equation: copies = "$10^{(Ct-b)/a}$," where the cell number was derived from (2). The final step was the interpretation of the data (Figure 1(d)). With this approach, the amount of damaged mtDNA copies/cell, total mtDNA copies/cell, and baseline mtDNA damage (ratio of damaged mtDNA/total mtDNA) were quantified simultaneously.

3.2. Dynamic Range, Linearity, Specificity, and Reproducibility of DNA Markers. The standard curve and the melting curve for CO2, D-loop, and calicin amplification were evaluated (Figure 2). Each data point was run in triplicates. The threshold cycles (Ct) of CO2, D-loop, and calicin amplification were based on 10X serially diluted standards ranging from 3×10^7 to 30 copies and were shown in Figures 2(a), 2(c), and 2(e). The PCR amplification efficiencies were 95.8%, 95.7%, and 95.4% for CO2, D-loop, and calicin, respectively. Linearity of the standard curve amplification was maintained in the dynamic range of 10 to 10^7 since the R-values of linear regression lines were 0.9998 for CO2, 0.9988 for D-loop, and

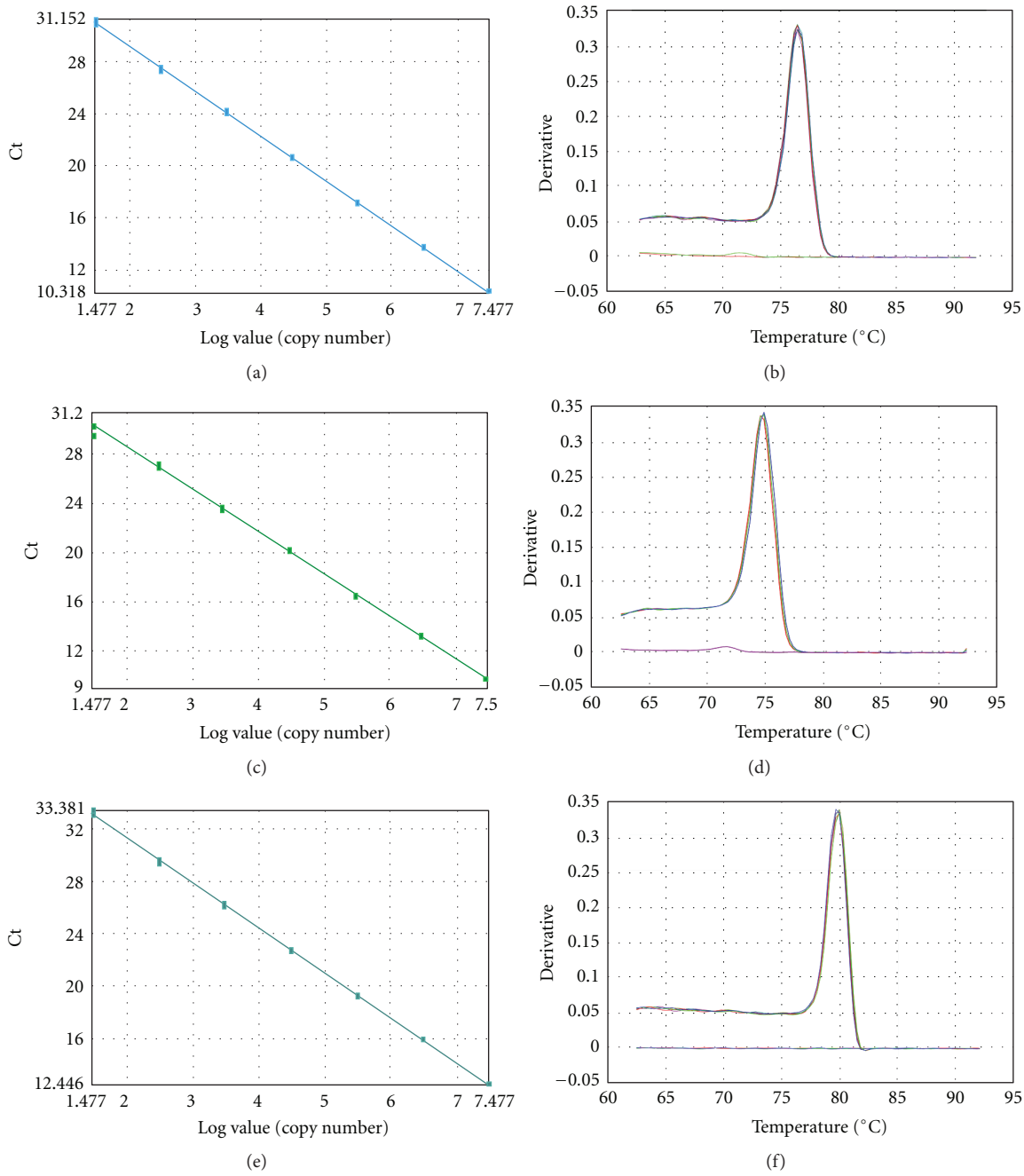

FIGURE 2: Dynamic range, linearity, specificity, and reproducibility. QPCR amplification of 7-point standard curves from 3×10^7 to 30 copies of (a) CO2, (c) D-loop, and (e) calicin markers. Melting curves showing the negative first derivative of the fluorescence signal of (b) CO2, (d) D-loop, and (f) calicin PCR product.

0.9996 for calicin. A single uniform melting peak at 76°C, 75°C, and 79°C was observed for CO2, D-loop, and calicin, respectively, demonstrating the high specificity of the primers (Figures 2(b), 2(d), and 2(f)). The intra-assay reproducibility of the standard was analyzed by calculating the coefficient of variation (CV) of the triplicates. The intra-assay median CV were 0.27%, 0.17%, and 0.12% for CO2, D-loop, and calicin, respectively (Table 2). The interassay CV was calculated with data from two or more independent experiments: the CV were 0.33%, 0.10%, and 0.62% for CO2, D-loop, and calicin, respectively (Table 2). These low CV values demonstrated very high intra- and interassay reproducibility of these new DNA markers.

3.3. Total Absolute Quantification of mtDNA Content and Baseline mtDNA Damage in Lymphocytes and Prostate Cancer Cells. Lymphocyte samples and two isogenic prostate cancer

Table 2: Intra- and interassay CV for standards.

Standards	Intra-assay CV (%)	Interassay CV (%)
CO2	0.27 (0.10–0.72)	0.33 (0.11–0.80)
D-loop	0.18 (0.03–0.16)	0.10 (0.05–0.78)
calicin	0.12 (0.02–0. 67)	0.62 (0.09–1.74)

Median CV value with CV range.

Table 3: Intra- and interassay CV for samples.

Sample type	Intra-assay CV (%)	Interassay CV (%)
Prostate cell lines*	0.74 (0.26–1.86)	1.20 (0.68–1.85)
Lymphocytes	1.87 (1.18–2.51)	2.33 (1.45–4.66)

Median CV value with CV range
*RWPE-1, C4-2, LNCaP, PC-3.

cell lines, LNCaP and C4-2, were analyzed for mtDNA content and baseline damage. The prostate cancer cell lines served a reference in method development because the ss-qPCR method was previously developed with these cell lines [6, 31, 35]. In lymphocytes, the total mtDNA content was quantified at an average of 153.25 ± 21.02 copies/cell from 4 individual samples, among which the amount of damaged mtDNA molecules was averaged at 41.44 ± 7.87 copies/cell (Figure 3(a)). In comparison, significantly higher mtDNA contents were detected in prostate cancer cells C4-2 (1495.35 ± 12.45, $P < 0.01$) and LNCaP (3086.61 ± 48.27, $P < 0.01$). The damaged mtDNA copies were 466.44 ± 8.64 and 990.41 ± 6.77 copies/cell, respectively. The baseline damage was calculated with the ratio of damaged mtDNA over total mtDNA: 27.04% of the total mtDNA content was damaged for lymphocytes versus 31.19% and 32.09% for C4-2 and LNCaP, respectively (Figure 3(b)). This assay was highly reproducible; the median intra- and interassay CV were 0.74% and 1.20% for cell lines and 1.87% and 2.33% for lymphocytes, respectively (Table 3). Furthermore, the use of different mtDNA markers, CO2 and D-loop, generated near identical results in terms of total mtDNA content, damaged mtDNA, and baseline damage detected (Figure 3(c)). Indeed, the average CV value obtained between CO2 and D-loop markers was calculated at 0.51%. Thus, these two mtDNA markers were highly consistent and interchangeable in quantitative mtDNA analyses. It was interesting to note that the absolute number of damaged mtDNA molecules was proportionally higher in samples with increased total copy numbers (Figure 3(a)). As such, the ratio between damaged and total copy numbers was a better indicator of the baseline level of DNA damage in a cell (Figure 3(b)). Taken together, the new quantification platform developed in this study provided a highly reproducible method for simultaneous analysis of absolute mtDNA copy number, damaged molecules, and baseline damage in both isolated lymphocytes and cancer cell lines.

3.4. Ex Vivo mtDNA Damage Responses to Exogenous H_2O_2 in Isolated Lymphocytes and in Whole Blood. Isolated lymphocytes from 9 healthy men were treated with 0 or 120 μM H_2O_2 for 15 min to evaluate induced mtDNA damage and repair activity after 60 min of recovery. The average mtDNA copy number of the untreated control samples was 161.78 ± 31.67 copies/cell (Figure 4(a)). The total mtDNA copy number was not affected by H_2O_2 treatment and remained stable across all treatment groups (Figure 4(a)). However, rapid mtDNA damage response was observed. The average baseline damage of untreated control samples was 27.63% (Figure 4(b)). Upon H_2O_2 exposure, the fraction of damaged mtDNA increased to 58.19% in lymphocytes, representing a 110.6% increase in induced damage from the control ($P < 0.001$). Interestingly, the induced damage was not repaired after 60 min of recovery, suggesting a lack of repair activity during the recovery period.

As an alternative to the isolated lymphocytes, a small amount of whole blood samples (<1 mL each) from four healthy subjects was tested using the same procedure. The average total mtDNA content of untreated control was 109.4± 22.40 copies/cell (Figure 5(a)). Similar to lymphocytes, the average baseline mtDNA damage of the untreated control samples was 26.6% (Figure 5(b)). When treated with 120 μM H_2O_2, the damaged fraction of mtDNA increased to 36.7%, representing a 38.0% increase in induced damage as compared to the baseline levels ($P < 0.05$), while the total mtDNA content remained the same (Figure 5(b)). An absence of repair activity was also observed within 60 min recovery after the H_2O_2 treatment. However, the whole blood samples had slightly lower mtDNA content and less pronounced mtDNA damage responses as compared to the lymphocytes. This could be caused by the complexity of different types of white blood cells present in whole blood samples. Despite this difference, the overall stress response pattern was similar between the isolated lymphocytes and the whole blood. Thus, the latter may serve as a convenient alternative to isolated lymphocytes in the analysis of mtDNA stress responses in circulating blood.

4. Discussion

Based on our previously developed ss-qPCR method [6, 31, 35], we propose a quantitative approach for precise and rapid detection of mtDNA structural damage and copy number change in isolated lymphocytes in a single analysis. We have demonstrated that the new approach had a wide dynamic range and was highly specific and reproducible. A relatively low mtDNA content and baseline level of damage were observed in lymphocytes of healthy men, and the lymphocytes were shown for the first time to exhibit a significant increase in mtDNA damage, followed by little repair activity after 1 h of recovery in an *ex vivo* challenge experiment with H_2O_2. This lack of repair activity to H_2O_2-induced damage after 1 h of recovery is consistent with a study from Collins et al. in which nuclear DNA repair activity was only observed after several hours (>2 h) [34]. Moreover, we showed that 1 mL of whole blood may serve as a convenient alternative

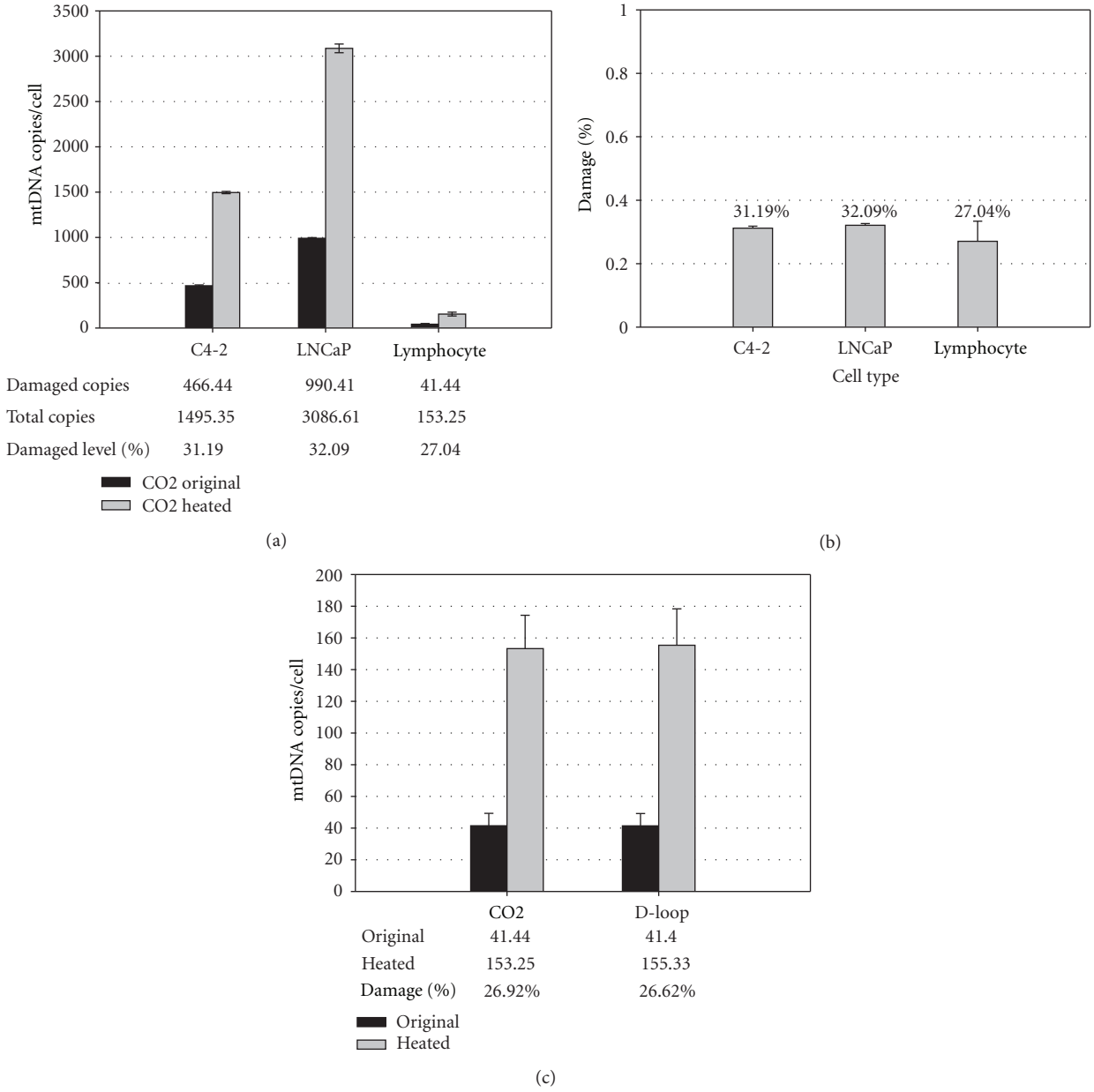

Figure 3: Absolute quantification of total mtDNA and baseline mtDNA damage in lymphocytes and prostate cancer cells. C4-2 (n = 2), LNCaP (n = 2), and lymphocytes (n = 4) were analyzed by ss-qPCR for total mtDNA content, damaged mtDNA number, and level of baseline damage. The cell number was calculated from the copy numbers of calicin, a single copy nuclear marker. (a) With mtDNA CO2 marker, the original (CO2 original) and preheated (CO2-heated) DNA templates were quantified for damaged copies and total mtDNA copies, respectively. (b) The baseline damage level was obtained by dividing damaged copies over total copies. (c) Comparison of CO2 versus D-loop markers in lymphocyte samples (n = 4).

to the isolated lymphocytes in the mtDNA analysis. Thus, mtDNA in blood may be explored as a sensitive surrogate to systemic oxidative stress by simultaneous analysis of multiple end-points in a single test.

The absolute quantification system developed in this study provides a standard method for the reliable quantification of the precise mtDNA copy number in lymphocytes and whole blood cells. This is achieved through well-defined mtDNA and single-copy nuclear DNA markers and by taking into account the DNA structural effects on qPCR amplification [31]. The relatively low mtDNA copy number revealed in isolated lymphocytes is consistent with very limited data reported in the literature. For example, one study detected ~87 to 579 copies/cell with a different real-time PCR method [36] and the other ~70 to 320 copies/cell with competitive PCR in lymphocytes [37]. Many studies report mtDNA content on a relative scale [19, 38–41]. However, the relative analysis is limited by the difficulty of comparing results from one

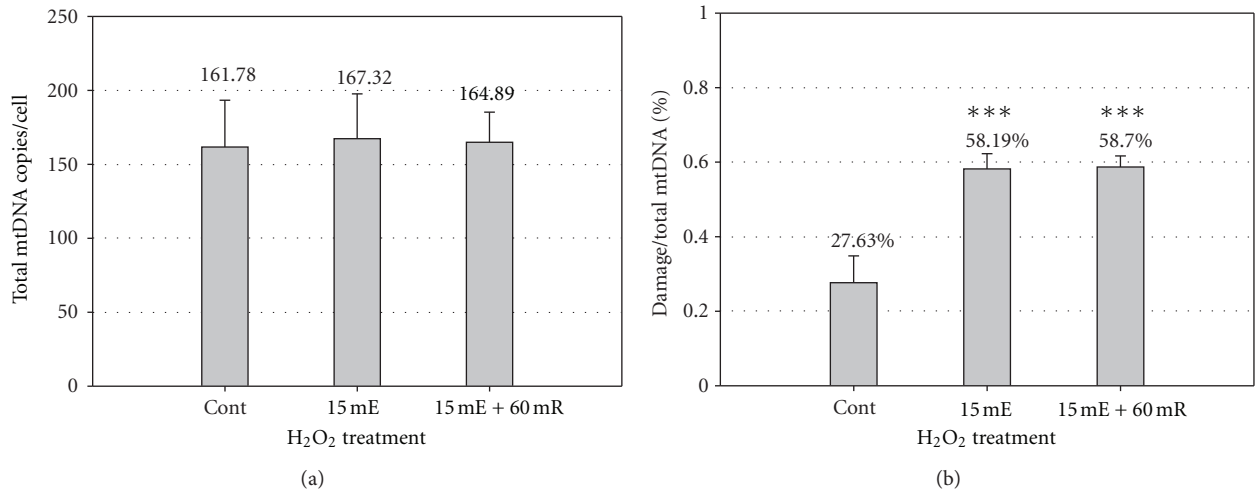

Figure 4: *Ex vivo* mtDNA damage response to exogenous H_2O_2 in isolated lymphocytes and whole blood. Experiments were performed to detect the baseline damage level, induced damage by H_2O_2 treatment, and repair capacity of white blood cells from healthy volunteers. Lymphocytes were isolated from fresh blood of three volunteers and stored at −80°C. The lymphocytes were split into three groups: untreated control ($n = 9$), 15 min of exposure to 120 μM H_2O_2 ($n = 9$), and 15 min of exposure + 60 min recovery ($n = 6$). (a) Total mtDNA content of lymphocytes. (b) MtDNA damage response of lymphocyte samples. ($^{***}P < 0.001$).

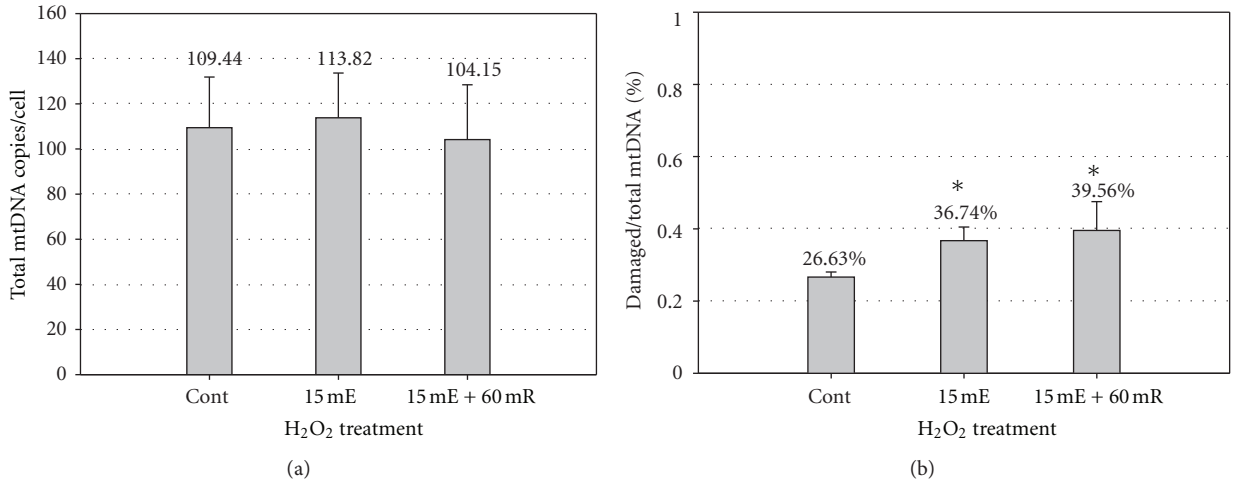

Figure 5: *Ex vivo* mtDNA damage response to exogenous H_2O_2 whole blood. Blood from six healthy male volunteers were collected and stored at −80°C. Blood cells from the whole blood samples were separated into three groups in the same manner as lymphocyte samples in Figure 4. (a) Total mtDNA content of whole blood. (b) MtDNA damage response of whole blood. ($^{*}P < 0.05$).

study to another and by the significant variations observed in mtDNA content between individuals [42]. To account for the inhibitory effect of the supercoiled DNA structure on qPCR amplification, we have taken steps to ensure an accurate measurement by disrupting the supercoiled mtDNA conformation with a preheating step prior to qPCR analysis. This step is necessary for precise quantification of mtDNA content but has largely been ignored in previous reports. Depending on the manufacturers of the qPCR machinery and chemistry kits, there are wide variations in the duration of the initial hot-activation step for hot-start DNA polymerases, which varies from 10 min to as short as 20 sec (e.g., ABI 7500 Fast System). We have shown that shorter denaturation time at 95°C was insufficient to disrupt all the supercoiled mtDNA conformation in a time- and dose-dependent experiment in prostate cancer cell lines [31]. Therefore, the inclusion of a preheating step in the template preparation is crucial for the accurate mtDNA measurement. In addition to measuring the total mtDNA content, our new system also provides a novel approach for direct quantification of the absolute copies of damaged mtDNA with qPCR. This is in contrast to mtDNA conformational study based on gel electrophoresis coupled with Southern Blot, which requires tedious post-PCR manipulations and is semiquantitative in nature. On the other hand, popular assays such as the comet test for detecting nuclear DNA strand breaks are not applicable to mtDNA due to its small size [34]. The quantification of structural mtDNA damage reported in this study mainly

reflects the damage caused by single- and double-stranded breaks, as it was shown that other type of DNA damage such as base lesions or abasic sites had little, if any, effect on the structure [31]. It is interesting to note that the amount of damaged mtDNA changes with the total mtDNA content in a cell. The direct comparison of the damaged mtDNA molecules from different individuals can be compounded by variations in the total content. To normalize this variation, we propose to calculate mtDNA damage based on the percentage of damaged versus total mtDNA molecules in a cell; this ratio of damage is relatively stable and more informative for comparative studies [43]. Moreover, the ratio of damage can be used to infer the baseline or endogenous damage in the isolated lymphocytes or whole blood from the untreated samples; it also quantifies induced mtDNA damage in isolated lymphocytes or a small amount of whole blood cells under oxidative stress. The ability of our approach to measure both endogenous and induced damage/repair responses in *ex vivo* treatments may be used to explore the state of oxidative defence and/or repair capability of individuals with different disease conditions. Indeed, previous studies have suggested that there is an association between systemic oxidative stress and diseases, such as an association of the high prostate cancer risk with severe damage response and poor repair capacity of nuclear DNA in lymphocytes [14].

In conclusion, we have developed an absolute quantification system for rapid measurement of mtDNA structural damage, copy number change, and damage response in isolated lymphocytes and whole blood cells. Systemic oxidative stress is associated with diverse pathological conditions, ranging from neurodegenerative diseases to many types of cancers. It is conceivable that the blood analysis with the multiple mtDNA end-points proposed in the this study may provide a simple and sensitive test to interrogate the nature and extent of systemic oxidative stress for a broad spectrum of clinical investigations, especially when coupled with other established tests such as cell-free circulating mtDNA, the comet assays targeting the nuclear DNA, and the detection of 8-oxo-G base lesions.

Abbreviations

mtDNA: Mitochondrial DNA
qPCR: Quantitative real-time polymerase chain reaction
8-oxo-G: 8-oxoguanine
ss-qPCR: Supercoiling-sensitive real-time PCR
SSB: Single-strand breaks
DSB: Double-strand breaks.

Conflict of Interests

The authors do not have any conflict of interests with the content of the paper.

Acknowledgments

The authors would like to thank Ms. Y. Han for her comments on an early version of this paper. This work was supported by a Canada Foundation for Innovation Grant (no. 11623) and the McGill Urology Research Funds to J. Z. Chen.

References

[1] D. C. Wallace, "A mitochondrial paradigm of metabolic and degenerative diseases, aging, and cancer: a dawn for evolutionary medicine," *Annual Review of Genetics*, vol. 39, pp. 359–407, 2005.

[2] J. Chen and F. Kadlubar, "Mitochondrial mutagenesis and oxidative stress in human prostate cancer," *Journal of Environmental Science and Health*, vol. 22, no. 1, pp. 1–12, 2004.

[3] C. Richter, "Oxidative damage to mitochondrial DNA and its relationship to ageing," *International Journal of Biochemistry and Cell Biology*, vol. 27, no. 7, pp. 647–653, 1995.

[4] S. Toyokuni, "Persistent oxidative stress in cancer," *FEBS Letters*, vol. 358, no. 1, pp. 1–3, 1995.

[5] J. Z. Chen, N. Gokden, G. F. Greene, B. Green, and F. F. Kadlubar, "Simultaneous generation of multiple mitochondrial DNA mutations in human prostate tumors suggests mitochondrial hyper-mutagenesis," *Carcinogenesis*, vol. 24, no. 9, pp. 1481–1487, 2003.

[6] S. W. Chan, P. N. Nguyen, D. Ayele, S. Chevalier, A. Aprikian, J. Z. Chen et al., "Mitochondrial DNA damage is sensitive to exogenous H_2O_2 but independent of cellular ROS production in prostate cancer cells," *Mutation Research*, vol. 716, no. 1-2, pp. 40–50, 2011.

[7] H. R. Griffiths, "ROS as signalling molecules in T cells$_2$evidence for abnormal redox signalling in the autoimmune disease, rheumatoid arthritis," *Redox Report*, vol. 10, no. 6, pp. 273–280, 2005.

[8] P. J. Barnes, S. D. Shapiro, and R. A. Pauwels, "Chronic obstructive pulmonary disease: molecular and cellular mechanisms," *European Respiratory Journal*, vol. 22, no. 4, pp. 672–688, 2003.

[9] G. E. Gibson and H. M. Huang, "Oxidative stress in Alzheimer's disease," *Neurobiology of Aging*, vol. 26, no. 5, pp. 575–578, 2005.

[10] M. M. Elahi and B. M. Matata, "Functional adaptation to oxidative stress by memory T cells: an analysis of the role in the cardiovascular disease process," *Biochemical and Biophysical Research Communications*, vol. 376, no. 3, pp. 445–447, 2008.

[11] C. L. Allen and U. Bayraktutan, "Oxidative stress and its role in the pathogenesis of ischaemic stroke," *International Journal of Stroke*, vol. 4, no. 6, pp. 461–470, 2009.

[12] A. De Vizcaya-Ruiz, O. Barbier, R. Ruiz-Ramos, and M. E. Cebrian, "Biomarkers of oxidative stress and damage in human populations exposed to arsenic," *Mutation Research*, vol. 674, no. 1-2, pp. 85–92, 2009.

[13] L. Lavie, L. Dyugovskaya, and A. Polyakov, "Biology of peripheral blood cells in obstructive sleep apnea—he tip of the iceberg," *Archives of Physiology and Biochemistry*, vol. 114, no. 4, pp. 244–254, 2008.

[14] K. L. Lockett, M. C. Hall, P. E. Clark et al., "DNA damage levels in prostate cancer cases and controls," *Carcinogenesis*, vol. 27, no. 6, pp. 1187–1193, 2006.

[15] D. J. Waters, S. Shen, H. Xu et al., "Noninvasive prediction of prostatic DNA damage by oxidative stress challenge of peripheral blood lymphocytes," *Cancer Epidemiology Biomarkers and Prevention*, vol. 16, no. 9, pp. 1906–1910, 2007.

[16] O. Yossepowitch, I. Pinchuk, U. Gur, A. Neumann, D. Lichtenberg, and J. Baniel, "Advanced but not localized prostate cancer

is associated with increased oxidative stress," *Journal of Urology*, vol. 178, no. 4, part 1, pp. 1238–1244, 2007.

[17] Q. Wei, L. Cheng, W. K. Hong, and M. R. Spitz, "Reduced DNA repair capacity in lung cancer patients," *Cancer Research*, vol. 56, no. 18, pp. 4103–4107, 1996.

[18] D. T. Saha, B. J. Davidson, A. Wang, A. J. Pollock, R. A. Orden, and R. Goldman, "Quantification of DNA repair capacity in whole blood of patients with head and neck cancer and healthy donors by comet assay," *Mutation Research*, vol. 650, no. 1, pp. 55–62, 2008.

[19] J. Xing, M. Chen, C. G. Wood et al., "Mitochondrial DNA content: its genetic heritability and association with renal cell carcinoma," *Journal of the National Cancer Institute*, vol. 100, no. 15, pp. 1104–1112, 2008.

[20] M. Y. Wu, C. S. Kuo, C. Y. Lin, C. L. Lu, and R. F. Syu Huang, "Lymphocytic mitochondrial DNA deletions, biochemical folate status and hepatocellular carcinoma susceptibility in a case-control study," *British Journal of Nutrition*, vol. 102, no. 5, pp. 715–721, 2009.

[21] C. Richter, J. W. Park, and B. N. Ames, "Normal oxidative damage to mitochondrial and nuclear DNA is extensive," *Proceedings of the National Academy of Sciences of the United States of America*, vol. 85, no. 17, pp. 6465–6467, 1988.

[22] P. Mecocci, U. MacGarvey, A. E. Kaufman et al., "Oxidative damage to mitochondrial DNA shows marked age-dependent increases in human brain," *Annals of Neurology*, vol. 34, no. 4, pp. 609–616, 1993.

[23] M. Hayakawa, T. Ogawa, S. Sugiyama, M. Tanaka, and T. Ozawa, "Massive conversion of guanosine to 8-hydroxyguanosine in mouse liver mitochondrial DNA by administration of azidothymidine," *Biochemical and Biophysical Research Communications*, vol. 176, no. 1, pp. 87–93, 1991.

[24] G. Colonna-Romano, A. Cossarizza, A. Aquino et al., "Age- and gender-related values of lymphocyte subsets in subjects from Northern and Southern Italy," *Archives of Gerontology and Geriatrics*, vol. 35, no. 8, pp. 99–107, 2002.

[25] N. Mehra, M. Penning, J. Maas, N. Van Daal, R. H. Giles, and E. E. Voest, "Circulating mitochondrial nucleic acids have prognostic value for survival in patients with advanced prostate cancer," *Clinical Cancer Research*, vol. 13, no. 2, part 1, pp. 421–426, 2007.

[26] J. Ellinger, S. C. Müller, N. Wernert, A. Von Ruecker, and P. J. Bastian, "Mitochondrial DNA in serum of patients with prostate cancer: a predictor of biochemical recurrence after prostatectomy," *BJU International*, vol. 102, no. 5, pp. 628–632, 2008.

[27] J. Ellinger, P. Albers, S. C. Müller, A. Von Ruecker, and P. J. Bastian, "Circulating mitochondrial DNA in the serum of patients with testicular germ cell cancer as a novel noninvasive diagnostic biomarker," *British Journal of Urology International*, vol. 104, no. 1, pp. 48–52, 2009.

[28] C. S. Liu, C. S. Tsai, C. L. Kuo et al., "Oxidative stress-related alteration of the copy number of mitochondrial DNA in human leukocytes," *Free Radical Research*, vol. 37, no. 12, pp. 1307–1317, 2003.

[29] C. S. Liu, C. L. Kuo, W. L. Cheng, C. S. Huang, C. F. Lee, and Y. H. Wei, "Alteration of the copy number of mitochondrial DNA in leukocytes of patients with hyperlipidemia," *Annals of the New York Academy of Sciences*, vol. 1042, pp. 70–75, 2005.

[30] C. M. Chen, Y.-R. Wu, M.-L. Cheng et al., "Increased oxidative damage and mitochondrial abnormalities in the peripheral blood of Huntington's disease patients," *Biochemical and Biophysical Research Communications*, vol. 359, no. 2, pp. 335–340, 2007.

[31] J. Chen, F. F. Kadlubar, and J. Z. Chen, "DNA supercoiling suppresses real-time PCR: a new approach to the quantification of mitochondrial DNA damage and repair," *Nucleic Acids Research*, vol. 35, no. 4, pp. 1377–1388, 2007.

[32] H. C. Wu, J. T. Hsieh, M. E. Gleave, N. M. Brown, S. Pathak, and L. W. K. Chung, "Derivation of androgen-independent human LNCaP prostatic cancer cell sublines: role of bone stromal cells," *International Journal of Cancer*, vol. 57, no. 3, pp. 406–412, 1994.

[33] L. Cheng, L. E. Wang, M. R. Spitz, and Q. Wei, "Cryopreserving whole blood for functional assays using viable lymphocytes in molecular epidemiology studies," *Cancer Letters*, vol. 166, no. 2, pp. 155–163, 2001.

[34] A. R. Collins, A. A. Oscoz, G. Brunborg et al., "The comet assay: topical issues," *Mutagenesis*, vol. 23, no. 3, pp. 143–151, 2008.

[35] S. W. Chan and J. Z. Chen, "Measuring mtDNA damage using a supercoiling-sensitive qPCR approach," *Methods in Molecular Biology*, vol. 554, pp. 183–197, 2009.

[36] M. E. Gahan, F. Miller, S. R. Lewin et al., "Quantification of mitochondrial DNA in peripheral blood mononuclear cells and subcutaneous fat using real-time polymerase chain reaction," *Journal of Clinical Virology*, vol. 22, no. 3, pp. 241–247, 2001.

[37] A. Cossarizza, M. Pinti, L. Moretti et al., "Mitochondrial functionality and mitochondrial DNA content in lymphocytes of vertically infected human immunodeficiency virus-positive children with highly active antiretroviral therapy-related lipodystrophy," *Journal of Infectious Diseases*, vol. 185, no. 3, pp. 299–305, 2002.

[38] J. Shen, M. Platek, A. Mahasneh, C. B. Ambrosone, and H. Zhao, "Mitochondrial copy number and risk of breast cancer: a pilot study," *Mitochondrion*, vol. 10, no. 1, pp. 62–68, 2010.

[39] G. M. Aldrovandi, C. Chu, W. T. Shearer et al., "Antiretroviral exposure and lymphocyte mtDNA content among uninfected infants of HIV-1-infected women," *Pediatrics*, vol. 124, no. 6, pp. e1189–e1197, 2009.

[40] S. W. Weng, T.-K. Linb, C.-W. Liou et al., "Peripheral blood mitochondrial DNA content and dysregulation of glucose metabolism," *Diabetes Research and Clinical Practice*, vol. 83, no. 1, pp. 94–99, 2009.

[41] A. D. D'Souza, N. Parikh, S. M. Kaech, and G. S. Shadel, "Convergence of multiple signaling pathways is required to coordinately up-regulate mtDNA and mitochondrial biogenesis during T cell activation," *Mitochondrion*, vol. 7, no. 6, pp. 374–385, 2007.

[42] C. T. Moraes, "What regulates mitochondrial DNA copy number in animal cells?" *Trends in Genetics*, vol. 17, no. 4, pp. 199–205, 2001.

[43] S. Maynard, N. C. de Souza-Pinto, M. Scheibye-Knudsen, and V. A. Bohr, "Mitochondrial base excision repair assays," *Methods*, vol. 51, no. 4, pp. 416–425, 2010.

Hindawi Publishing Corporation
BioMed Research International
Volume 2013, Article ID 239257, 10 pages
http://dx.doi.org/10.1155/2013/239257

Research Article

An Inherited Heteroplasmic Mutation in Mitochondrial Gene COI in a Patient with Prostate Cancer Alters Reactive Oxygen, Reactive Nitrogen and Proliferation

Rebecca S. Arnold,[1,2] Qian Sun,[1] Carrie Q. Sun,[1] Jendai C. Richards,[1] Sean O'Hearn,[3] Adeboye O. Osunkoya,[1,2,4,5] Douglas C. Wallace,[3,6,7] and John A. Petros[1,2,4,5]

[1] *Department of Urology, School of Medicine, Emory University, 1365 Clifton Rd. Building B, Atlanta, GA 30322, USA*
[2] *Winship Cancer Institute, Emory University, Atlanta, GA 30322, USA*
[3] *Center for Molecular and Mitochondrial Medicine and Genetics (MAMMAG), University of California Irvine, Irvine, CA 92697, USA*
[4] *Department of Pathology and Laboratory Medicine, Emory University, Atlanta, GA 30322, USA*
[5] *Department of Urology, The Atlanta VA Medical Center, Decatur, GA 30033, USA*
[6] *Center for Mitochondrial and Epigenomic Medicine, Children's Hospital of Philadelphia and Department of Pathology and Laboratory Medicine, University of Pennsylvania, Philadelphia, PA 19104, USA*
[7] *Department of Pathology, University of Pennsylvania, Philadelphia, PA 19104, USA*

Correspondence should be addressed to John A. Petros; jpetros@emory.edu

Received 6 June 2012; Revised 8 August 2012; Accepted 9 August 2012

Academic Editor: Gurmit Singh

Mitochondrial DNA (mtDNA) mutations have been found in many cancers but the physiological derangements caused by such mutations have remained elusive. Prostate cancer is associated with both inherited and somatic mutations in the cytochrome c oxidase (COI) gene. We present a prostate cancer patient-derived rare heteroplasmic mutation of this gene, part of mitochondrial respiratory complex IV. Functional studies indicate that this mutation leads to the simultaneous decrease in cytochrome oxidation, increase in reactive oxygen, and increased reactive nitrogen. These data suggest that mitochondrial DNA mutations resulting in increased reactive oxygen and reactive nitrogen generation may be involved in prostate cancer biology.

1. Introduction

The mitochondrion contains the only functional DNA outside the eukaryotic cell nucleus and mutations in this genome have been linked to a vast array of human disease including pediatric neurologic disease, degenerative muscular disease, and blindness in the pediatric population and more recently to chronic diseases of adults including diabetes, Alzheimer's dementia, Parkinson's disease, cardiovascular disease, and cancer [1]. Because of the critical role the mitochondria play in normal human cell physiology, severe mutations that cause dramatic derangements of mitochondrial function can be fatal [2]. Indeed, recent evidence indicates that severe mutations are culled from the germ line through depletion of mutant germ cells in the ovary [3]. Severe mutations can exist and even be passed between generations if they exist in a state of heteroplasmy where some copies of the genome contain the mutation and some are wild type. For this reason, one indication that a mitochondrial DNA (mtDNA) mutation is potentially pathogenic is that it exists in a heteroplasmic state, though this is not strictly necessary in all cases.

Prostate cancer is one example of an adult disease tightly linked to ageing for which there is evidence linking both inherited and somatic mtDNA mutations to disease [4]. Mutations in the mitochondrial cytochrome c oxidase subunit I (COI) gene are found at disproportionately high rates in prostate cancer patients compared to either the general population or rigorously defined controls without prostate cancer [5]. A population-based case-control study of African Americans found 2 single nucleotide polymorphisms in this

gene significantly associated with prostate cancer ($P < 0.05$) and in strong linkage disequilibrium with each other ($r > 0.6$) [6]. MtDNA mutations are easily detected in early stage prostate cancer tissues and can also be found in the serum and urine from the same individuals [7]. MtDNA content has been linked to androgen responsiveness of prostate cancer cells *in vitro* [8] and analysis of clinical samples suggests that mtDNA content is higher in prostate cancer compared to adjacent normal prostatic tissue in the same individual [9]. A specific mtDNA deletion mutation may have utility in identifying adult cancer not apparent in clinical prostate biopsies [10].

While multiple independent investigators have confirmed mtDNA mutations in prostate cancer, there is little understanding of the cell biologic and biochemical consequences of specific prostate cancer-associated mtDNA mutations. We investigated the mtDNA from a patient with prostate cancer and found a heteroplasmic missense mutation in the mitochondrial COI gene that impairs the oxidation of cytochrome c (respiratory complex IV inhibition) and increases the generation of both reactive oxygen species (ROS) and reactive nitrogen species (RNS).

2. Materials and Methods

2.1. Cytochrome c Oxidase Subunit I (COI) Gene Sequencing. The mtDNA region encompassing COI was amplified using a forward primer starting at nucleotide position (np) 5772 (5′ AGG TTT GAA GCT GCT TCT TC 3′) and a reverse primer ending at np 7600 (5′ CGC TGC ATG TGC CAT TAA GA 3′). The template was denatured at 95°C for 7 min and primers extended for 35 cycles of 94°C for 1 min, then 55°C for 1 min, and 72°C for 1 min. Both strands of the COI polymerase chain reaction (PCR) product were cycle-sequenced using the slip primers in the forward direction starting at np 6080 (5′ TCT ACA ACG TTA TCG TCA CA 3′) and at np 6930 (5′ TGC AGT GCT CTG AGC CCT AG 3′) and in the reverse direction starting at np 6340 (5′ CTA GGT GTA AGG AGA AGA TG 3′) and at np 7150 (5′ GAT TTA CGC CGA TGA ATA TG 3′). The templates were denatured at 96°C and primers extended in the presence of "Big Dye Terminators" for 25 cycles of 96°C for 10 sec, then 55°C for 5 sec, and 60°C for 4 min. The reactions were chilled to 4°C, and the excess dye terminators removed by Centri-Sep Columns. The trace files were determined using an Applied Biosystems (ABI) Prism 3100 genetic analyzer, analyzed using Sequencher gene analysis software v 4.1 (Gene Codes, Ann Arbor, MI), and interpreted within the context of MITOMAP (http://www.mitomap.org/). Full mtDNA sequencing was performed as described above using primer sets that span the full length of the mitochondrial DNA [11].

2.2. Laser Capture Microdissection (LCM). LCM was carried out by the Winship Cancer Institute Pathology Core using the Molecular Machines & Industries, Inc. Cell cut laser microdissector to isolate pure populations of prostatic epithelium (malignant and benign) and stromal cells. DNA was purified from LCM of frozen tissue using PicoPure DNA Extraction Kit (Arcturus, Mt View, CA) according to the recommended protocol.

2.3. Epstein-Barr Transformation. Lymphocytes were isolated from whole blood by centrifugation and diluted with phosphate buffered saline (PBS). Red cells were lysed by the addition of H_2O. After 20 s, osmolarity was restored with 10x concentrated PIPES (piperazine-*N*,*N*′-bis-[2-ethanosulfonic-acid]) buffer, centrifuged, and the pellet was resuspended in RPMI with fetal bovine serum (FBS) and incubated for 45 min in 5% CO_2 at 37°C. The nonadherent cells were washed and collected and lymphocytes pelleted. Lymphocytes were infected with the B95-8 strain of Epstein-Barr Virus (EBV) and cultured in RPMI-1640 medium supplemented with 10% heat-inactivated fetal bovine serum, 2 mM l-glutamine, 100 U/mL penicillin, and 100 mg/mL streptomycin, at 37°C in a humid atmosphere saturated with 5% CO_2 until cryopreservation or use [12].

2.4. Mitochondrial Preparation and Isolation. Mitochondria were isolated by cell fractionation and centrifugation. All procedures were carried out on ice. Cells were pelleted and washed in cold PBS and resuspended in 10 volumes of isolation buffer (250 mM sucrose, 10 mM HEPES, 1 mM EDTA, pH 7.35). Cell lysis was performed with 5 passes of a hand held Dounce homogenizer and centrifuged at 500 g (4°C) for 5 min. The supernatant was reserved and the pellet was resuspended in isolation buffer, rehomogenized, and centrifuged. This process was repeated a third time and supernatants combined and centrifuged 12,000 g at 4°C for 10 min to pellet mitochondria which were then washed in isolation buffer and repelleted three times. Following the final wash, mitochondria were resuspended in reaction buffer (1 mL/mL of original cell pellet), and frozen until assayed.

2.5. Cytochrome c Oxidase Activity. Cytochrome c oxidase activity of isolated mitochondrial preparations was measured by dual wavelength spectrophotometry (550/540 nm) as previously described [13]. Briefly, mitochondria were suspended in reaction buffer (250 mM Sucrose, 10 mM HEPES, 1 mM $MgCl_2$, pH 7.35). An aliquot of mitochondria suspension (~300 ug mitochondrial protein) was added to the cuvette containing reaction buffer plus ~5 uM reduced cytochrome c in a final volume of 700 uL. The oxidation of cytochrome c was recorded over time and the cytochrome c oxidase specific activity was calculated. Mitochondrial protein was determined by the Bradford method [14].

2.6. Cybrid Formation. Mitochondrial donors (patient lymphoblasts) were enucleated by short term incubation with Actinomycin D, which was subsequently removed from the culture medium by centrifugation and washing. These cytoplasts were then rescued by polyethylene glycol (PEG)-induced fusion with 143B rho zero cells. Fusions are monitored by phase contrast microscopy and isolated by ring cloning. Clones were expanded and genotyped to assure that the donor mtDNA had been incorporated (sequencing) and that a single nucleus was present (Karyotyping).

2.7. Flow Cytometric Assay for ROS and RNS. Peroxides Assay: Lymphoblasts were grown in suspension in flasks. When cells were in growth phase, 1×10^6 cells per sample were removed, pelleted, and resuspended in 2 μM CM-DCFDA (5-(and -6)-chloromethyl-2′,7′-dichlorodihydrofluorescein diacetate) (Life Technologies, Grand Island, NY). Cells were placed in a dark room at room temperature while gently rocking for 30 minutes (CM-DCFDA). Following this incubation, samples were kept on ice until counting on a Becton Dickinson FACScan flow cytometer. 10,000 cells were counted and analyzed by FlowJo 7.6.4 to compare mean values of DCF fluorescence intensity. All samples were repeated in triplicate. Some sample tubes also contained 10 M FCCP (Mesoxalonitrile 4-trifluoromethoxyphenylhydrazone) and were preincubated with the lymphoblasts prior to the addition of CM-DCFDA. Cybrid cell lines were also treated with CM-DCFDA. Briefly, adherent cells were grown to 70% confluency, washed with PBS, and cells were removed from the plate by the addition of trypsin-EDTA (Mediatech, Inc, Manassas, VA). Cells were pelleted at 400 g for 5 minutes at room temperature and the cells were resuspended in CM-DCFDA and assay continued as described above. Mitochondrial Superoxide Assay: Media (RPMI 1640 containing 10% fetal bovine serum) was replaced on cells in growth phase with media containing 5 μM MitoSOX (Life Technologies). Cells were incubated in the dark at 37°C, 5% CO_2 for 10 minutes. Following this incubation, cells were harvested by trypsin digestion, pelleted, and resuspended in HANKS Buffer containing 10% FBS. Samples were kept on ice until counting on a Becton Dickinson LSRII flow cytometer as described above. NO Assay: Media (RPMI 1640 containing 10% fetal bovine serum) was replaced on cells in growth phase with media containing 4 μM 4-amino-5-methylamino-2′,7′-difluorofluorescein diacetate (DAF-FM DA) (Life Technologies). Cells were incubated in the dark at 37°C, 5% CO_2 for 30 minutes, DAF-FM DA was removed and replaced with media and incubated in the dark at 37°C, 5% CO_2 for a additional 20 minutes. Following this incubation, cells were harvested by trypsin digestion, pelleted, and resuspended in HANKS Buffer containing 10% FBS. Samples were kept on ice until counting on a Becton Dickinson LSRII flow cytometer as described above. Time between dye loading and reading was 30 minutes and all samples were treated identically. The DAF experiment was done in the presence of serum.

2.8. Cell Proliferation Assay. Cell were plated in 6 well plates, 18,000 cells per well in triplicate for each time point and grown in RPMI 1640 (Mediatech) containing 15% Fetal Bovine Serum. Cells were harvested after 1, 2, 3, or 4 days and cell number was determined using FluoReporter Blue Fluorometric dsDNA Quantitation Kit (Life Technologies) according to manufacturer's protocol.

2.9. Reverse Transcription and PCR. In order to determine which isoform of Nitric Oxide Synthase (NOS) is present in our cybrid cell lines we performed RT-RCR on RNA from the cybrid cell lies and a positive control. cDNA was obtained from the RNA of 6124WT, 6124Mut, and BT474 (positive control) by reverse transcription using Advantage RT for PCR from Clontech (a Takara Bio Company, Mountain View, CA) according to protocol. The presence of NOS1, NOS2, and NOS3 were examined. Using the Amplitaq Gold Kit (Life Technologies), reactions were as follows: cDNA, 1XBuffer, 1.5 mM $MgCl_2$, 0.2 mM each dNTPs, 150 nM each forward and reverse primers for NOS1 (Forward 5′ CGA CAC CAC TAG CAC TTA CCA G 3′; Reverse 5′ CAG ACT CGG AAG TCG TGC TTG 3′), NOS2 (Forward 5′ TCG GCT GCA GAA TCC TTC ATG A 3′; Reverse 5′ CAT TGT CTT GCG CAT CAG CAT AC 3′) or NOS3 (Forward 5′ GAA GCA CCT GGA GAA TGA GCA G 3′; Reverse 5′ CTT CAC TCG CTT CGC CAT CAC 3′) and 5 units of Taq for a final volume of 100 uL. Primers were designed to cross two introns and amplify all major isoforms of NOS1. The PCR reaction included an initial cycle of 95°C for 10 min followed by 40 cycles of 95°C for 30 sec and 61°C for 30 sec, 72°C for 1 min. A 3% agarose gel was run after PCR. The presence of NOS1, NOS2, and NOS3 were indicated by the presence of a 261 nt band, 288 nt or a 274 nt band, respectively.

2.10. Western Blot Analysis. Whole-cell extracts were obtained by lysing cells with lysis buffer containing 50 mmol/L, Tris Base, 5 mmol/L EGTA, 150 mmol/L NaCl, and 1% Triton X-100 (pH 7.4). One tablet of protease inhibitor (Roche Applied Science, Indianapolis, IN) was dissolved in 7 mL of lysis buffer. Total protein 30 μg/well was loaded in 4–12% gradient NuPAGE MES SDS gel (Life Technologies) and transferred into Immun-Blot PVDF Membrane (BIO-RAD, Hercules, CA). The membrane was immunoblotted with anti-PARP (Cell Signaling Technology, Danvers, MA) at 1 : 2000 dilution and anti-β-actin (Sigma, St. Louis, MO) at 1 : 2000 dilution. Immunodetection was completed by using the corresponding secondary horseradish peroxide- conjugated antibodies (Amersham, Piscataway, NJ). Horseradish peroxide activity was detected using enhanced chemiluminescence from ECL Western Blotting Analysis System (Amersham).

2.11. Mice. Male nu/nu mice, 6–8-weeks old, were purchased from Charles River Laboratories (Wilmington, MA) and housed in ventilated cages under sterile conditions. For surgical manipulation, mice were anesthetized with an intramuscular injection of a mixture of ketamine hydrochloride, Xylazine, and Acepromazine.

2.12. In Vivo Tumor Study. Mice were injected subcutaneously in the neck with 3 separate 6124WT clones for a total of 29 mice and 3 separate 6124Mut clones for a total of 30 mice. 2.5×10^5 cells, resuspended in PBS, were injected per mouse. Mice were checked daily for tumor growth. When tumors were visually observed they were measured twice a week and the tumor volumes calculated using the formula [length $\times$ $(\text{width})^2$]/2 [15]. Experiment was repeated 2 additional times. Mice were sacrificed when the tumors reached 10% of body weight. Tumor tissues were dissected for further study.

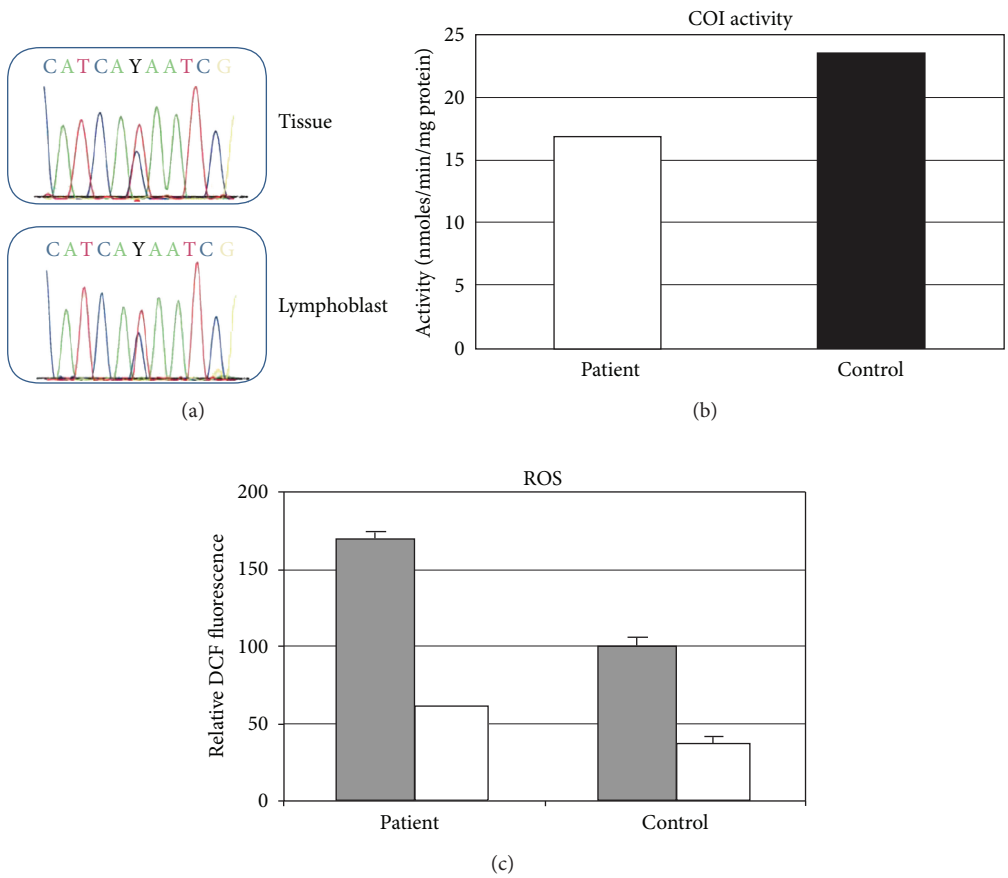

Figure 1: Detection of heteroplasmic point mutation of mitochondrial cytochrome oxidase subunit I (COI) mitochondrial gene from a single individual with prostate cancer. (a) Sequencing chromatograms of prostatic tissue and an Epstein-Barr transformed lymphoblast cell line show approximately equal levels of both the wild type (T) and mutant (C) DNA base. (b) Activity of cytochrome oxidase measured in isolated mitochondria prepared from the patient's heteroplasmic lymphoblasts (see Section 2 for details) compared to the average of two-lymphoblast lines from controls with only the wild type base at position 6124. (c) Flow cytometric analysis of DCF fluorescence in the patient's heteroplasmic lymphoblasts compared to the average of two-lymphoblast lines from controls with only the wild type base at position 6124 (gray bars). Cells were also analyzed for DCF fluorescence in the presence of FCCP (white bars). Error bars represent the standard deviation of 2–4 data points.

3. Results

3.1. Mutation Analysis. A 60-year old patient underwent radical prostatectomy after presenting to his primary care physician with an elevated-serum-prostate-specific antigen (PSA = 5.5 ng/mL) that prompted a prostate biopsy revealing a Gleason 6 prostatic adenocarcinoma. Histopathologic examination of the radical prostatectomy specimen revealed a Gleason's score 6 (moderately differentiated-grade G2) conventional (acinar) prostatic adenocarcinoma involving ~5% of the left lobe of the prostate with negative surgical margins (pathologic stage pT2a). Follow-up of over 7 years with history, physical examinations and serum PSA determinations found the patient to be without evidence of prostate cancer recurrence. There was no family history of prostate cancer and the patient was otherwise healthy. DNA from the prostate tissue was the first specimen to be sequenced from this patient and this demonstrated a heteroplasmic point mutation at nucleotide position (np) 6124 of the mitochondrial genome. The sequencing chromatogram demonstrated approximately equal proportions of the wild type base (T) and mutant base (C) (Figure 1(a)). The mutation changes amino acid 74 from the nonpolar, methionine (sulfur side chain) to the polar, threonine (hydroxyl side chain). This is a highly conserved amino acid, being methionine in 95% of all species ($N = 61$) for which the sequence has been determined. This conservation index (CI) of 95 is at the very upper end of what is observed for "adaptive mutations" (CI = 85 ± 9%) and significantly above the CI of "neutral polymorphisms" (CI = 23 ± 15%), making it highly likely to be functional in terms of mitochondrial physiology [1]. Another indicator of the uniqueness of this base and amino acid change is that this patient remains the only example of this base change in MITOMAP and mutation at this nucleotide position has not been found in the 2704 complete mtDNA sequences reported in the online database mtDB [16], where 2704 out of 2704 individuals have the wild type base (T). Subsequent sequencing of patient peripheral blood DNA, lymphoblast cell lines, and laser capture microdissection of various cellular compartments of the prostate all revealed similar levels of

heteroplasmic mutation at this base, confirming inheritance in the germ line and maintenance of the mutation in the prostate. The entire mitochondrial DNA sequence for this patient was determined and all changes from the revised Cambridge reference sequence are shown in Table 1. The mutation at n.p. 6124 was the only heteroplasmic mutation and the only mutation that had not been previously found in the 2407 complete mtDNA sequences published in the online database mtDB.

3.2. Cytochrome Oxidase Enzyme Activity. In order to study the biochemical consequences of this mutation we studied reactive oxygen production and enzymatic activity of respiratory complex (RC) IV (cytochrome oxidoreductase). The COI polypeptide forms the catalytic core of this enzyme. Cytochrome oxidation was measured in mitochondria isolated from the patient's lymphoblast cell line and compared to other lymphoblast cell lines from two unrelated, individuals' lymphoblast lines, sequence proven to be wild type at the COI locus (Figure 1(b)). The mutation is associated with a 29% decrease in COI activity.

3.3. Reactive Oxygen. Mutations in the COI polypeptide that lead to decreased RCIV activity could potentially lead to increased reactive oxygen [17]. In order to determine if this was occurring, we assayed the lymphoblast cell line of the patient for increased peroxide levels using dichlorofluorescin (DCF) and compared the results to the two-wild type patients described above. There was a marked increase (1.75 fold) in DCF fluorescence in the lymphoblast cell line containing the mutation compared to wildtype (Figure 1(c), gray bars). The majority of the increase in DCF fluorescence can be attributed to the mitochondria as demonstrated when oxidative phosphorylation is inhibited with FCCP (white bars), DCF fluorescence levels are decreased to similar levels. More detailed analysis of the effect of the 6124 mutation on ROS generation was obtained in the cybrid experiments, results highlighted below ("Cybrid ROS and RNS").

3.4. Cybrid Generation. In order to eliminate the potential confounding effects of the nuclear genome we made cytoplasmic hybrids (cybrids) that combined either pure mutant or pure wild type genomes from this patient with a stable nuclear background (143 B cells). The resultant pair of cybrids thus have the exact same nucleus (different from the patient), and the exact same mitochondrial DNA sequence except for the single base mutation at n.p. 6124. MtDNA genotypes were sequence verified in cybrids.

3.5. Cybrid In Vitro Proliferation. Three cybrids 6124 wild type clones and three 6124 mutant clones were analyzed for proliferation in culture. All three mutant 6124 cybrid clones grew faster than the three wild type clones with an average doubling time of 1.57 ± 0.12 days compared to 2.81 ± 0.56 days, mutant to wild type, respectively, ($P \leq 0.098$) (Figure 2).

Table 1: Patient mitochondrial DNA mutations. Patient peripheral blood, lymphoblast, and cybrid mtDNA was sequenced in its entirety. All changes from rCRS are shown as is the region in which the change occurs and the amino acid alteration when applicable. AI (allelic index) is the measure of the frequency of the mutation when compared to mtDB—Human Mitochondrial Genome Database [16]. Cybrid mtDNA was identical to peripheral blood with the exception of n.p. 6124 at which point the cybrids were determined to be either homoplasmic mutant or wild type.

ΔrCRS	Amino acid	Region	AI
A73G	noncoding	D-loop	83.4
A263G	noncoding	D-loop	99.7
309insC	noncoding	D-loop	
311insC	noncoding	D-loop	
523delA	noncoding	D-loop	
524delC	noncoding	D-loop	
G709A	noncoding	12S rRNA	16.4
A750G	noncoding	12S rRNA	99.2
A1438G	noncoding	12S rRNA	96.9
G1888A	noncoding	16s rRNA	5.3
A2706G	noncoding	16s rRNA	80.5
T4216C	Tyr → His	ND1	9.0
A4769G	Met	ND2	99.0
A4917G	Asn → Asp	ND2	4.8
T6124 T&C	Met → Thr	COI	unique
C7028T	Ala	COI	81.3
8270-8278del	noncoding	NC7	
G8697A	Met	ATPase6	4.7
G8854A	Ala → Thr	ATPase6	0.1
A8860G	Thr → Ala	ATPase6	99.8
T10463C	noncoding	tRNA Arg	4.7
A11251G	Leu	ND4	8.7
G11719A	Gly	ND4	77.7
A11812G	Leu	ND4	3.3
G13368A	Gly	ND5	4.9
A14233G	Asp	ND6	3.4
C14766T	Ile → Thr	Cytb	77.4
G14905A	Met	Cytb	5.1
A15326G	Thr → Ala	Cytb	99.4
C15452A	Leu → Ile	Cytb	8.7
A15607G	Lys	Cytb	5.5
G15928A	noncoding	tRNA Thr	4.9
T16126C	noncoding	D-loop	8.9
T16189C	noncoding	D-loop	28.0
C16278T	noncoding	D-loop	7.7
C16294T	noncoding	D-loop	5.7
C16296T	noncoding	D-loop	2.4
T16519C	noncoding	D-loop	59.7

3.6. Cybrid ROS and RNS. We then compared multiple wild type and mutant clones for reactive oxygen species (ROS) and reactive nitrogen species generation using flow cytometry and ROS and RNS sensitive fluorescent dyes. In order to study the cellular peroxide levels in cells that were either

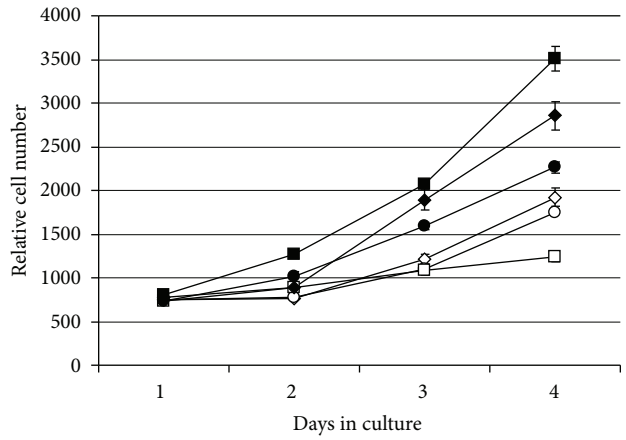

Figure 2: Cybrid cell lines with the T6124C mutation show increased proliferation. Proliferation was measured in 3 separate 6124WT clones and 3 separate 6124Mut clones using FluoReporter Blue Fluorometric dsDNA Quantitiation Kit (see Section 2). Symbols represent the following clones: ◊-6124WT3; ○-6124WT5; □-6124WT6, ◆-6124Mut1; ●-6124Mut2; ■-6124Mut4. Error bars represent the standard error of the mean of triplicate data.

entirely mutant or entirely wild type at this base, cybrid cell lines were made and multiple clones assayed by DCF fluorescence. Overall, 6 individual mutant clones showed a consistent increase in peroxide levels when compared to 5 individual wildtype clones (data not shown). When averaging the relative level of fluorescence in all wildtype clones compared to mutant clones, the mutation is associated with a statistically significant ($P \leq 0.0001$) increase in DCF fluorescence (Figure 3(a)). Similarly, in order to determine mitochondrial superoxide levels, there was a slight overall decrease in mitochondrial superoxide in the 6124Mut cell lines when compared to 6124WT ($P \leq 0.04$) (Figure 3(b)). A substantial and significant increase was observed in nitric oxide (NO) levels in the same 6124Mut and 6124WT cell lines (Figure 3(c)). When treated with DAF-FM diacetate, 6124Mut cell lines showed an average of 5.2-fold increase in NO levels compared to 6124WT ($P \leq 0.00001$). For comparison, NO was also measured cybrids containing 8993WT or Mut. 8993Mut cells had 1.8-fold higher NO when compared to 8993WT ($P \leq 0.0003$). Finally, there were no differences in the overall levels of hydroxyl radicals and peroxynitrite anions as measured by hydroxyphenylfluorescein (HPF) (Figure 3(d)).

3.7. Nitric Oxide Synthases (NOS) in Cybrids Cell Lines. In order to determine the possible source of the increased NO, we harvested RNA from the 6124WT and 6124Mut cybrids cell lines, followed by reverse transcription and PCR. There were no detectable levels of NOS1 or NOS3 observed (data not shown). However, NOS2 was demonstrated to be in both WT and Mut cell lines (Figure 4). The breast cancer cell line BT474 is used as a robustly positive control for NOS2 RNA.

3.8. Apoptosis. PAPR (poly ADP ribose polymerase) cleavage was analyzed to determine if changes in cellular proliferation were in part due to changes in apoptosis. Western blot analysis of PARP cleavage demonstrates that PARP cleavage was reduced in 6124Mut cybrids compared to 6124WT (Figure 5).

3.9. In Vivo Proliferation. 6124Mut cybrid cell lines grew faster *in vivo* when compared to 6124WT cybrids cells (Figure 6). There was some variability within each group as to the number and size of tumor, but at all time points there was a statistically significant increase in the size of tumors from 6124Mut cybrids cell lines ($P \leq 0.001$ at day 32). The animals injected with cybrids showed no systemic symptoms in response to tumor injection or growth.

4. Discussion

The mitochondrially encoded COI gene was first implicated in cancer biology in 1998 when a somatically acquired chain termination mutation was reported in colon cancer by the Vogelstein group at Johns Hopkins [18]. In 2005 an analysis of 260 patients with prostate cancer revealed that 31 (12%) had an inherited mutation in COI compared to <2% of no-cancer controls. Similarly, a case-control analysis of African-American men revealed that two COI gene single nucleotide polymorphisms (SNPs) (T6221C and T7389C) were significantly associated with prostate cancer ($P < 0.05$) and in strong linkage disequilibrium with each other ($r^2 > 0.6$). It is therefore likely that COI gene mutations predispose individuals to the development of prostate cancer. For this reason we have sequenced the COI gene from 482 prostate cancer patients and identified missense mutations in 116 (24.1%) [19]. The patient reported in this paper is part of that cohort.

The biochemical analysis of mtDNA mutations requires that viable cells are obtained from patients with such mutations and that potentially confounding nuclear events are controlled. This is made possible by the combination of capturing clinically relevant mutations in patient lymphoblast cell lines and the subsequent formation of cybrids with a common nuclear background. The cybrid formation process has the further advantage of allowing the mutant base to be studied separately from the wild type base. This paper documents that a prostate cancer-associated COI mutation affects the normal functioning of respiratory complex (RC) IV (cytochrome oxidase) in at least two distinct ways: decreasing the rate of mitochondrial cytochrome c oxidation and increasing the rate of ROS and NO generation in intact cells. It therefore seems likely that both of these effects are a direct consequence of the mutation. As Figure 3 depicts, not all ROS are affected equally by the 6124 mutation. In particular, peroxides are elevated, superoxide is depressed and there is no difference in hydroxyl radicals. One possible explanation for the decrease in superoxide levels in the presence of abundant superoxide dismutase that results in the rapid conversion of superoxide to hydrogen peroxide. Hydrogen peroxide is stable and able to accumulate while superoxide anion is transient and highly reactive.

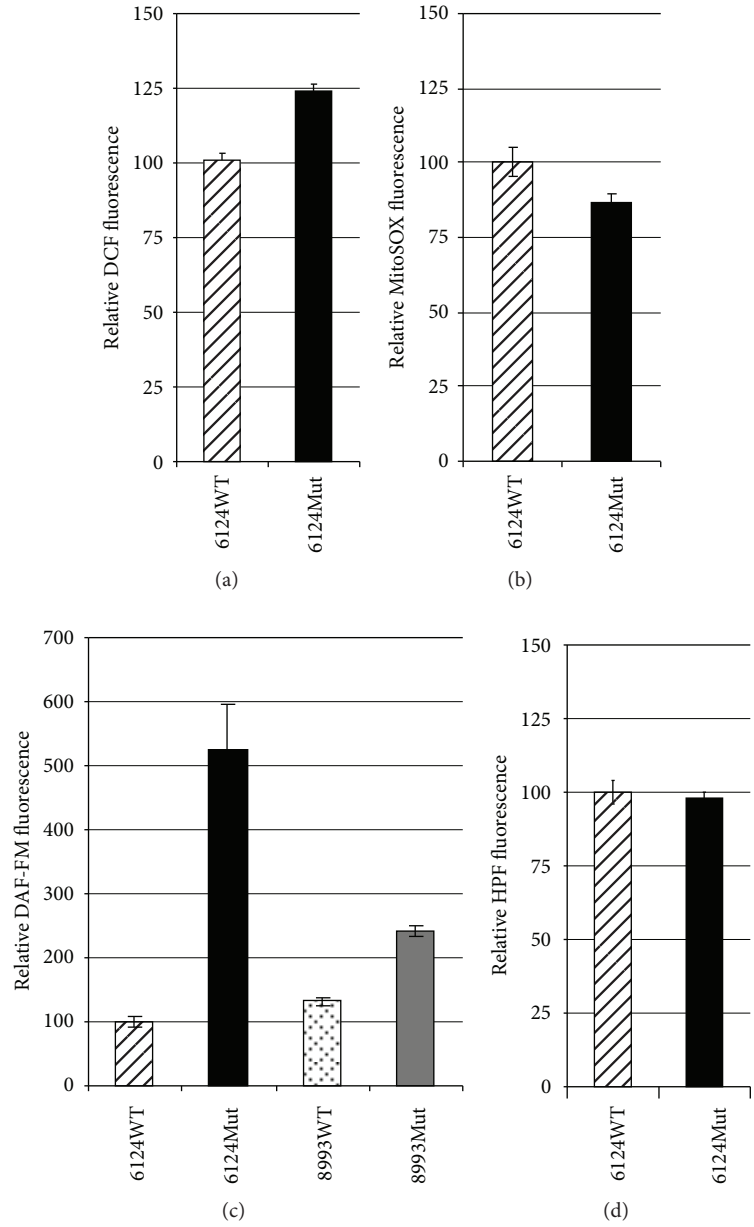

Figure 3: Peroxide and Nitric Oxide are elevated in 6124 mutant cybrid cells. (a) Peroxide levels are elevated in 6124Mut cell lines as measured by flow cytometric analysis of DCF fluorescence. 143B cybrids cell lines containing either the wild type base at position 6124WT or the mutation at position 6124Mut were analyzed. The average DCF fluorescence of five wild type and six mutant clonal cell lines are shown. Mutant cybrids produce significantly more peroxides ($P \leq 0.0001$). Error bars represent the standard error of the mean of 10 data points (WT) and 12 data points (Mut). (b) Mitochondrial superoxide levels are decreased in 6124Mut cell lines compared to 6124WT ($P \leq 0.04$). The average MitoSOX fluorescence of three wild type and three mutant clonal cell lines are shown. Error bars represent the standard error of the mean of 9 data points each WT and Mut. (c) NO levels are highly elevated in 6124Mut cells compared to 6124WT as measured by DAF-FM Fluorescence ($P \leq 0.00001$). For comparison, 143B cybrids cell lines containing a separate patient mtDNA with either a mutation at position 8993 (8993Mut) or wild type 8993 (8993WT) is shown. Error bars represent the standard error of the mean of 9 data points each 6124WT, 6124Mut, and 3 data points each 8993WT and 8993Mut. (d) Hydroxyl radicals and peroxynitrite anions as measured by hydroxyphenylfluorescein (HPF) remain unchanged. Error bars represent the standard error of the mean of 9 data points each 6124WT and 6124Mut.

The possible tumorigenic effects of increases in ROS are well known and include (at least) an increased rate of DNA mutations and ROS-induced promitogenic signaling [20–22]. These are common findings in prostate cancer and other solid tumors [23, 24]. It is likely that the cumulative effect over a lifetime of a tonic increase in cellular ROS increases the chances of malignant transformation. It is uncertain whether the prostate is more susceptible to this influence than other

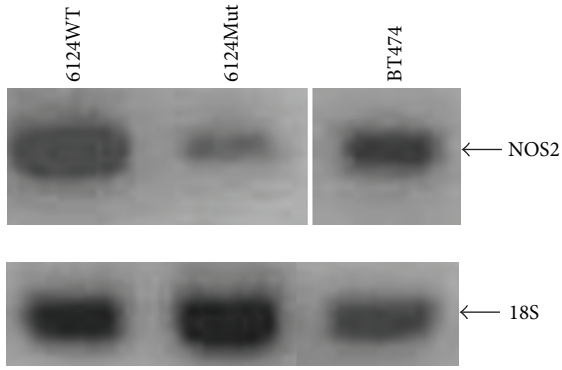

Figure 4: iNOS RNA is present in the cybrids cells. Reverse transcription followed by standard PCR was performed with iNOS specific primers. iNOS RNA was present in both 6124WT and 6124Mut cell lines. The breast cancer cell line BT474 is used as a robustly positive control for iNOS RNA. and 18S RNA was used as a quality control.

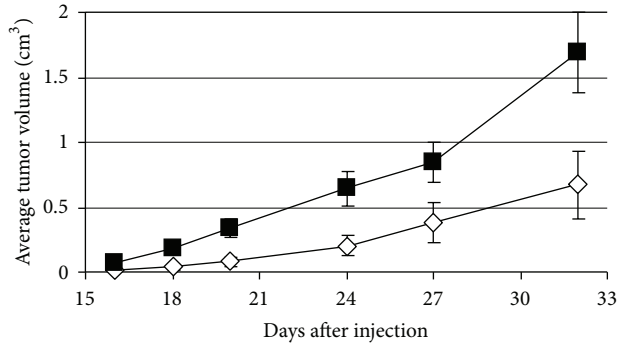

Figure 6: 6124Mut cell lines grow faster in nude mice. Growth curves of tumor xenografts in nude mice. Each line represents a cohort of 29-30 animals injected with the 6124WT cybrids cells (◊) or 6124Mut cybrids cells (■). Error bars denote the standard error of the mean for each cohort at each time. Data are representative of 3 individual experiments.

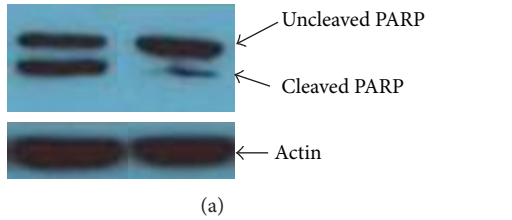

(a)

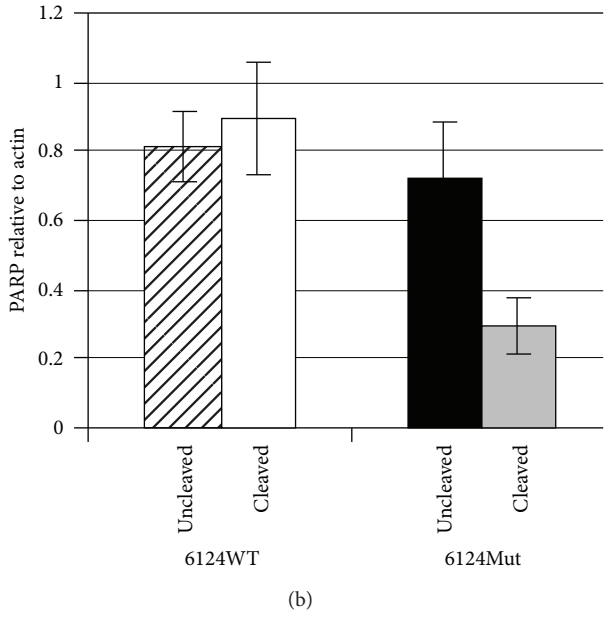

(b)

Figure 5: PARP cleavage is decreased in 6124Mut cybrids cells. (a) Western Blot analysis of uncleaved and cleaved PARP in 6124WT (left) and 6124Mut (right) cells. Figure is representative of three 6124WT and three 6124Mut clones. (b) Densitometric analysis of Western Blot results of three 6124WT and three 6124Mut clones using ImageJ software. Error bars represent the standard error of the mean of the three WT and three Mut clones.

organs, but the association of COI mutations with disease suggests some specificity.

The possible mechanism by which a decreased efficiency of oxidative phosphorylation is related to malignant transformation is less obvious. It is probably relevant to the so called "Warburg Effect" wherein tumor cells exhibit defective oxidative phosphorylation and increased glycolysis as a primary means of ATP generation [25]. It is possible that inherited or somatically acquired mtDNA mutations are partially or wholly responsible for this effect. It is possible that the decrease in oxidative phosphorylation is not in and of itself causally related to the increased risk of cancer, but that the relation to cancer risk is conferred predominantly by the increased ROS generation and that compromises to oxidative phosphorylation are merely a bystander effect of no direct consequence to tumorigenesis. This remains to be determined.

The possible tumorigenic effects of increases in RNS are also well known. Nitric oxide (NO) is generated enzymatically by synthases (NOS), which oxidize L-arginine to L-citrulline. The inducible form, iNOS, is present in a variety of cell types. Over the past 20 years iNOS expression has been associated with various human tumors including: breast, brain, lung, prostate, colorectal, and melanoma [26–32]. NO action is concentration-dependent. Increased cGMP-mediated ERK phosphorylation is associated with low levels of NO in cancer cells whereas HIF-1a stabilization is associated with intermediate levels [33]. Though NO has been shown to induce apoptosis it can transcriptionally enhance MMP-1 via the ERK and p38 MAPK pathways resulting in tumor progression and also can result in the overproduction of VEGF [33]. Although NO levels are transient, iNOS generated NO fluctuations varying from seconds to days can influence the antiapoptotic/proapoptotic effects of NO [33].

We have demonstrated that the T6124C (M74T) mutation was inherited in a heteroplasmic state by a patient that developed prostate cancer and that the mutation not only causes increased ROS and nitric oxide but also induces increased cellular proliferation, decreased apoptosis, and

increased *in vivo* tumor growth. These are quintessential characteristics of the malignant phenotype. These results are concordant with other studies that demonstrate a profound effect of mtDNA mutations on tumor cell biology. In 2008 Ishikawa demonstrated that mtDNA mutations determined the metastatic potential of lung cancer cell lines independent of the characteristics of the cancer cell nucleus. Specifically, high-metastatic cell lines lost their metastatic potential when the mtDNA was replaced with mtDNA from low-metastatic cell lines and low-metastatic cell lines acquired high-metastatic capabilities when mtDNA from high metastatic lines were inserted [34]. The metastatic capacity could be eliminated by treatment with antioxidants indicating the central importance of ROS-induced signaling in metastasis. Similarly, an ATP6 (ATP synthase subunit 6) missense mutation in the mitochondrial genome (T8993G) causes increased ROS in prostate cancer cell lines and increased tumor growth [5].

5. Conclusions

Mitochondrial DNA from a prostate cancer patient with an inherited-heteroplasmic-mtDNA mutation in COI, the catalytic core of mitochondrial respiratory complex IV was studied. In the laboratory, this mutation was found to simultaneously decrease the activity of the respiratory complex as measured by the rate of cytochrome c oxidation and to increase the rate of mitochondrial reactive oxygen generation. Other mutation-induced biochemical changes included increased generation of nitric oxide. Cells harboring the mutation proliferated faster *in vitro* and caused increased tumor growth *in vivo*. These findings suggest a possible molecular substrate (mtDNA mutation) for the "Warburg effect" of anaerobic metabolism exhibited by some tumors and increased cellular reactive oxygen, a common finding in solid tumors.

Acknowledgments

This work is supported by NIH Grant nos. CA98912 (Petros), CA96994 (Petros), and NS21328 (Wallace). It is also supported by a VA MERIT award (Petros). The authors wish to thank Mr. Larry Williams (The Breckenridge Group) for his personal support of this research and the Evans County Cares Foundation. In addition, cytochrome oxidase activity assays performed by Leslie Costello, Ph.D. (University of Maryland). Technical help was also provided by Amanda Parrish Ph.D. and Carina Fenandez-Golarz M.D.

References

[1] D. C. Wallace, "A mitochondrial paradigm of metabolic and degenerative diseases, aging, and cancer: a dawn for evolutionary medicine," *Annual Review of Genetics*, vol. 39, pp. 359–407, 2005.

[2] S. I. Zhadanov, E. Y. Grechanina, Y. B. Grechanina et al., "Fatal manifestation of a de novo ND5 mutation: insights into the pathogenetic mechanisms of mtDNA ND5 gene defects," *Mitochondrion*, vol. 7, no. 4, pp. 260–266, 2007.

[3] W. Fan, K. G. Waymire, N. Narula et al., "A mouse model of mitochondrial disease reveals germline selection against severe mtDNA mutations," *Science*, vol. 319, no. 5865, pp. 958–962, 2008.

[4] M. Gómez-Zaera, J. Abril, L. González et al., "Identification of somatic and germline mitochondrial DNA sequence variants in prostate cancer patients," *Mutation Research*, vol. 595, no. 1-2, pp. 42–51, 2006.

[5] J. A. Petros, A. K. Baumann, E. Ruiz-Pesini et al., "MtDNA mutations increase tumorigenicity in prostate cancer," *Proceedings of the National Academy of Sciences of the United States of America*, vol. 102, no. 3, pp. 719–724, 2005.

[6] A. M. Ray, K. A. Zuhlke, A. M. Levin, J. A. Douglas, K. A. Cooney, and J. A. Petros, "Sequence variation in the mitochondrial gene cytochrome c oxidase subunit I and prostate cancer in African American men," *Prostate*, vol. 69, no. 9, pp. 956–960, 2009.

[7] C. Jerónimo, S. Nomoto, O. L. Caballero et al., "Mitochondrial mutations in early stage prostate cancer and bodily fluids," *Oncogene*, vol. 20, no. 37, pp. 5195–5198, 2001.

[8] M. Higuchi, T. Kudo, S. Suzuki et al., "Mitochondrial DNA determines androgen dependence in prostate cancer cell lines," *Oncogene*, vol. 25, no. 10, pp. 1437–1445, 2006.

[9] T. Mizumachi, L. Muskhelishvili, A. Naito et al., "Increased distributional variance of mitochondrial DNA content associated with prostate cancer cells as compared with normal prostate cells," *Prostate*, vol. 68, no. 4, pp. 408–417, 2008.

[10] J. Maki, K. Robinson, B. Reguly et al., "Mitochondrial genome deletion aids in the identification of false- and true-negative prostate needle core biopsy specimens," *American Journal of Clinical Pathology*, vol. 129, no. 1, pp. 57–66, 2008.

[11] B. A. Aldridge, S. D. Lim, A. K. Baumann et al., "Automated sequencing of complete mitochondrial genomes from laser-capture microdissected samples," *BioTechniques*, vol. 35, no. 3, pp. 606–612, 2003.

[12] J. M. Seigneurin, B. Guilbert, M. J. Bourgeat, and S. Avrameas, "Polyspecific natural antibodies and autoantibodies secreted by human lymphocytes immortalized with Epstein-Barr virus," *Blood*, vol. 71, no. 3, pp. 581–585, 1988.

[13] L. C. Costello, Z. Guan, B. Kukoyi, P. Feng, and R. B. Franklin, "Terminal oxidation and the effects of zinc in prostate versus liver mitochondria," *Mitochondrion*, vol. 4, no. 4, pp. 331–338, 2004.

[14] M. M. Bradford, "A rapid and sensitive method for the quantitation of microgram quantities of protein utilizing the principle of protein dye binding," *Analytical Biochemistry*, vol. 72, no. 1-2, pp. 248–254, 1976.

[15] D. Hammond-McKibben, P. Lake, J. Zhang, N. Tart-Risher, R. Hugo, and M. Weetall, "A high-capacity quantitative mouse model of drug-mediated immunosuppression based on rejection of an allogeneic subcutaneous tumor," *Journal of Pharmacology and Experimental Therapeutics*, vol. 297, no. 3, pp. 1144–1151, 2001.

[16] M. Ingman and U. Gyllensten, "mtDB: human mitochondrial genome database, a resource for population genetics and medical sciences," *Nucleic Acids Research*, vol. 34, pp. D749–751, 2006.

[17] J. F. Turrens, "Mitochondrial formation of reactive oxygen species," *Journal of Physiology*, vol. 552, no. 2, pp. 335–344, 2003.

[18] K. Polyak, Y. Li, H. Zhu et al., "Somatic mutations of the mitochondrial genome in human colorectal tumours," *Nature Genetics*, vol. 20, no. 3, pp. 291–293, 1998.

[19] T. A. Scott, R. Arnold, and J. A. Petros, "Mitochondrial cytochrome c osidase subunit 1 sequence variation in prostate cancer," *Scientifica*, vol. 2012, Article ID 701810, 7 pages, 2012.

[20] Y. Zhang, Y. Du, W. Le, K. Wang, N. Kieffer, and J. Zhang, "Redox control of the survival of healthy and diseased cells," *Antioxid Redox Signal*, vol. 15, no. 11, pp. 2867–2908, 2011.

[21] D. Ziech, R. Franco, A. Pappa, and M. I. Panayiotidis, "Reactive Oxygen Species (ROS)—induced genetic and epigenetic alterations in human carcinogenesis," *Mutation Research*, vol. 711, no. 1-2, pp. 167–173, 2011.

[22] G. Gupta-Elera, A. R. Garrett, R. A. Robison, and K. L. O'Neill, "The role of oxidative stress in prostate cancer," *European Journal of Cancer Prevention*, vol. 21, no. 2, pp. 155–162, 2012.

[23] T. P. Szatrowski and C. F. Nathan, "Production of large amounts of hydrogen peroxide by human tumor cells," *Cancer Research*, vol. 51, no. 3, pp. 794–798, 1991.

[24] H. Wiseman and B. Halliwell, "Damage to DNA by reactive oxygen and nitrogen species: role in inflammatory disease and progression to cancer," *Biochemical Journal*, vol. 313, pp. 17–29, 1996.

[25] O. Warburg, "On respiratory impairment in cancer cells," *Science*, vol. 124, no. 3215, pp. 269–270, 1956.

[26] C. S. Cobbs, J. E. Brenman, K. D. Aldape, D. S. Bredt, and M. A. Israel, "Expression of nitric oxide synthase in human central nervous system tumors," *Cancer Research*, vol. 55, no. 4, pp. 727–730, 1995.

[27] S. Ambs, W. G. Merriam, W. P. Bennett et al., "Frequent nitric oxide synthase-2 expression in human colon adenomas: implication for tumor angiogenesis and colon cancer progression," *Cancer Research*, vol. 58, no. 2, pp. 334–341, 1998.

[28] S. Ekmekcioglu, J. Ellerhorst, C. M. Smid et al., "Inducible nitric oxide synthase and nitrotyrosine in human metastatic melanoma tumors correlate with poor survival," *Clinical Cancer Research*, vol. 6, no. 12, pp. 4768–4775, 2000.

[29] S. H. Aaltomaa, P. K. Lipponen, and V. M. Kosma, "Inducible nitric oxide synthase (iNOS) expression and its prognostic value in prostate cancer," *Anticancer Research*, vol. 21, no. 4B, pp. 3101–3106, 2001.

[30] P. K. Lala and C. Chakraborty, "Role of nitric oxide in carcinogenesis and tumour progression," *The Lancet Oncology*, vol. 2, no. 3, pp. 149–156, 2001.

[31] D. Massi, A. Franchi, I. Sardi et al., "Inducible nitric oxide synthase expression in benign and malignant cutaneous melanocytic lesions," *The Journal of Pathology*, vol. 194, no. 2, pp. 194–200, 2001.

[32] A. S. Bulut, E. Erden, S. D. Sak, H. Doruk, N. Kursun, and D. Dincol, "Significance of inducible nitric oxide synthase expression in benign and malignant breast epithelium: an immunohistochemical study of 151 cases," *Virchows Archiv*, vol. 447, no. 1, pp. 24–30, 2005.

[33] S. Singh and A. K. Gupta, "Nitric oxide: role in tumour biology and iNOS/NO-based anticancer therapies," *Cancer Chemotherapy and Pharmacology*, vol. 67, no. 6, pp. 1211–1224, 2011.

[34] K. Ishikawa, K. Takenaga, M. Akimoto et al., "ROS-generating mitochondrial DNA mutations can regulate tumor cell metastasis," *Science*, vol. 320, no. 5876, pp. 661–664, 2008.

Hindawi Publishing Corporation
BioMed Research International
Volume 2013, Article ID 379438, 7 pages
http://dx.doi.org/10.1155/2013/379438

Research Article

Paired Ductal Carcinoma In Situ and Invasive Breast Cancer Lesions in the D-Loop of the Mitochondrial Genome Indicate a Cancerization Field Effect

Andrea Maggrah,[1] Kerry Robinson,[1] Jennifer Creed,[1] Roy Wittock,[1] Ken Gehman,[2] Teresa Gehman,[2] Helen Brown,[3] Andrew Harbottle,[3] M. Kent Froberg,[4] Daniel Klein,[1] Brian Reguly,[1] and Ryan Parr[1]

[1] *Mitomics Inc., 290 Munro Street, Suite 1000, Thunder Bay, ON, Canada P7A 7T1*
[2] *Department of Surgery, Thunder Bay Regional Health Sciences Centre, 980 Oliver Road, Thunder Bay, ON, Canada P7B 6V4*
[3] *Mitomics Inc., UK Ltd. Cels At Newcastle, Medical School, University of Newcastle, Framlington Place, Newcastle Upon Tyne NE2 4HH, UK*
[4] *Department of Pathology, Saint Mary's Duluth Clinic, 400 East Third Street, Duluth, MN 55805, USA*

Correspondence should be addressed to Andrea Maggrah; a.maggrah@mitomicsinc.com

Received 6 July 2012; Accepted 26 September 2012

Academic Editor: John Jakupciak

Alterations in the mitochondrial genome have been chronicled in most solid tumors, including breast cancer. The intent of this paper is to compare and document somatic mitochondrial D-loop mutations in paired samples of ductal carcinoma *in situ* (DCIS) and invasive breast cancer (IBC) indicating a potential breast ductal epithelial cancerization field effect. Paired samples of these histopathologies were laser-captured microdissected (LCM) from biopsy, lumpectomy, and mastectomy tissues. Blood samples were collected as germplasm control references. For each patient, hypervariable region 1 (HV1) in the D-loop portion of the mitochondrial genome (mtGenome) was sequenced for all 3 clinical samples. Specific parallel somatic heteroplasmic alterations between these histopathologies, particularly at sites 16189, 16223, 16224, 16270, and 16291, suggest the presence of an epithelial, mitochondrial cancerization field effect. These results indicate that further characterization of the mutational pathway of DCIS and IBC may help establish the invasive potential of DCIS. Moreover, this paper indicates that biofluids with low cellularity, such as nipple aspirate fluid and/or ductal lavage, warrant further investigation as early and minimally invasive detection mediums of a cancerization field effect within breast tissue.

1. Introduction

In 2010, close to 207,090 new cases of IBC were diagnosed in the United States, and DCIS was identified in an additional 54,010 women who did not yet have IBC [1]. These statistics indicate that breast cancer and the often associated precursor lesion, DCIS, are global health problems.

Although DCIS masses are often small by comparison to IBC masses, DCIS is typically detected through mammography or self-examination. However, there are significant shortcomings to these methods. Mammography is generally used to identify breast masses within a resolution limit of 1 cm, and the Van Nuys prognostic index (VNPI) for DCIS does not score tumors less than 1.5 cm. This means that a subset of smaller lesions which may have significant future clinical impact remain undetected and/or evaluated. Breast self-examination has also been extensively shown to be an ineffective detection tool for Asian women [2, 3].

Currently, there is no clinical means to distinguish between the heterogeneous types of DCIS and recognize the carcinomas that will progress into invasive, metastatic breast cancer. The mechanism that drives this transformation from DCIS to IBC is also not well understood. Hence, when mammography detects DCIS, a full diagnostic workup and treatment is required [4]. As such, a huge need exists for the development of early detection procedures or tools for

preinvasive lesions. If a link is established between smaller DCIS lesions and larger IBC lesions, or if a distinction can be made between invasive and noninvasive masses, it may then be possible to apply this knowledge to the development of early detection tools and chemopreventive treatment for women at risk.

The progression of DCIS is poorly understood because the technology used to detect it relies on tissue mass. Indeed, the identification of DCIS via mammography is low compared to larger tumors. If a significant proportion of IBC cases originate as DCIS, then successful detection and stratification of these lesions will assist the clinician and the patient with determining potential monitoring and treatment strategies. A recent review articulated the need for a combined research effort directed towards this clinical need [5].

This study proposes using somatic mitochondrial D-loop mutations in paired samples of DCIS and IBC to identify a potential breast ductal epithelial "cancerization" field effect. Alterations in the mitochondrial genome have been chronicled in most solid tumors, including breast cancer [6]. Since the mtGenome has an accelerated mutation rate in association with the beginning or presence of malignant transformation, patient-matched characterization of this genome in both DCIS and IBC may reveal a common related or progressive mutation pattern between these two lesions.

Mitochondrial D-loop mutations can be evaluated using tissue samples from solid tumors. Using biofluids with low cellularity such as nipple aspirate fluid (NAF) or ductal lavage (DL) represents a much less invasive route for developing early detection tests. The mtGenome is ideal for these investigations because it has a high copy number per cell, when compared to the nuclear archive of DNA.

There are other characteristics suggesting that the mtGenome may be an ideal "biosensor" as follows: (1) each copy of the mtGenome is clonal; (2) the mtGenome has a maternal inheritance pattern which precludes generational recombination; (3) somatic mutations appearing in a subset of mtGenomes, known as heteroplasmy, afford early disease detection; (4) the modest size of the mtGenome (16,568 bp) allows inexpensive, targeted, and concentrated genetic analyses; (5) the mtGenome has a 10–100-fold copy advantage over the nuclear genome; (6) the mitochondrial organelle is the center of ATP synthesis and is the mediator of cell apoptosis, and for successful tumorigenesis to occur, energy production must be replaced by an alternative process and apoptosis must be by-passed; (7) mitochondrial DNA (mtDNA) has an accelerated somatic mutation rate in which mutations occur within years, and perhaps months, from when molecular pathways are altered by early molecular changes associated with malignant transformation; (8) mutations in the mtGenome have been attested in a wide variety of solid tumors.

2. Materials and Methods

2.1. Patients and Samples. Women who were referred to a surgical oncologist for a clinical breast examination and had a biopsy with positive results were recruited to this study. Patients having a biopsy, lumpectomy, or mastectomy were selected based on a pathology report which identified both DCIS and IBC. Two patients had both a biopsy and a secondary procedure (lumpectomy and mastectomy). All patients were procured in accordance with the ethical guidelines of the Thunder Bay Regional Health Sciences Research Ethics Board in adherence to the Tri-Council Policy Statement on Ethical Conduct for Research Involving Humans. Written consent was obtained from the patients for publication of the study. Patients were selected based on review of biopsy and/or surgical pathology reports. A total of 34 patients were identified, however, upon sectioning of requested samples, only 15 had sufficient quantities of both IBC and DCIS to warrant LCM. After complete sample processing (extraction through sequencing), 5 patients were further eliminated due to sample drop-out. A total of 34 samples, including blood, were contributed by a suite of 10 patients (Table 1). Blood from a finger prick was collected on IsoCode cards (Whatman, Piscataway, NJ). DNA was extracted using a QIAcube (Qiagen, Germantown, MD) and QIAamp DNA mini kit (Qiagen, Germantown, MD) using the protocol for DNA purification for dried blood.

2.2. Laser Capture Microdissection. Requested tissues (biopsy and mastectomy samples) were sectioned from formalin-fixed paraffin-embedded (FFPE) blocks and processed for LCM. LCM was performed by two qualified, gowned, gloved, and masked technicians who captured both DCIS and IBC from each patient. By direct observation of the process, about 3-4 cells were harvested per laser pulse, or capture event, and approximately 2,000 captures were recovered from each tissue type. DNA was liberated from LCM samples by an overnight digestion at 65°C in 50 μL of 100 mM Tris-HCl (pH 8.0), 10 mM EDTA, 1% Tween 20, and 20 mg/mL Proteinase K. The following morning, the reactions were inactivated at 95°C for 10 minutes. A total of 24 FFPE samples were processed. DNA was extracted using a QIAcube and QIAamp DNA mini kit tissue protocol, with the addition of heating each sample at 90°C for 1 hour after incubation of the sample at 56°C with 180 μL of Buffer ATL plus 20 μL Proteinase K. The samples were eluted in 200 μL of Buffer AE. Samples were dried down and resuspended in 30 μL of ddH_20.

2.3. Mitochondrial D-Loop Amplification. A portion of the D-loop was amplified with primer sets MT1, 2, 3 forward and reverse (MitoScreen Assay Kit, Transgenomic, Omaha, NE) using the following reagent concentrations per reaction: 1X FastStart High Fidelity Reaction Buffer, 1.8 mM $MgCl_2$, and 0.25 U FastStart High Fidelity Enzyme Blend (Roche, Burgess Hill, UK); 0.2 mM of each dNTP; 0.3 μM of each primer; 2.5 μL of tissue extract or 1 μL of DNA recovered from blood, with the final reaction volume adjusted to 25 μL with ddH_20. Reactions were activated at 95°C for 6 minutes, then amplified with the following profile for 42 cycles: 95°C, 30 seconds; 56°C, 30 seconds; 72°C, 1 minute; followed by a final extension for 7 minutes at 72°C.

2.4. Denaturing High Performance Liquid Chromatography (DHPLC). Following amplification, DHPLC was used to

Table 1: Clinical, pathological information with parallel mutation sites in common between both DCIS and IBC for each patient, inclusive of all patient tissue samples. Heteroplasmic sites are scored as mutations.

Patient	Age	Sample	Est	Pro	HER2	Grade	NG	TF	MS	BR	EIC	Parallel mutations	Haplotype
33	65	Mast	−	−	+	3	3	2	3	8	+	192, 224, 304, 311	U5a
36	67	Lump	+	−	−	1	1	1	1	3	−	188, 189, 223, 224, 270, 291, 311, 319, 362, 390	H
43	51	Biopsy					2					93, 189, 298	V
	52	Lump	+	+		2	2	2	2	6	−		
46	66	Biopsy	−	+	−	2	2	3	1	6	−	126, 189, 223, 291, 357, 362, 390	J
57	41	Lump	+	+	−	3	2	3	3	8	+	189, 291, 390	H
64	51	Biopsy										182, 183, 249	H
	51	Mast	−	−	+	3	3	3	3	9	−		
74	39	Biopsy	−	−	+							203, 304	K
	40	Mast				2	3	2	1	6	+		
83	49	Lump	+	−	−	2	2	3	1	6	−	189	H
89	41	Lump	−	−	−	3	3	3	3	9	−	189, 223, 224, 291, 298, 311, 362, 390	K
94	50	Lump	+	+		1	2	2	1	5	−	93, 189, 224, 291, 311	H

Unavailable information is left blank. NG: nuclear grade; MS: mitotic score; BR: modified Bloom-Richardson grade; EIC: extensive intraductal component.

identify areas of mtGenome alterations. Sample analysis temperatures were predicted using Navigator software (Transgenomic, Omaha, NE). The gradient mobile phase consisted of Buffer A (0.1 M Triethylammonium Acetate pH 7.0) and Buffer B (0.1 M Triethylammonium Acetate pH 7.0) and 25% Acetonitrile. These buffers were mixed to provide a linear gradient varying Buffer B, for MT1 59–67, MT2 57–65, and MT3 59–67 over a 4-minute period. After each analysis, the column was cleaned with 100% Buffer B and then equilibrated for 2 minutes with Buffers A : B 54 : 56 (MT1 and MT3) 52 : 58 (MT2). Analysis temperatures were 58°C for MT1, 60°C for MT2, and 57°C and 59°C for MT3. Prior to injection, the samples were heteroduplexed by heating to 95°C for 5 minutes and then cooling at 1.5°C per minute down to 25°C.

2.5. Amplification of Altered Sequences Identified by DHPLC. Due to the low amount of template recovered from the LCM procedure, sequencing efforts were limited to a target sequence through and around hypervariable region 1 (HV1; 16,024–16,383). HV1 has a 2-fold higher mutation rate than HV2 [7]. A large fragment (1264 bp), including HV1, was amplified as previously mentioned with the following changes: primers MT2 and 19 from the MitoScreen Assay Kit (Transgenomic, Omaha, NE) concentrations were increased to 0.4 μM, cycle number was reduced to 35, and the extension time was increased to 3 minutes.

This provided a low yield product which was amplified for a smaller sequence (627 bp) with nested primer D1 [8], which contains standard sequencing primer sites. The target sequence amplified by these primers specifically encompasses HV1 and flanking segments.

Reaction conditions were again the same as mentioned previously with the following changes: primer concentrations were increased to 0.6 μM, and 1 μL of the preceding product was used to seed the reaction which was run with the following conditions: 95°C for 6 minutes, 14 cycles of 94°C for 1 minute, 65°C for 1 minute (0.5°C per cycle), and 72°C for 1 minute. Then 20 cycles of 94°C for 1 minute, 58°C for 1 minute, 72°C for 1 minute, followed by a final extension of 72°C for 8 minutes.

2.6. Sequencing. Primer set MT2/MT19 (15424-102) was used to generate template for nested amplification with D1 primers (15898–16525). Both sets of primers were tested for null amplification against Rho 0 derived template [9] using the PCR conditions described previously to preclude the possibility of coamplification of numts. This mandatory precaution has been chronicled elsewhere [10, 11]. In addition, results were compared to the HV1 sequence signature of everyone directly involved with handling the samples to detect any incidental contamination by laboratory personnel. Finally, the corresponding germ plasma-derived DNA was amplified and sequenced from each patient as a direct comparative to control for actual somatic mutations as opposed to maternal variation.

Amplified template was sequenced at Genevision (Newcastle Upon Tyne, UK). Both Geneious bioinformatics software (Biomatters) and Sequencher 4.5 (Gene Codes) were used for sequence analyses.

2.7. Statistical Analyses. Analyses were performed on HV1 mutation patterns and all applicable parameters listed in the pathology report: age, receptor status, tumor grade, nuclear grade, tubule formation, mitotic score, modified Bloom-Richardson grade, and presence or absence of extensive intraductal component. Attempts to correlate the diagnostic rankings and per-site mutation results were made using point-biserial and rank-biserial statistics. Pearson rank correlation was used to identify the strength of the relationship between HVR1 relative substitution rates and the prevalence of each mutation site in the patient data. IBC and DCIS sample populations were considered separately in order to determine if any patterns existed in the mutation load of the individual sample types as well as to discover the presence

Table 2: HV1 somatic mutations are bolded, while mutations persisting in all patient samples are also italicized. Patient histologies are compared to the corresponding sequence of their germplasm or blood (B) to detect mutations. Only those sites appearing in all histologies for a given patient are identified.

	93	126	188	189	192	203	223	224	249	270	291	298	304	311	319	357	362	390
RCRS	T	T	C	T	C	A	C	T	T	C	C	T	T	T	G	T	T	G
33 B	T	T	C	T	T	A	C	T	T	T	C	T	C	T	G	T	T	G
33 MIBC	N	N	C	T	**C**	A	C	**C**	T	T	C	T	**T**	**C**	G	T	T	G
33 MDCIS	T	**Y**	C	T	**C**	A	C	**Y**	T	**Y**	C	T	**Y**	**Y**	G	T	T	G
36 B	T	T	T	T	C	A	C	T	T	C	C	T	T	T	A	T	T	G
36 LIBC	T	T	**C**	**Y**	C	A	**Y**	**Y**	T	**Y**	**Y**	T	T	**Y**	**G**	T	**Y**	**R**
36 LDCIS	T	T	**C**	**Y**	C	A	**Y**	**Y**	T	**T**	**Y**	T	T	**Y**	**G**	T	**Y**	**R**
43 B	C	T	C	T	C	A	C	T	T	C	C	C	T	T	G	T	T	G
43 BIBC	**T**	T	C	**Y**	C	A	C	**Y**	T	**Y**	C	**T**	T	T	G	T	T	G
43 BDCIS	**T**	T	C	**Y**	C	A	C	**Y**	T	C	C	**T**	T	T	G	T	T	G
43 LDCIS	**T**	**C**	C	**Y**	C	A	**Y**	T	T	C	**Y**	**T**	**Y**	T	G	T	**Y**	G
46 B	T	C	C	T	C	A	C	T	T	C	C	T	T	T	G	C	T	G
46 BIBC	T	**T**	C	**Y**	C	A	**Y**	T	T	C	**Y**	T	T	T	G	**T**	**Y**	**R**
46 BDCIS	T	**T**	C	**C**	C	A	**T**	T	T	C	**T**	T	T	T	G	**T**	**C**	**A**
57 B	T	T	C	**T**	C	A	C	T	T	C	C	T	T	T	G	T	T	G
57 LIBC	N	N	C	**Y**	C	A	**T**	T	T	C	**T**	T	T	T	G	T	**C**	**A**
57 LDCIS	T	T	C	**Y**	C	A	C	**Y**	T	**Y**	**Y**	T	T	Y	G	T	T	**R**
64 B	T	T	C	C	C	A	C	T	C	C	C	T	T	T	G	T	T	G
64 MIBC1	N	N	C	C	C	A	**Y**	**Y**	**Y**	**Y**	**Y**	T	T	**Y**	G	T	**Y**	**R**
64 MIBC2	T	T	C	**Y**	C	A	**Y**	T	**T**	C	**Y**	T	T	T	G	T	**Y**	**R**
64 MDCIS	T	T	C	**Y**	C	A	C	**Y**	**Y**	**Y**	C	T	T	**Y**	G	T	T	G
74 B	T	T	C	T	C	G	C	T	T	C	C	T	C	T	G	T	T	G
74 BIBC	T	T	C	**Y**	C	**A**	**Y**	T	T	C	**Y**	T	**T**	T	G	T	**Y**	**R**
74 BDCIS	T	T	C	**Y**	C	**A**	**T**	T	T	C	**Y**	T	**T**	T	G	T	**Y**	**R**
74 MIBC	T	T	C	T	C	**A**	C	**Y**	T	**Y**	C	T	**T**	T	G	T	T	G
74 MDCIS	T	T	C	**Y**	C	**A**	**Y**	T	T	C	**Y**	T	**T**	T	G	T	**Y**	**R**
83 B	T	T	C	C	C	A	C	T	T	C	C	T	T	T	G	T	T	G
83 BIBC	T	T	C	**T**	C	A	**Y**	T	T	C	C	T	T	T	G	T	T	G
83 BDCIS	T	T	C	**T**	C	A	C	**C**	T	C	C	T	T	**C**	G	T	T	G
89 B	T	T	C	T	C	A	C	C	T	C	C	C	T	C	G	T	T	G
89 BIBC	N	N	C	**Y**	C	A	**Y**	**T**	T	C	**Y**	**T**	T	**T**	G	T	**Y**	**R**
89 BDCIS	N	N	C	**Y**	C	A	**Y**	**Y**	T	**Y**	**Y**	**T**	**Y**	**Y**	G	T	**Y**	**R**
94 B	C	T	C	C	C	A	C	T	T	T	T	T	T	T	G	T	T	G
94 BIBC	**T**	T	C	**T**	C	A	C	**Y**	T	**C**	**C**	T	T	**Y**	G	T	T	G
94 BDCIS	**T**	T	C	**T**	C	A	C	**C**	T	T	**C**	T	T	**C**	G	T	T	G

IBC: invasive breast carcinoma, DCIS: ductal carcinoma *in situ*. Prefixes: B: biopsy, L: lumpectomy, and M: mastectomy. The revised Cambridge reference sequence (RCRS) is used as a standard comparison. The first 2 and/or 3 digits for each site have been removed to avoid redundancy.

of any interactions between the two tissue types. Again, Pearson correlations were used as statistics for this analysis.

3. Results

Mutations were identified in HV1 which was reamplified with Rho 0 null primers and sequenced. All patients in this study demonstrate heteroplasmy in all of the associated histologies in comparison to germ plasma, or blood. It is important to note that 18 sites had homoplasmic and/or heteroplasmic mutation sites in common between DCIS and IBC lesions recovered from the same patient. All patients had at least 1 corresponding homoplasmic and/or heteroplasmic site in both DCIS and IBC. These results parallel similar observations noting that other biomarkers are held in common between DCIS and IBC [12]. Two patients (43 and 74) had equivalent mutations in both biopsy samples and tissue from follow-up procedures (lumpectomy and mastectomy). See Tables 1 and 2 for an overview of clinical pathology and HV1 somatic mutations, respectively. No exogenous contamination from laboratory personnel, via comparison to HV1 sequence from germplasm, was observed.

3.1. Site Specific Mutations. Of the patients in this study, 9/10 had a mutation at positions 16189 and 16224 in at least one of their samples. Site 16189 may be of particular interest, as it is found in both DCIS and IBC in every patient. Mutations at position 16270 occur in 80% of the patients studied, but only about one third of these patients had this mutation in both histopathologies. 37.5% of the patients had this mutation in DCIS only, and 37.5% had this mutation in IBC exclusively. Three other sites, 16223, 16270, and 16291, occur in 8 patients, 2 sites (16311, 16362) in 7 patients, 1 site (16390) in 6 patients, 1 site (16304) in 4 patients, 1 site (16126) in 3 patients, and 2 sites (16093 and 16298) in 2 patients. Finally, 6 sites (16188, 16192, 16203, 16249, 16319, and 16357) are exclusive to 6 individual patients.

3.2. Clinical Correlation and Mutation Load. There appears to be no statistically significant correlation between single individual mutation sites and specific gradings; namely, the modified Bloom-Richardson grade, nuclear grade, tubule formation, and mitotic score.

The mutation loads of the IBC and DCIS samples were similar, even though up to a third of the mutations for a given patient differed. The average mutation load per patient was the same.

Considering IBC and DCIS mutation load from a per-site perspective, the two populations strongly correlate ($r = 0.929$, $P < 0.001$), meaning that the mutation load at a given site is consistent, regardless of tissue type. This may imply that the same damage is occurring in both tissues and that the disease processes may be similar.

4. Discussion

The observed frequency of mutations in the study population indicates a medium correlation with the relative mutation rates in HV1. All of the identified sites have estimated relative rates greater than zero, and 65% of the sites are classified as "fast" by multiple studies since they have a greater tendency to mutate than other neighboring sites. Using the same metric (substitution rate >2), 88% of the identified sites could be classified as "fast" [7].

The mutation sites identified by this study appear predisposed towards mutation. Since sites such as 16189 and 16224 are present in almost every patient, they demonstrate near confluence in this small cohort. This is perhaps due to a biological propensity to rapid mutation. As such, this attribute could be used as a breast cancer marker if this behavior is consistent in transforming breast tissue.

These results are consistent with a field effect demonstrated in epithelial tissues in general, including those cells lining the mammary ducts [13]. This field effect was also observed by Xu et al. in a small segment of the D-loop referred to as D310 [14]. This idea is demonstrated in multiple matching heteroplasmic and homoplasmic changes in HV1 in corresponding patient-matched DCIS and IBC samples from 10 patients in the study. A gland-wide influence is further suggested by the results of patients 43 and 74. Here, common mutations are observed in tissues from separate clinical procedures. Patient 43 has 3 mutations which occur in both biopsy and lumpectomy samples, in DCIS and IBC captured from biopsy and DCIS taken from a later lumpectomy. Patient 74 has 5 parallel alterations between IBC and DCIS from biopsy and DCIS recovered after a mastectomy. The IBC from mastectomy share 2 of these sites. This sample also has 2 unique changes.

Unfortunately, only patients 43 and 74 had follow-up procedures allowing this level of comparative analyses. The IBC and DCIS from the remaining 8 study participants were associated with 1 procedure, a biopsy, lumpectomy, or mastectomy. Absence of a 1 : 1 correlation between the mutation patterns of IBC and DCIS for a given patient and between separate procedures is likely a result of capturing ducts from tissue cross-sections and the convoluted anatomy of ductal tissue (i.e., patient 43). The extent and effect of the field may vary among associated, parallel ducts. Also, heteroplasmic signal detection up to 20% may not have been reached in all comparative patient samples.

Both telomere content (TC) and allelic imbalance (AI) have been documented in histologically normal breast tissue at 1 cm from a tumor focus. At 5 cm from a focus, TC and AI reflect normal parameters. This field could be much wider than 1 cm, since data was collected only at 1 and 5 cm intervals [15]. Similar epithelial field attributes have also been noted in lung cancer [16]. Also, extensive cancerization fields have been described in both head and neck cancers (7 cm in diameter) and colon cancer (3–10 cm in diameter) [17, 18]. The size of these fields may depend on the biological characteristics of the specific biomarkers.

It has been reported that D-loop mutations are associated with tumors which are both estrogen and progesterone receptor negative in women 50 years of age or older [18]. That pattern was not seen here which means that the D-loop alterations identified in this study would be suitable for use in a broad age range of women. Moreover, women with alterations in the D-loop experience poorer outcomes than those free of mutations [19]. This suggests that HV1 mutations found in both DCIS and IBC, when found in patients with DICS only, may be indicators of DCIS with potential aggressive behavior.

In other work, NAF was successfully retrieved from 82% of the participants with 96% yielding fluid from both breasts [20]. Given that the alterations displayed by the mtGenome demonstrate a field effect in breast tissue, there is merit in assessing NAF or DL recovered from women with both DCIS and IBC histopathologies. This applies to other abnormal breast histopathologies as well, such as atypical ductal hyperplasia. Both NAF and DL have been investigated as a source of biomarkers and for biological indications of breast cancer [16, 20–31]. Given the high copy number of the mtGenome and its rapid mutation rate, sequence analysis of the D-loop may identify mutations associated with these lesions in glandular organ-associated biofluids which are low in both volume and cellularity. Full mtGenome sequencing was successful for NAF and blood from 19 women referred to a surgical oncologist for a clinical breast examination and who had a nonmalignant outcome. A subset of these patients had a single mutation each (4/19, 21%) in the entire mtGenome. Unfortunately, no follow-up information was

available for these women, and thus, comments regarding the association of the mutations observed with a disease state could not be reported.

5. Conclusions

This study was able to identify mtGenome alterations that occur in both DCIS and IBC within individual patients that are suggestive of a cancerization field effect, and DCIS that may be aggressive in nature. Other work demonstrates that large amounts of genetic information can be recovered from the high-copy-number mtGenome in low volume biofluids [20]. Identification of biomarkers with early detection and/or diagnostic capacity that utilize the mtGenome and its characteristics, in combination with the epithelial field effect and the use of NAF and/or DL as the detection medium, may have important clinical applications. Further studies are warranted to help unravel the mechanisms linking DCIS and IBC, as well as the mechanism that drives the transition from the smaller DCIS lesions to larger IBC lesions.

Conflict of Interests

A. Maggrah, K. Robinson, J. Creed, R. Wittock, H. Brown, A. Harbottle, D. Klein, B. Reguly, and R. Parr work for Mitomics Inc. and A. Harbottle, D. Klein, and R. Parr own stocks in Mitomics Inc.

Acknowledgments

All funding sources are Canadian and contributed equally to this study: Industrial Research Assistance Program, FedNor, Northern Ontario Heritage Foundation, Mitomics Inc.

References

[1] Cancer Facts & Figures Atlanta: American Cancer Society, p. 68, 2008.

[2] D. B. Thomas, D. L. Gao, R. M. Ray et al., "Randomized trial of breast self-examination in Shanghai: final results," *Journal of the National Cancer Institute*, vol. 94, no. 19, pp. 1445–1457, 2002.

[3] D. B. Thomas, D. L. Gao, S. G. Self et al., "Randomized trial of breast self-examination in Shanghai: methodology and preliminary results," *Journal of the National Cancer Institute*, vol. 89, no. 5, pp. 355–365, 1997.

[4] J. E. Joy, E. E. Penhoet, D. B. Petitti et al., Eds., *Saving Women's Lives: Strategies for Improving Breast Cancer Detection and Diagnosis*, National Academies Press, 2005.

[5] H. M. Kuerer, C. T. Albarracin, W. T. Yang et al., "Ductal carcinoma in situ: state of the science and roadmap to advance the field," *Journal of Clinical Oncology*, vol. 27, no. 2, pp. 279–288, 2009.

[6] R. L. Parr, J. P. Jakupciak, M. A. Birch-Machin, and G. D. Dakubo, "The mitochondrial genome: a biosensor for early cancer detection?" *Expert Opinion on Medical Diagnostics*, vol. 1, no. 2, pp. 169–182, 2007.

[7] S. Meyer, G. Weiss, and A. von Haeseler, "Pattern of nucleotide substitution and rate heterogeneity in the hypervariable regions I and II of human mtDNA," *Genetics*, vol. 152, no. 3, pp. 1103–1110, 1999.

[8] R. M. Andrews, I. Kubacka, P. F. Chinnery, R. N. Lightowlers, D. M. Turnbull, and N. Howell, "Reanalysis and revision of the Cambridge reference sequence for human mitochondrial DNA," *Nature Genetics*, vol. 23, no. 2, p. 147, 1999.

[9] R. L. Parr, G. D. Dakubo, K. A. Crandall et al., "Somatic mitochondrial DNA mutations in prostate cancer and normal appearing adjacent glands in comparison to age-matched prostate samples without malignant histology," *The Journal of Molecular Diagnostics*, vol. 8, no. 3, pp. 312–319, 2006.

[10] B. Parfait, P. Rustin, A. Munnich, and A. Rötig, "Co-amplification of nuclear pseudogenes and assessment of heteroplasmy of mitochondrial DNA mutations," *Biochemical and Biophysical Research Communications*, vol. 247, no. 1, pp. 57–59, 1998.

[11] R. L. Parr, J. Maki, B. Reguly et al., "The pseudo-mitochondrial genome influences mistakes in heteroplasmy interpretation," *BMC Genomics*, vol. 7, article 185, 2006.

[12] D. C. Allred, Y. Wu, S. Mao et al., "Ductal carcinoma in situ and the emergence of diversity during breast cancer evolution," *Clinical Cancer Research*, vol. 14, no. 2, pp. 370–378, 2008.

[13] G. D. Dakubo, J. P. Jakupciak, M. A. Birch-Machin, and R. L. Parr, "Clinical implications and utility of field cancerization," *Cancer Cell International*, vol. 7, article 2, 2007.

[14] C. Xu, D. Tran-Thanh, C. Ma et al., "Mitochondrial D310 mutations in the early development of breast cancer," *British Journal of Cancer*, vol. 106, pp. 1506–1511, 2012.

[15] C. M. Heaphy, M. Bisoffi, C. A. Fordyce et al., "Telomere DNA content and allelic imbalance demonstrate field cancerization in histologically normal tissue adjacent to breast tumors," *International Journal of Cancer*, vol. 119, no. 1, pp. 108–116, 2006.

[16] K. Steiling, J. Ryan, J. S. Brody, and A. Spira, "The field of tissue injury in the lung and airway," *Cancer Prevention Research*, vol. 1, no. 6, pp. 396–403, 2008.

[17] B. J. M. Braakhuis, C. R. Leemans, and R. H. Brakenhoff, "Expanding fields of genetically altered cells in head and neck squamous carcinogenesis," *Seminars in Cancer Biology*, vol. 15, no. 2, pp. 113–120, 2005.

[18] T. Tanaka, "Colorectal carcinogenesis: review of human and experimental animal studies," *Journal of Carcinogenesis*, vol. 8, article 5, 2009.

[19] L. M. Tseng, P. H. Yin, C. W. Chi et al., "Mitochondrial DNA mutations and mitochondrial DNA depletion in breast cancer," *Genes Chromosomes and Cancer*, vol. 45, no. 7, pp. 629–638, 2006.

[20] J. P. Jakupciak, A. Maggrah, S. Maragh et al., "Facile whole mitochondrial genome resequencing from nipple aspirate fluid using MitoChip v2.0," *BMC Cancer*, vol. 8, article 95, 2008.

[21] T. M. Pawlik, H. Fritsche, K. R. Coombes et al., "Significant differences in nipple aspirate fluid protein expression between healthy women and those with breast cancer demonstrated by time-of-flight mass spectrometry," *Breast Cancer Research and Treatment*, vol. 89, no. 2, pp. 149–157, 2005.

[22] S. A. Khan, E. L. Wiley, N. Rodriguez et al., "Ductal lavage findings in women with known breast cancer undergoing mastectomy," *Journal of the National Cancer Institute*, vol. 96, no. 20, pp. 1510–1517, 2004.

[23] K. A. Baltzell, M. Moghadassi, T. Rice, J. D. Sison, and M. Wrensch, "Epithelial cells in nipple aspirate fluid and subsequent breast cancer risk: a historic prospective study," *BMC Cancer*, vol. 8, article 75, 2008.

[24] E. R. Sauter, C. Wagner-Mann, H. Ehya, and A. Klein-Szanto, "Biologic markers of breast cancer in nipple aspirate fluid and nipple discharge are associated with clinical findings," *Cancer Detection and Prevention*, vol. 31, no. 1, pp. 50–58, 2007.

[25] W. Zhu, W. Qin, P. Bradley, A. Wessel, C. L. Puckett, and E. R. Sauter, "Mitochondrial DNA mutations in breast cancer tissue and in matched nipple aspirate fluid," *Carcinogenesis*, vol. 26, no. 1, pp. 145–152, 2005.

[26] J. Li, J. Zhao, X. Yu et al., "Identification of biomarkers for breast cancer in nipple aspiration and ductal lavage fluid," *Clinical Cancer Research*, vol. 11, no. 23, pp. 8312–8320, 2005.

[27] W. L. Buntain, M. M. Woolley, G. H. Mahour et al., "Pulmonary sequestration in children: a twenty five year experience," *Surgery*, vol. 81, no. 4, pp. 413–420, 1977.

[28] W. C. Dooley, B. M. Ljung, U. Veronesi et al., "Ductal lavage for detection of cellular atypia in women at high risk for breast cancer," *Journal of the National Cancer Institute*, vol. 93, no. 21, pp. 1624–1632, 2001.

[29] E. R. Sauter, H. Ehya, J. Babb et al., "Biologic markers of risk in nipple aspirate fluid are associated with residual cancer and tumour size," *British Journal of Cancer*, vol. 81, no. 7, pp. 1222–1227, 1999.

[30] E. R. Sauter, E. Ross, M. Daly et al., "Nipple aspirate fluid: a promising non-invasive method to identify cellular markers of breast cancer risk," *British Journal of Cancer*, vol. 76, no. 4, pp. 494–501, 1997.

[31] M. R. Wrensch, N. L. Petrakis, E. B. King et al., "Breast cancer incidence in women with abnormal cytology in nipple aspirates of breast fluid," *American Journal of Epidemiology*, vol. 135, no. 2, pp. 130–141, 1992.

Hindawi Publishing Corporation
BioMed Research International
Volume 2013, Article ID 825065, 8 pages
http://dx.doi.org/10.1155/2013/825065

Review Article

Oxidative Stress Induces Mitochondrial DNA Damage and Cytotoxicity through Independent Mechanisms in Human Cancer Cells

Yue Han and Junjian Z. Chen

Division of Urology, Department of Surgery, Research Institute of McGill University Health Center, Room R1-107, 1650 Cedar Avenue, Montreal, QC, Canada H3G 1A4

Correspondence should be addressed to Junjian Z. Chen; junjian.chen@mcgill.ca

Received 9 June 2012; Revised 22 August 2012; Accepted 23 August 2012

Academic Editor: Ryan Parr

Intrinsic oxidative stress through increased production of reactive oxygen species (ROS) is associated with carcinogenic transformation, cell toxicity, and DNA damage. Mitochondrial DNA (mtDNA) is a natural surrogate to oxidative DNA damage. MtDNA damage results in the loss of its supercoiled structure and is readily detectable using a novel, supercoiling-sensitive real-time PCR method. Our studies have demonstrated that mtDNA damage, as measured by DNA strand breaks and copy number depletion, is very sensitive to exogenous H_2O_2 but independent of endogenous ROS production in both prostate cancer and normal cells. In contrast, aggressive prostate cancer cells exhibit a more than 10-fold sensitivity to H_2O_2-induced cell toxicity than normal cells, and a cascade of secondary ROS production is a critical determinant to the differential response. We propose a new paradigm to account for different mechanisms governing cellular oxidative stress, cell toxicity, and DNA damage with important ramifications in devising new techniques and strategies in prostate cancer prevention and treatment.

1. Introduction

Persistent oxidative stress due to reactive oxygen species (ROS) has been associated with carcinogenesis and cancer progression [1–3], along with various aggressive cancer cell phenotypes [4]. The superoxide anion ($O_2^{\bullet -}$), the primary type of ROS generated through various cellular metabolic pathways and through exposure to ionizing radiation [5], is converted into hydrogen peroxide (H_2O_2) and hydroxyl radical ($OH^{\bullet}$) via biological and antioxidant processes within the cell [6]. The hydroxyl radical, generated through the Fenton, or Haber-Weiss, reaction, is more reactive than either superoxide or hydrogen peroxide and causes direct damage to DNA and other macromolecules [7–9], resulting in DNA strand breaks and mutations.

The electron transport chain (ETC), one of the intracellular sources of ROS production, is located in the inner mitochondrial membrane and involved in the production of cellular energy through oxidative phosphorylation [10, 11]. Due to its proximity to the ETC, mitochondrial DNA (mtDNA) is sensitive to oxidative stress-related damage, which may be responsible for altered mitochondrial gene expression and somatic mutations in many human cancers [12–16]. A mitochondrial mutator phenotype has been proposed to account for the accumulation of extensive somatic mutations in clinical tumors [17]. Mitochondrial DNA is a supercoiled, closed-circular molecule with multiple copies and an average of 100 negatively superhelical turns [18]. The supercoiled structure has been identified as a functional substrate for mtDNA replication and transcription initiation in cells [19–21]. It is thus logical that disruptions to the supercoiled structure (i.e., strand breaks) would have direct effects on mitochondrial bioenergetics and mutagenesis.

In addition to DNA damage, cellular ROS can also induce cell proliferation and toxicity. The high levels of ROS generation and accumulation can lead to cell toxicity and death, making some tumor cells possible targets for ROS-induced apoptosis [22, 23], while the low levels of ROS activate signal pathways that lead to cell growth and proliferation [24]. Many human cancer cells, such as prostate, breast, colon, and

malignant mesothelioma, as well as mouse colon and liver hepatoma, are shown to have increased levels of indigenous ROS and are thus under persistent oxidative stress [4, 25–27]. This may be due to upregulation of membrane-bound NAD(P)H oxidases (NOX) [28], altered energy metabolism associated with mitochondrial dysfunction [12, 29–32], and reduced antioxidant activities in superoxide dismutase and GSH pathways [6, 25]. Therefore, a bell-shaped response curve has been proposed to account for the relationship between the level of ROS and the rate of cell proliferation [25]. The increased baseline levels of ROS in tumor cells can lead to differential responses to further oxidative injury as compared to normal cells [25, 33].

In this paper, we will introduce the use of real-time PCR as a new method of assessing mitochondrial DNA damage through quantification of damaged forms (relaxed circular and linear) of supercoiled mtDNA, a concept previously introduced by our group [34]; examine some surprising interactions among cytotoxicity, ROS production, and oxidative DNA damage in prostate cancer and normal cells [33]; propose a new paradigm to explain these intriguing phenomena.

2. A Novel Method for Sensitive Quantification of mtDNA Damage, Repair, and Copy Number Change

The real-time PCR is a valuable tool often used to quantify starting amounts of nucleic acids in a PCR reaction without post-PCR manipulation [35, 36]. For mtDNA quantification, the relative mtDNA content is calculated as the ratio of mtDNA versus a reference nuclear gene. However, we have previously shown that different structural conformations of mtDNA (supercoiled, nicked circular, linear) have different effects on real-time PCR quantification [34]. Based on this observation, we have developed a supercoiling-sensitive quantitative PCR assay (ss-qPCR) to quantify oxidative damage in the supercoiled DNA [34, 37].

The principle of this new approach can be illustrated by model molecules. The supercoiled pBR322 plasmid DNA is previously shown to be a reliable model for mtDNA conformational studies [38]. In a comparative analysis undertaken previously [34], both supercoiled DNA molecules were digested with enzymes that altered their supercoiled DNA structure. pBR322 was treated with EcoR 1 (a single restriction site in pBR322 DNA) to generate its linear form and with N.BstNB1 (two nicking sites in pBR322 DNA) to generate a nicked (or relaxed) circular form. Total genomic DNA (containing mtDNA) from the LNCaP cells, a type of androgen responsive prostate cancer cell, was treated with EcoR 1 to linearize mtDNA. Together, two nuclear DNA, multiple mtDNA, and two plasmid DNA markers were analyzed for real-time PCR amplification using the MyiQ real-time PCR system as well as the SYBR Green I intercalation dye [34]. In this analysis, we observed that there was a 6-fold increase in the amplification of nicked circular and linear forms of plasmid DNA as compared to its untreated and supercoiled form and a 2-fold increase in the amplification of the closed-circular form of DNA when the same amount of starting template material was used (see Figure 1C in [34]). A 2-fold increase in amplification was observed in EcoR-1-treated mtDNA as compared to amplification of its untreated form in the same study. We concluded that the negatively supercoiled structure of DNA was a poor substrate for real-time PCR amplification and that a disruption of the supercoiled structure by either cutting (producing a linear molecule) or nicking (nicked circular form produced by single-strand breaks) the double-stranded molecule significantly increased the efficiency of qPCR amplification. As such, amplification efficiency can be used to determine the degree to which a supercoiled DNA sample is damaged. A heat-denaturing step at the onset of qPCR amplification can be used to introduce strand breaks into all initial mtDNA, thus enabling accurate measurement of total initial mtDNA copy number in a sample without interference from the supercoiled structure. Coupled with the quantification of DNA structural damage, the percentage of damaged mtDNA in a total sample can be calculated and the degree of oxidative stress the cell is subjected to can be inferred. A quantitative evaluation of mtDNA degradation through copy number loss can also be achieved with qPCR.

While useful, the ss-qPCR protocol used for the quantification of mtDNA damage has the potential of introducing artificial strand breaks into the sample. The initial heat-denaturing step at 95°C for three minutes, while necessary to initiate the amplification process, was observed to significantly increase qPCR amplification in mtDNA [34]. In an effort to reduce artifact, we subsequently developed a new two-step qPCR protocol with a shortened initial denaturing time at 95°C followed by a significantly lowered denaturing temperature of 80°C for the remaining cycles [33]. This 2-step procedure, by reducing both the duration and intensity of heat imposed upon the DNA substrates, led to a reduced baseline reading of mtDNA damage and increased sensitivity with regard to detecting induced mtDNA damage in different prostate cell lines. Indeed, an almost 2-fold decrease in baseline mtDNA damage levels from 44.2% to 24.6% was detected between the regular protocol and the new two-step protocol (Figure 1(a)) (Figure 1A in [33]).

The total mtDNA content per cell for different prostate cell lines and the number of damaged (or relaxed) mtDNA copies per cell can be determined using an absolute quantification approach (Figure 1(b)) (Figure 1B in [33]). Although the absolute number of mtDNA copies varies significantly, the percentage of damaged mtDNA is relatively stable across cell lines (Figure 1(c)). As such, we propose to present the level of mtDNA damage as the percentage of damaged mtDNA in the total DNA content as opposed to the absolute number of damaged molecules. Since different cell lines have different amount of mitochondria and mtDNA damage is induced within each mitochondrion, cell lines with increased levels of mitochondria may exhibit greater absolute mtDNA damage when in fact each mitochondrion has the same amount of DNA damage. Thus, the percentage of damaged mtDNA is independent from the mitochondrial content in each cell. This provides a method of evaluating the constitutively different cell lines and tissues on equal footing and gives

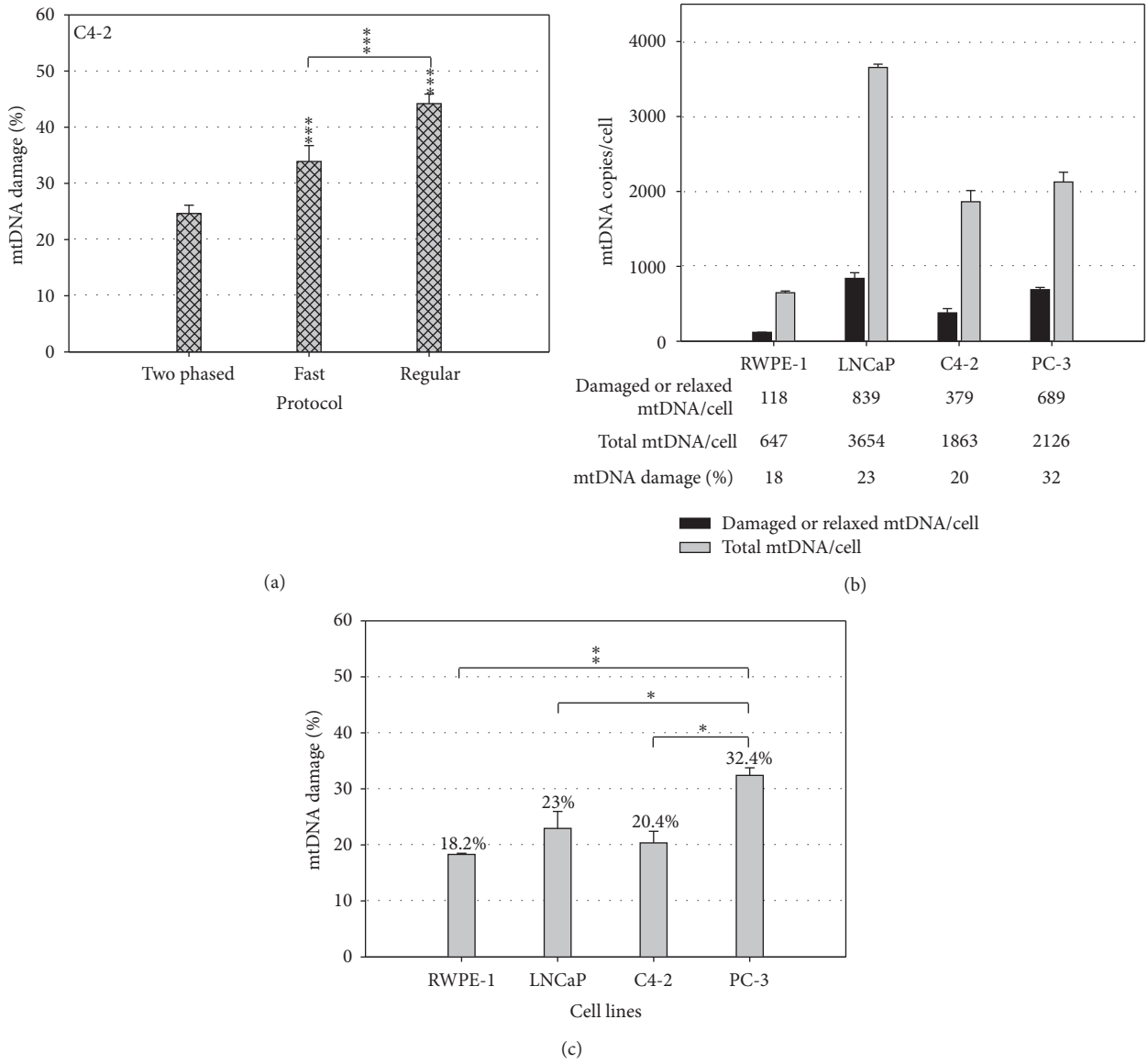

Figure 1: Two-phased, supercoiling-sensitive qPCR for improved mtDNA damage detection [33]. The percentage of relaxed/damaged mtDNA in C4-2 cancer cell line detected by a two-phased protocol and protocols previously reported as Fast and Regular ones (a). The absolute copy numbers of damaged and total mtDNA molecules were detected in normal RWPE-1 and three prostate cancer cell lines (LNCaP, C4-2, and PC-3) (b). The basal levels of mtDNA damage were calculated as the ratio of damaged versus total mtDNA copy numbers (c). Student's t-test was used for significant analysis. ($^{*}P < 0.05$, $^{**}P < 0.01$).

a more accurate view into oxidative mtDNA damage between tumor and normal cells.

3. Differential Responses to Oxidative Injury between Prostate Cancer and Normal Cells

It is increasingly recognized that cellular ROS have a signaling role in stimulating cancer growth [2]. Therefore, intrinsic oxidative stress through enhanced levels of endogenous ROS in prostate and other cancers may be a phenotype actively selected for in cancer progression. However, which cellular processes contribute to ROS propagation in cancer and how such changes modify cancer cell responses to further oxidant injury remain to be fully elucidated. Using H_2O_2 as an exogenous stimulus, we previously investigated differential responses to cell toxicity, cellular ROS production, and oxidative DNA damage between prostate cancer and normal cell lines [33]. We demonstrated that aggressive prostate cancer cells exhibited a low threshold effect and increased susceptibility to extrinsic oxidative injury. Using the MTT assay, small amounts of exogenous H_2O_2 caused significant early redox damage and late cytotoxicity in androgen-insensitive and highly aggressive cancer cells (C4-2, PC-3) and, to a lesser extent, in androgen-sensitive cancer cells (LNCaP). However, higher doses of H_2O_2 were required to trigger transient cytotoxic effects in immortalized prostate epithelial

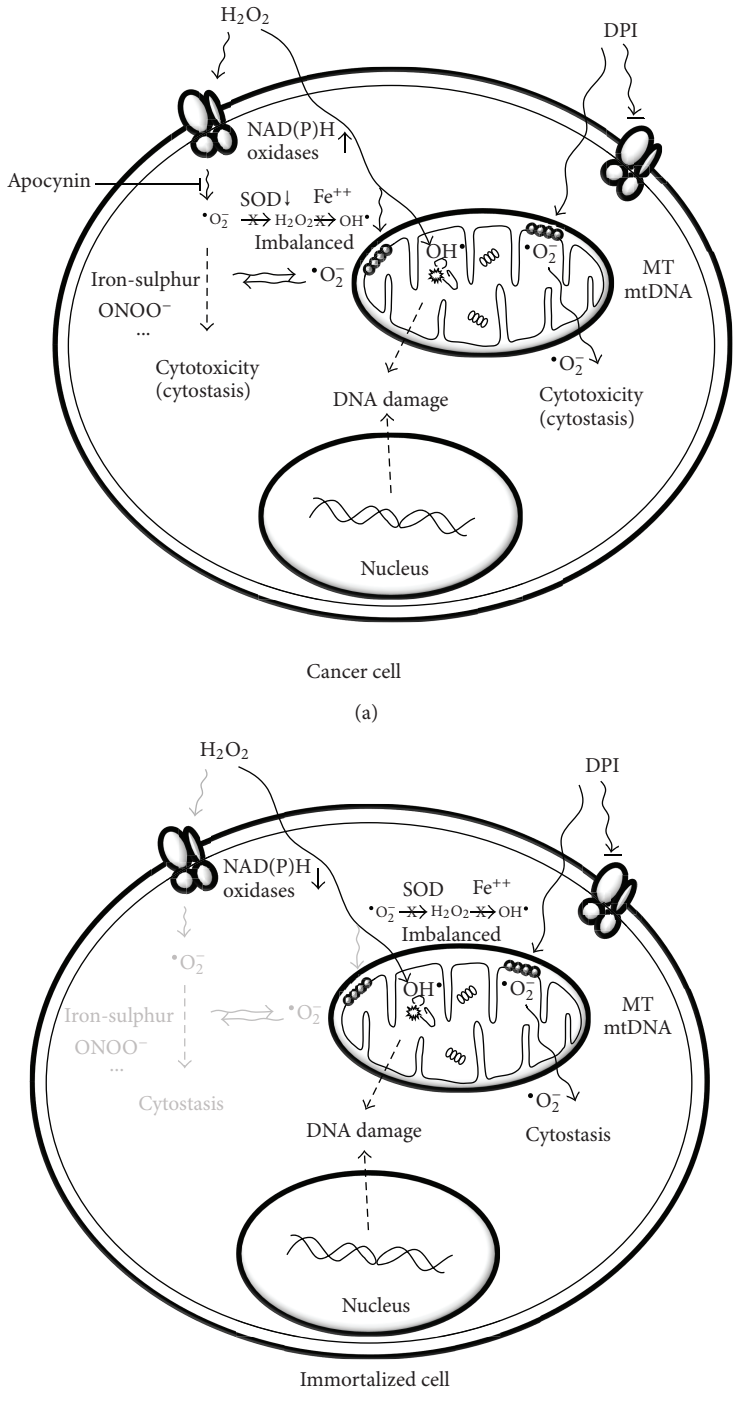

Figure 2: A new paradigm of oxidative injury in prostate cancer versus normal cells. Aggressive prostate cancer cells exhibit increased susceptibility to oxidant injury and DNA damage through independent mechanisms (a). See text for details. Immortalized epithelial cells are resistant to H_2O_2-induced cell toxicity but sensitive to oxidative DNA damage (b). The strong resistance is correlated to a lack of sustained $O_2^{\bullet-}$ production through NAD(P)H oxidases, while the sensitive mtDNA damage is due to direct infiltration of H_2O_2 and its $HO^{\bullet}$ derivative.

cells (RWPE-1), as evidenced by a 10-fold difference in 50% growth inhibition (EC_{50}) values between RWPE-1 and C4-2 cell lines [33].

Using the $O_2^{\bullet-}$ specific fluorescent probe dihydroethidium (DHE), the basis of increased susceptibility to oxidative injury was shown to be associated with both a high level of endogenous $O_2^{\bullet-}$ and a marked induction of secondary $O_2^{\bullet-}$ production in aggressive cancer cells. Indeed, we found that the isogenic LNCaP and C4-2 cells had over 5-fold higher basal ROS levels, and PC-3, 3-fold higher levels, when

compared to RWPE-1 [33]. In addition, low H_2O_2 doses induced persistent secondary $O_2^{\bullet-}$ generation in tumor cells, yet high doses only produced transient secondary $O_2^{\bullet-}$ propagation in normal cells. These findings point to a new mechanism by which exogenous H_2O_2 exerts its differential effects by triggering a sustained $O_2^{\bullet-}$ propagation that amplifies cell toxicity in aggressive prostate cancer cells.

Cellular $O_2^{\bullet-}$ is the first line of ROS production of several processes, including upregulation of membrane-bound NAD(P)H oxidases and alterations in mitochondrial respiration. We further demonstrated that the H_2O_2-induced $O_2^{\bullet-}$ propagation specific to aggressive cancer cells is likely associated with the activation of NAD(P)H oxidases. Indeed, apocynin, a specific inhibitor of NAD(P)H oxidases, markedly reduced H_2O_2-induced $O_2^{\bullet-}$ propagation and cytotoxicity in aggressive C4-2 cells [33]. This finding is consistent with the stimulating effect of H_2O_2 on NAD(P)H oxidases-mediated $O_2^{\bullet-}$ production reported in human SMC, endothelial and cancer cells [39–41], and is further supported by upregulation of several isoforms of NAD(P)H oxidases in prostate cancer cell lines and tumor tissues [4, 28]. It is interesting to point out that other sources of $O_2^{\bullet-}$ production downstream of NAD(P)H oxidases may be required to maintain persistent $O_2^{\bullet-}$ accumulation in aggressive cancer cells, such as impaired mitochondrial respiration and oxidative DNA damage. Thus, upregulation of NAD(P)H oxidases likely confers an increased metastatic potential through enhanced levels of endogenous ROS in aggressive cancer cells, but subjects the same cells to increased susceptibility to oxidant toxicity through NAD(P)H oxidases-mediated $O_2^{\bullet-}$ burst.

4. mtDNA Damage Is Sensitive to Exogenous H_2O_2 but Independent of Cellular ROS Production

The mitochondrion is both a major source of ROS production and a primary target of oxidative damage in the cell. The supercoiled mtDNA serves as a natural surrogate to oxidative DNA damage due to its close proximity to the site of ROS production [34]. The supercoiling-sensitive qPCR method provides a new opportunity to investigate whether oxidative DNA damage contributes to H_2O_2-induced differential cell toxicity or associates with cellular ROS production [33]. As elucidated in the MTT assay, H_2O_2 exposure yielded EC_{50} values of 46–112 μM for prostate cancer cells (i.e., C4-2, PC-3, LNCaP) and 470 μM for RWPE-1 cells after 24 h treatment, equating to a much higher resistance to oxidative stress-related cytotoxicity in normal cells when compared with cancer cell lines. However, when treated with subtoxic levels of H_2O_2 (30 μM), RWPE-1 cells exhibited significant mtDNA damage, which increased dose-dependently with treatments of up to 240 μM for 1 h. Administration of 120 μM H_2O_2 resulted in more than 80% early structural mtDNA damage in RWPE-1 cells and induced a more than 10-fold copy number reduction in 24 h recovery, although noticeable supercoiled-structure recovery in mtDNA was also observed. Furthermore, application of 30–240 μM H_2O_2 to C4-2 cells also resulted in prominent mtDNA damage and copy number loss. As such, exogenous H_2O_2 was shown to cause a very dynamic process with mtDNA damage, repair, and copy number depletion cooccurring in both prostate cancer and normal cell lines, which is in direct contrast with the differing effect it had on EC_{50} values in the different cell types. Therefore, mtDNA damage is prevalent in all cell lines but not correlated to the differential cytotoxicity between prostate cancer and normal cell lines induced by exogenous H_2O_2. However, it remains to be illustrated if this conclusion applies to individual cell by cell basis.

This surprising finding also suggests that acute mtDNA damage requires the presence of H_2O_2 and its $HO^{\bullet}$ derivative, but is independent of cellular $O_2^{\bullet-}$ production in prostate cell lines. This observation is further supported by the lack of induced mtDNA damage in both C4-2 and RWPE-1 cell lines when treated by $O_2^{\bullet-}$-producing agents, diphenyleneiodonium (DPI), and rotenone [33]. DPI is known to reduce $O_2^{\bullet-}$ production by inhibiting NAD(P)H oxidases but to increase cellular $O_2^{\bullet-}$ by impairing mitochondrial respiration depending on the dose and cell type used [42–44]. We demonstrated that DPI induced dose-dependent ROS production and growth inhibition in C4-2 and RWPE-1 cell lines. However, no effect was detected on either mtDNA structural damage or copy number change in both cell lines treated by DPI [33]. This result was further corroborated by the rotenone treatment that targeted specifically complex 1 of the mitochondrial ETC [33]. It is conceivable that DPI induces imbalanced $O_2^{\bullet-}$ accumulation without being converted to $HO^{\bullet}$ through H_2O_2. Indeed, DPI has been shown to induce $O_2^{\bullet-}$ production in many cell types [43, 44] but to suppress H_2O_2 production in several prostate cancer cell lines [4] and in the mitochondria of rat skeletal muscle [45]. Thus, contrary to the common assumption that cellular $O_2^{\bullet-}$ is tightly balanced with H_2O_2 in a cell, we suggest that imbalanced accumulation of different ROS species may occur under stressed conditions, leading to very different functional consequences.

5. A New Paradigm of Oxidative Injury and Its Implications

We propose a new paradigm of oxidative injury in prostate cancer cells (Figure 2). Aggressive cancer cells exhibit intrinsic oxidative stress based on the type and source of different ROS [4, 6, 12, 25–32]. We have demonstrated that H_2O_2 exposure induces differential cell toxicity and sensitive oxidative DNA damage in prostate cancer cells through different mechanisms. A cascade of cellular $O_2^{\bullet-}$ production is shown to be a critical determinant of selective toxicity in aggressive cancer cells [33], which is mediated by the activation of elevated NAD(P)H oxidases [28] and by crosstalk with impaired mitochondrial respiration in cancer cells [13] (Figure 2(a)). Conversely, the resistance to H_2O_2-induced cytotoxicity in normal cells may be attributed to a low cellular level of NAD(P)H oxidases and the normal mitochondrial function (Figure 2(b)). On the other hand, a significant level of oxidative DNA damage is induced by exogenous H_2O_2 in both cancer and normal cells, but is independent of cellular $O_2^{\bullet-}$

steady-state levels. We propose that selective accumulation of cellular $O_2^{\bullet-}$ (e.g., DPI) is cytotoxic regardless of cell types [43] but is independent to $HO^{\bullet}$-mediated DNA damage [33]. The $O_2^{\bullet-}$ accumulation may be exacerbated by a difference in the rate of $O_2^{\bullet-}$ accumulation and conversion to H_2O_2 and $HO^{\bullet}$ in stressed cancer cells. Alternatively, $O_2^{\bullet-}$ may be metabolized promptly with other reactive species such as nitric oxide (NO). NO is shown to interact with $O_2^{\bullet-}$ to generate peroxynitrite anions (ONOO-) and nitrogen oxides (NO_x) [22], which could attenuate the formation of the highly reactive $HO^{\bullet}$ and oxidative DNA damage.

The new paradigm has important implications in designing new strategies in cancer prevention and therapy. Selective production of cellular $O_2^{\bullet-}$ rather than $HO^{\bullet}$ is a promising strategy for preferential killing of aggressive cancer cells. This can be achieved by targeted activation of NAD(P)H oxidases in prostate cancer cells, which may be further sensitized by modulating other sources of cellular $O_2^{\bullet-}$ production. In contrast, $HO^{\bullet}$ is a potent mutagen that may cause mtDNA damage and copy number depletion under subtoxic conditions; these active responses to DNA damage provide a new explanation to the accumulation of extensive mtDNA damage and somatic mutations in clinical tumors and aging tissues under physiological and/or pathological conditions [11, 17]. Thus, minimizing cellular $HO^{\bullet}$ production is better suited for cancer prevention by reducing the long-term accumulation of oxidative DNA damage and mutagenesis. Besides, the recognition of cellular partitioning and functional separation of major ROS in prostate cancer cells will likely shed new lights on the evolution of aggressive phenotype in prostate cancer. Additional investigations are desirable to test the applicability of the implications in other human cancers.

The development of a very sensitive approach to analyze structure-mediated DNA damage using real-time PCR provides a powerful, quantitative new approach to the study of mtDNA damage, repair, and copy number change in a single test [34]. This quantitative approach is in contrast to the semiquantitative analysis on mtDNA structural damage based on gel electrophoresis and southern blot [46]. Therefore, this new technical platform may find broad applications to study oxidative stress in cultured cells, clinical samples, and model animals. Indeed, mtDNA may serve as a sensitive surrogate for precise quantification of oxidative DNA damage locally in diseased tissues and systemically in circulating blood of cancer patients. We have developed a comprehensive strategy to measure multiple mtDNA endpoints in circulating lymphocytes to study systemic stress in clinical investigations [47] and to study the influence of microsurgical varicocelectomy on human sperm mtDNA copy number [48]. Finally, this method also has the potential to quantify specific oxidative base lesions accumulated in supercoiled mtDNA when coupled with lesion-specific repair enzymes.

6. Conclusion

Cellular ROS are natural byproducts of metabolic processes, but persistent accumulation of ROS can lead to cellular oxidative injury, including DNA damage and cell toxicity. Damage to mtDNA results in the loss of its supercoiled structure, which is readily detectable with a two-step, supercoiling-sensitive qPCR assay. Our previous studies have demonstrated that mtDNA damage is very sensitive to exogenous H_2O_2 but independent of endogenous ROS accumulation in both prostate cancer and normal cells. In contrast, aggressive prostate cancer cells exhibit a more than 10-fold sensitivity to H_2O_2-induced cell toxicity than normal cells, suggesting a very different mechanism of action. We propose a new paradigm to account for different mechanisms governing oxidative stress, cell toxicity and DNA damage with important ramifications in devising new techniques and strategies in cancer prevention and treatment.

Acknowledgments

This work was supported by a Canada Foundation for Innovation Grant (no. 11623) and the McGill Urology Research Funds to J. Z. Chen.

References

[1] A. L. Jackson and L. A. Loeb, "The contribution of endogenous sources of DNA damage to the multiple mutations in cancer," *Mutation Research*, vol. 477, no. 1-2, pp. 7–21, 2001.

[2] M. Benhar, D. Engelberg, and A. Levitzki, "ROS, stress-activated kinases and stress signaling in cancer," *EMBO Reports*, vol. 3, no. 5, pp. 420–425, 2002.

[3] L. Behrend, G. Henderson, and R. M. Zwacka, "Reactive oxygen species in oncogenic transformation," *Biochemical Society Transactions*, vol. 31, no. 6, pp. 1441–1444, 2003.

[4] B. Kumar, S. Koul, L. Khandrika, R. B. Meacham, and H. K. Koul, "Oxidative stress is inherent in prostate cancer cells and is required for aggressive phenotype," *Cancer Research*, vol. 68, no. 6, pp. 1777–1785, 2008.

[5] K. J. A. Davies, "The broad spectrum of responses to oxidants in proliferating cells: a new paradigm for oxidative stress," *IUBMB Life*, vol. 48, no. 1, pp. 41–47, 1999.

[6] V. J. Thannickal and B. L. Fanburg, "Reactive oxygen species in cell signaling," *American Journal of Physiology*, vol. 279, no. 6, pp. L1005–L1028, 2000.

[7] M. Dizdaroglu, G. Rao, B. Halliwell, and E. Gajewski, "Damage to the DNA bases in mammalian chromatin by hydrogen peroxide in the presence of ferric and cupric ions," *Archives of Biochemistry and Biophysics*, vol. 285, no. 2, pp. 317–324, 1991.

[8] J. A. Imlay, S. M. Chin, and S. Linn, "Toxic DNA damage by hydrogen peroxide through the fenton reaction in vivo and in vitro," *Science*, vol. 240, no. 4852, pp. 640–642, 1988.

[9] B. Halliwell and J. M. C. Gutteridge, *Free Radicals in Biology and Medicine*, Clarendon Press, Oxford, UK, 1999.

[10] J. F. Turrens and A. Boveris, "Generation of superoxide anion by the NADH dehydrogenase of bovine heart mitochondria," *Biochemical Journal*, vol. 191, no. 2, pp. 421–427, 1980.

[11] C. Richter, "Oxidative damage to mitochondrial DNA and its relationship to ageing," *International Journal of Biochemistry and Cell Biology*, vol. 27, no. 7, pp. 647–653, 1995.

[12] S. Toyokuni, "Persistent oxidative stress in cancer," *FEBS Letters*, vol. 358, no. 1, pp. 1–3, 1995.

[13] P. C. Herrmann, J. W. Gillespie, L. Charboneau et al., "Mitochondrial proteome: altered cytochrome c oxidase subunit levels in prostate cancer," *Proteomics*, vol. 3, no. 9, pp. 1801–1810, 2003.

[14] M. S. Fliss, H. Usadel, O. L. Caballero et al., "Facile detection of mitochondrial DNA mutations in tumors and bodily fluids," *Science*, vol. 287, no. 5460, pp. 2017–2019, 2000.

[15] P. Parrella, Y. Xiao, M. Fliss et al., "Detection of mitochondrial DNA mutations in primary breast cancer and fine-needle aspirates," *Cancer Research*, vol. 61, no. 20, pp. 7623–7626, 2001.

[16] J. Z. Chen, N. Gokden, G. F. Greene, P. Mukunyadzi, and F. F. Kadlubar, "Extensive somatic mitochondrial mutations in primary prostate cancer using laser capture microdissection," *Cancer Research*, vol. 62, no. 22, pp. 6470–6474, 2002.

[17] J. Z. Chen, N. Gokden, G. F. Greene, B. Green, and F. F. Kadlubar, "Simultaneous generation of multiple mitochondrial DNA mutations in human prostate tumors suggests mitochondrial hyper-mutagenesis," *Carcinogenesis*, vol. 24, no. 9, pp. 1481–1487, 2003.

[18] R. Radloff, W. Bauer, and J. Vinograd, "A dye-buoyant-density method for the detection and isolation of closed circular duplex DNA: the closed circular DNA in HeLa cells," *Proceedings of the National Academy of Sciences of the United States of America*, vol. 57, no. 5, pp. 1514–1521, 1967.

[19] D. L. Robberson and D. A. Clayton, "Replication of mitochondrial DNA in mouse L cells and their thymidine kinase—derivatives: displacement replication on a covalently-closed circular template," *Proceedings of the National Academy of Sciences of the United States of America*, vol. 69, no. 12, pp. 3810–3814, 1972.

[20] D. Bogenhagen and D. A. Clayton, "Mechanism of mitochondrial DNA replication in mouse L-cells. Introduction of superhelical turns into newly replicated molecules," *Journal of Molecular Biology*, vol. 119, no. 1, pp. 69–81, 1978.

[21] D. A. Clayton, "Replication of animal mitochondrial DNA," *Cell*, vol. 28, no. 4, pp. 693–705, 1982.

[22] C. Nicco, A. Laurent, C. Chereau, B. Weill, and F. Batteux, "Differential modulation of normal and tumor cell proliferation by reactive oxygen species," *Biomedicine and Pharmacotherapy*, vol. 59, no. 4, pp. 169–174, 2005.

[23] Q. Kong, J. A. Beel, and K. O. Lillehei, "A threshold concept for cancer therapy," *Medical Hypotheses*, vol. 55, no. 1, pp. 29–35, 2000.

[24] R. H. Burdon, "Superoxide and hydrogen peroxide in relation to mammalian cell proliferation," *Free Radical Biology and Medicine*, vol. 18, no. 4, pp. 775–794, 1995.

[25] A. Laurent, C. Nicco, C. Chéreau et al., "Controlling tumor growth by modulating endogenous production of reactive oxygen species," *Cancer Research*, vol. 65, no. 3, pp. 948–956, 2005.

[26] N. Aykin-Burns, I. M. Ahmad, Y. Zhu, L. W. Oberley, and D. R. Spitz, "Increased levels of superoxide and H_2O_2 mediate the differential susceptibility of cancer cells versus normal cells to glucose deprivation," *Biochemical Journal*, vol. 418, no. 1, pp. 29–37, 2009.

[27] E. Ranzato, S. Biffo, and B. Burlando, "Selective ascorbate toxicity in malignant mesothelioma a redox trojan mechanism," *American Journal of Respiratory Cell and Molecular Biology*, vol. 44, no. 1, pp. 108–117, 2010.

[28] S. D. Lim, C. Sun, J. D. Lambeth et al., "Increased Nox1 and hydrogen peroxide in prostate cancer," *Prostate*, vol. 62, no. 2, pp. 200–207, 2005.

[29] O. Warburg, "On the origin of cancer cells," *Science*, vol. 123, no. 3191, pp. 309–314, 1956.

[30] J. S. Penta, F. M. Johnson, J. T. Wachsman, and W. C. Copeland, "Mitochondrial DNA in human malignancy," *Mutation Research*, vol. 488, no. 2, pp. 117–133, 2001.

[31] A. Dorward, S. Sweet, R. Moorehead, and G. Singh, "Mitochondrial contributions to cancer cell physiology: redox balance, cell cycle, and drug resistance," *Journal of Bioenergetics and Biomembranes*, vol. 29, no. 4, pp. 385–392, 1997.

[32] B. N. Ames, M. K. Shigenaga, and T. M. Hagen, "Oxidants antioxidants, and the degenerative diseases of aging," *Proceedings of the National Academy of Sciences of the United States of America*, vol. 85, pp. 6465–6467, 1988.

[33] S. W. Chan, P. N. Nguyen, D. Ayele, S. Chevalier, A. Aprikian, and J. Z. Chen, "Mitochondrial DNA damage is sensitive to exogenous H_2O_2 but independent of cellular ROS production in prostate cancer cells," *Mutation Research*, vol. 716, pp. 40–50, 2011.

[34] J. Chen, F. F. Kadlubar, and J. Z. Chen, "DNA supercoiling suppresses real-time PCR: a new approach to the quantification of mitochondrial DNA damage and repair," *Nucleic Acids Research*, vol. 35, no. 4, pp. 1377–1388, 2007.

[35] R. Higuchi, C. Fockler, G. Dollinger, and R. Watson, "Kinetic PCR analysis: real-time monitoring of DNA amplification reactions," *Bio/Technology*, vol. 11, no. 9, pp. 1026–1030, 1993.

[36] C. A. Heid, J. Stevens, K. J. Livak, and P. M. Williams, "Real time quantitative PCR," *Genome Research*, vol. 6, no. 10, pp. 986–994, 1996.

[37] S. W. Chan and J. Z. Chen, "Measuring mtDNA damage using a supercoiling-sensitive qPCR approach," *Methods in Molecular Biology*, vol. 554, pp. 183–197, 2009.

[38] M. Yaffee, P. Walter, C. Richter, and M. Müller, "Direct observation of iron-induced conformational changes of mitochondrial DNA by high-resolution field-emission in-lens scanning electron microscopy," *Proceedings of the National Academy of Sciences of the United States of America*, vol. 93, no. 11, pp. 5341–5346, 1996.

[39] W. G. Li, F. J. Miller, H. J. Zhang, D. R. Spitz, L. W. Oberley, and N. L. Weintraub, "H_2O_2-induced O_2.- production by a non-phagocytic NAD(P)H oxidase causes oxidant injury," *Journal of Biological Chemistry*, vol. 276, no. 31, pp. 29251–29256, 2001.

[40] C. H. Coyle, L. J. Martinez, M. C. Coleman, D. R. Spitz, N. L. Weintraub, and K. N. Kader, "Mechanisms of H_2O_2-induced oxidative stress in endothelial cells," *Free Radical Biology and Medicine*, vol. 40, no. 12, pp. 2206–2213, 2006.

[41] B. M. Boulden, J. D. Widder, J. C. Allen et al., "Early determinants of H_2O_2-induced endothelial dysfunction," *Free Radical Biology and Medicine*, vol. 41, no. 5, pp. 810–817, 2006.

[42] A. R. Cross and O. T. G. Jones, "The effect of the inhibitor diphenylene iodonium on the superoxide-generating system of neutrophils. Specific labelling of a component polypeptide of the oxidase," *Biochemical Journal*, vol. 237, no. 1, pp. 111–116, 1986.

[43] N. Li, K. Ragheb, G. Lawler et al., "DPI induces mitochondrial superoxide-mediated apoptosis," *Free Radical Biology and Medicine*, vol. 34, no. 4, pp. 465–477, 2003.

[44] C. Riganti, E. Gazzano, M. Polimeni, C. Costamagna, A. Bosia, and D. Ghigo, "Diphenyleneiodonium inhibits the cell redox metabolism and induces oxidative stress," *Journal of Biological Chemistry*, vol. 279, no. 46, pp. 47726–47731, 2004.

[45] A. J. Lambert, J. A. Buckingham, H. M. Boysen, and M. D. Brand, "Diphenyleneiodonium acutely inhibits reactive oxygen species production by mitochondrial complex I during reverse, but not forward electron transport," *Biochimica et Biophysica Acta*, vol. 1777, no. 5, pp. 397–403, 2008.

[46] P. B. Walter, M. D. Knutson, A. Paler-Martinez et al., "Iron deficiency and iron excess damage mitochondria and mitochondrial DNA in rats," *Proceedings of the National Academy of Sciences of the United States of America*, vol. 99, no. 4, pp. 2264–2269, 2002.

[47] S. W. Chan, *Mitochondrial DNA as a sensitive surrogate to oxidative stress in prostate cancer cells and circulating lymphocytes [M.S. thesis]*, McGill University, 2009.

[48] M. S. Gabriel, S. W. Chan, A. Alhathal, J. Z. Chen, and A. Zini, "Influence of microsurgical varicocelectomy on human sperm mitochondrial DNA copy number: a pilot study," *Journal of Assisted Reproduction and Genetics*, vol. 29, no. 8, pp. 759–764, 2012.

Hindawi Publishing Corporation
BioMed Research International
Volume 2013, Article ID 868131, 10 pages
http://dx.doi.org/10.1155/2013/868131

Research Article

p55PIK Transcriptionally Activated by MZF1 Promotes Colorectal Cancer Cell Proliferation

Yu Deng,[1,2] Jing Wang,[3] Guihua Wang,[1,2] Yuan Jin,[1] Xuelai Luo,[2] Xianmin Xia,[1] Jianping Gong,[2] and Junbo Hu[1,2]

[1] *Molecular Medical Center, Tongji Hospital, Huazhong University of Science and Technology, Wuhan 430030, China*
[2] *Department of Surgery, Tongji Hospital, Huazhong University of Science and Technology, Wuhan 430030, China*
[3] *Department of Immunology, Tongji Medical College, Huazhong University of Science and Technology, Wuhan 430030, China*

Correspondence should be addressed to Junbo Hu; jbhu@tjh.tjmu.edu.cn

Received 6 June 2012; Accepted 31 August 2012

Academic Editor: Ryan Parr

p55PIK, regulatory subunit of class IA phosphatidylinositol 3-kinase (PI3K), plays a crucial role in cell cycle progression by interaction with tumor repressor retinoblastoma (Rb) protein. A recent study showed that Rb protein can localize to the mitochondria in proliferative cells. Aberrant p55PIK expression may contribute to mitochondrial dysfunction in cancer progression. To reveal the mechanisms of p55PIK transcriptional regulation, the p55PIK promoter characteristics were analyzed. The data show that myeloid zinc finger 1, MZF1, is necessary for p55PIK gene transcription activation. ChIP (Chromatin immunoprecipitation) assay shows that MZF1 binds to the cis-element "TGGGGA" in p55PIK promoter. In MZF1 overexpressed cells, the promoter activity, expression of p55PIK, and cell proliferation rate were observed to be significantly enhanced. Whereas in MZF1-silenced cells, the promoter activity and expression of p55PIK and cell proliferation level was statistically decreased. In CRC tissues, MZF1 and p55PIK mRNA expression were increased ($P = 0.046$, $P = 0.047$, resp.). A strong positive correlation ($Rs = 0.94$) between MZF1 and p55PIK mRNA expression was observed. Taken together, we concluded that p55PIK is transcriptionally activated by MZF1, resulting in increased proliferation of colorectal cancer cells.

1. Introduction

Activation of the phosphatidylinositol 3-kinase (PI3K)/AKT pathway is thought to play a crucial role in the development of a variety of human cancers. Several academic efforts are underway to define therapeutic inhibitors of the pathway components [1, 2]. PI3K interacts with phosphatidylinositol-3-phosphate at the cell membrane and catalyzes the phosphorylation of downstream effector(s) such as Akt [1]. Class IA PI3Ks, consisting of a catalytic subunits p110 and regulatory subunit (p85, p55, and p50), play a critical role in cell proliferation and cell survival [3–6].

The p55PIK, also known as p55γ, is encoded by the pik3r3 gene [7, 8]. We previously reported that p55PIK, the N-terminal 24-amino-acid of which is associated with tumor suppressor retinoblastoma protein (Rb), may play an important role in cell cycle control [9]. Ectopic expression of N-terminal 24-amino-acid of p55PIK inhibited cell cycle progression in several cell lines, such as colorectal (HT29) and thyroid (FTC236) cancer cells [10]. One study reported that elevated p55PIK mRNA expression was observed in ovarian, liver, prostate, and breast cancers. A recent study showed that Rb protein can localize to the mitochondria in proliferative cells [11]. Aberrant p55PIK expression may contributes to mitochondrial dysfunction in cancer progression. In addition, apoptosis was observed in p55PIK downregulated ovarian cancer cell lines [12]. Further more, the insulin-like growth factor 2 (IGF2)-p55PIK interaction involved in promoting the growth of a subset of proliferative glioblastomas that lack EGF receptor amplification [13]. These findings suggest that p55PIK was aberrantly expressed in several human cancers and p55PIK may act as an important target for cancer treatment. The detailed mechanism, especially its transcriptional regulation mechanism, remains unknown. Disclosure of the factor(s) that contribute to the regulation of p55PIK expression may be useful in cancer treatment targeting p55PIK.

Table 1: Primers for reporter gene constructs of p55PIK.

Primer name	Sequence
pGL3-p55PIK-(−651/+45) up	5′-TTAATTGGTACCGGTCGGGTTGGTTCTTAC-3′
pGL3-p55PIK-(−839/+45) up	5′-TTAATTGGTACCGAATCCCGGTACATCG-3′
pGL3-p55PIK-(−1064/+45) up	5′-TTAATTGGTACCCACCCACCTTGCCTCT-3′
pGL3-p55PIK-(−1243/+45) up	5′-TTAATTGGTACCCTGCCTTTGTCCCGCTTA-3′
pGL3-p55PIK-(−1633/+45) up	5′-TTAATTGGTACCAGGTGGCAAGTGGGTT-3′
pGL3-p55PIK-shared down	5′-ATATATAGATCTCCAGTCTGCGTCATCG-3′

Several factor(s) have been reported to regulate p55PIK expression in different human disease models, such as mammary cancer [14] and cerebral ischemia-reperfusion [15]. One study has shown that p55PIK expression increased in the presence of doxorubicin, an anthracycline antibiotic that is used abroad in cancer chemotherapy, in breast cancer MDA-MB-231 cells but not in MCF-7 cells [14]. The genetic factors altered in MDA-MB-231 cells, which are p53/estrogen receptor/progesterone receptor negative, may be involved in regulation of p55PIK expression. Another study reported that the Insulin-like growth factor 2 (IGF2) and p55PIK are overexpressed in more proliferative glioblastomas [13]. In fatty acid and cholesterol biosynthesis, Sterol-regulatory element binding protein-1 (REBP-1) and Platelet-derived growth factor (PDGF) induce the expression of p55PIK in AG01518 human foreskin fibroblasts [16]. A recent study revealed that berberine, an effective candidate neuroprotective agent in clinical ischemic stroke, enhances p55PIK promoter activity during cerebral ischemia-reperfusion [15]. In *Mycobacterium tuberculosis* model of WI-38 cells, downregulated p55PIK expression was observed by recombinant *Mycobacterium tuberculosis* CFP-10/ESAT-6 protein treatment [17]. Despite the clarification of these factors, little is known about the mechanism of p55PIK transcriptional regulation.

The aim of the present study is to identify the cis-elements and transcription factor(s) involved in p55PIK transcriptional activation in colorectal cancer cells (CRCs). Firstly, we made *in silico* analysis and deletion analysis of the p55PIK gene promoter and determined the transcriptional factor(s) that may regulate p55PIK transcription. We also evaluated the influence of the transcriptional factors(s) on PI3K expression and the cell growth of CRC cells. Based on the results of this study, the transcription factor(s)-p55PIK axis may be suggested as the potentially crucial target(s) of CRC treatment.

2. Materials and Methods

2.1. Ethics Statement. All research involving human participants has been approved by the Huazhong University of Science and Technology Ethics committee. We obtained informed, written consent from all participants involved in this study.

2.2. Cell Culture and Transfection. Cell lines HepG2, HeLa, SW480, and LoVo were purchased from the American Type Culture Collection (Manassas, VA, USA) and cultured in DMEM supplemented with 10% fetal bovine serum (HyClone, Logan, UT, USA). These cell lines were cultured at 37°C in 5% CO_2/air atmosphere. Transfection was done using Lipofectamine 2000 (Invitrogen, Carlsbad, CA, USA) following the manufacturer's instructions.

2.3. Reporter Constructs and Expression Vectors. DNA fragments containing the same 3′ terminal and different 5′ terminal of p55PIK promoter (Table 1) were amplified by PCR from human genomic DNA and cloned into pGL3 Basic vectors (Promega, Madison, WI, USA) between kpn1 and Bgl II restriction enzyme sites. Reconstructed reporter plasmids were named as (−1633/+45)-p55PIK, (−1243/+45)-p55PIK, (−1064/+45)-p55PIK, (−839/+45)-p55PIK, or (−651/+45)-p55PIK), respectively. Before use, all constructs were verified as correct by sequencing. MZF1 expression vector MZF1-GFP and GFP-control vector were kindly provided by Zhou et al. [18].

2.4. Small Interfering RNA. Synthetic siRNA targeting human MZF1 (RuiBo, Guangzhou, China) was transfected into cultured cells. Transfection was done using Lipofectamine 2000 following manufacturer's instructions. Cells were cultured in 24-well plates in antibiotic-free 10% fetal bovine serum plus medium and transfected with 50 nmol/L siRNA at 70–80% confluency. Expression of MZF1 or p55PIK was detected at 24 h or 48 h after-transfection.

2.5. Site-Directed Mutagenesis. Constructs bearing mutant promoter variants of p55PIK were generated by PCR using the wildtype p55PIK reporter construct (−1243/+45)-p55PIK as template. Underlined nucleotides in Table 2 indicate mutated sequences. Primers were designed according to manufacturer's instructions and produced by Invitrogen. Site-directed mutagenesis was done according to manufacturer's protocol for the Quick Change site-directed mutagenesis kit (Stratagene, La Jolla, CA, USA). All mutants of (−1243/+45)-p55PIK were verified correctly by sequencing.

2.6. Dual-Luciferase Reporter Gene Assay. Cells were seeded in 24-well plates. After culturing for 24 h, cells were cotransfected with luciferase reporter plasmids and *Renilla* vector (pRL-TK) (Promega, Madison, WI, U.S.A). Luciferase activities were measured at 24 h post-transfection, using the Dual-Luciferase Reporter Assay System (Promega, Madison, WI, U.S.A). Luciferase activity was normalized for transfection efficiency using the corresponding *Renilla* luciferase activity. All experiments were performed independently at least four times.

Table 2: Primers for site-directed mutagenesis of construct (−1243/+45) p55PIK.

Name	Sequence change	Sense primer sequence (5′-3′)/antisense primer sequence (5′-3′)
RUNX1-mut	ACCACC to GTGTAT	GCAACCGGCCTCAGCCAATCGTGTATCACCTTGCCTCTCTTCCCTC
		GAGGGAAGAGAGGCAAGGTGATACACGATTGGCTGAGGCCGGTTGC
MZF1-mut1	TGGGGA to CTAGTG	GAAGCCTAGAGAGCGGCTAGTGGACGTGAAAGTCGAG
		CTCGACTTTCACGTCCACTAGCCGCTCTCTAGGCTTC
MZF1-mut2	GGGGG to TAGTC	CGTACCATTCTGATTGAGGCTTAGTCAGAGCGCGGATGGCTGATTGGG
		CCCAATCAGCCATCCGCGCTCTGACTAAGCCTCAATCAGAATGGTACG
MZF1-mut3	TGGGGA to CTAGTG	CGAGAGGCGTGGCTGATCTAGTGGCCGAAGCCTAGAGAGCGG
		CCGCTCTCTAGGCTTCGGCCACTAGATCAGCCACGCCTCTCG
YY1-mut	ACCAT to GTTGA	CCAGCGCCCGGATCGTGTTGATCTGATTGAGGCTGG
		CCAGCCTCAATCAGATCAACACGATCCGGGCGCTGG

2.7. Chromatin Immunoprecipitation (ChIP) Assay. The chromatin immunoprecipitation (ChIP) assay was used to show interactions between transcription factor(s) and p55PIK promoter DNA sequence in CRC cell lines or tissues samples. In brief, chromatin from SW480 cells or CRC tissues was sheared to DNA fragments with an average size of 200–500 bp. After cross-linking reversal and proteinase-K digestion, each individual IP was purified using QIAquick PCR purification kit (Qiagen, Valencia, CA, USA) followed by elution with 50 μL of elution buffer. After elution, IPs were amplified using PCR. To detect the transcription factor(s) binding motif in the p55PIK promoter, we used sense primer 5′-GAAGCCTAGAGAGCGGT-3′ and antisense primer 5′-TGTCAAGTGCCTGAGAAC-3′. MZF1 antibody (Santa Cruz, CA, USA) and control IgG (Santa Cruz, CA, USA) were used to immunoprecipitate the protein-DNA complex.

2.8. Real-Time PCR. The comparative Ct method with SYBR Green was conducted with the ABI 7300 Real-Time PCR System (Applied Biosystems, Foster City, CA, USAs). Forp55PIKdetection, the following primers were used: sense primer 5′-GAGTATGGACCGCGATGA-3′, antisense primer 5′-TTGGCTTAGGTGGCTTTG-3′; MZF1: sense primer 5′-AGTGTAAGCCCTCACCTCC-3′, antisense primer 5′-GGG TCCTGTTCACTCCTCAG-3′; GAPDH sense primer: 5-AACGGATTTGGTCGTATTG-3, antisense primer 5-GAA GATGGTGATGGGATT-3.

2.9. Western Blot Analysis. Cells were washed in cold PBS and incubated with RIPA buffer (Biomed, Beijing, China) for 30 min at 4°C. Cell lysates were centrifuged, and proteins were collected and separated by gel electrophoresis. The PVDF membranes were blocked in 5% (w/v) milk dissolved with PBS-0.1% Tween 20 (PBS-T) for 1 hr at room temperature. Membranes were then incubated with primary antibodies diluted in PBS-T overnight at 4°C. Membranes were washed with PBS-T and incubated with peroxidase-conjugated secondary antibody diluted in PBS-T for 1 hr at room temperature. Membranes were washed in PBS-T; bound antibody was detected with ECL western blotting detection reagents (Thermo Scientific, Rockford, IL, USA). The primary antibody was anti-MZF1, anti-p55PIK, or anti-GAPDH (all purchased from Santa Cruz, Biotechnology, Santa Cruz, CA, USA), respectively. All experiments were repeated 3 times. Protein bands were quantified using Quantity One software (Bio-Rad).

2.10. MTT Assay. For measurements of cell growth, cells were counted manually, plated in triplicate in 96-well plates at 3×10^3 and 1×10^4 cells/well, and transfected with plasmids or SiRNA for 72 h to 96 h; media were then removed and 50 μL of 3-[4,5 dimethylthiazol-2-y]-2,5-diphenyltetrazolium bromide (MTT; Sigma-Aldrich) was added to each well. After incubation for 4h, MTT-containing media were removed, and 100 μL of dimethyl sulfoxide (DMSO) was added to each well. Plates were placed on a plate shaker for 20 mins and the optical density was read immediately at 595 nm/650 nm with a model DTX 880 microplate reader (Beckman Coulter, Fullerton, CA, USA).

2.11. Statistics. All measurements were performed in at least three independent experiments. The means ± SD were calculated. Student's t test was used to compare two independent groups. For all tests, values of $P < .05$ were considered statistically significant.

3. Results and Discussion

3.1. Deletion Analysis of the p55PIK Promoter. p55PIK, the regulatory subunit of class IA phosphatidylinositol 3-kinase (PI3K), plays a crucial role in cell cycle progression. We previously reported that p55PIK, the 24-amino-acid N-terminal end (N24) of which is associated with tumor suppressor retinoblastoma protein (Rb), may play an important role in cell cycle control [9]. A recent study showed that Rb protein can localize to the mitochondria in proliferative cells [11]. Aberrant p55PIK expression may contributes to mitochondrial dysfunction in cancer progression. To reveal the mechanisms of p55PIK transcriptional regulation, the p55PIK promoter characteristics were analyzed.

To identify cis-acting elements within the p55PIK promoter, we constructed a series of luciferase reporter plasmids that contained 5′-deletions of the p55PIK promoter at nucleotides (nt) −1633, −1243, −1064, −839, and −651, with a common 3′-terminus at +45 (Figures 1(a), 1(b)). The promoter activities of the 5′-deletions mutants were assessed by

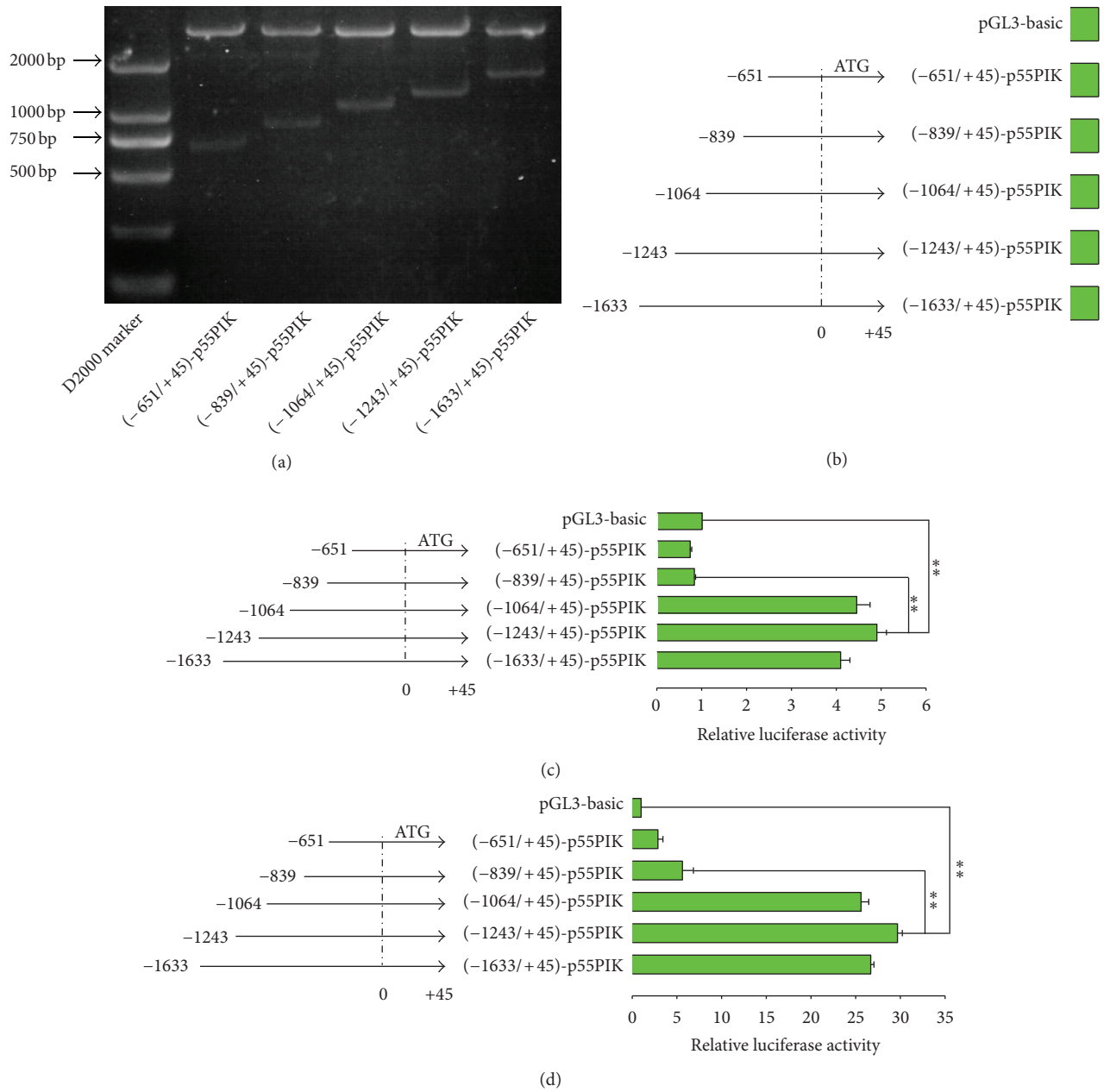

Figure 1: Main p55PIK promoter activity conferred by −1243/−840 upstream region sequence. (a) Series of 5′ end p55PIK promoter recombinant reporter plasmids; (b) DNA fragments with different lengths but with the same 3′ end of p55PIKpromoter cloned into pGL3-Basic reporter plasmids; (c, d) Relative luciferase activity (RLA) of p55PIK reporter plasmids was examined with Dual-Luciferase reporter assay in HepG2 and HeLa cell lines. Data are shown as mean ± SD ($n = 4$; $^{**}P < .01$, per Student's t -test.)

Dual-Luciferase Reporter Assay after transient transfection into two human cell lines: cervical carcinoma HeLa and hepatocellular carcinoma HepG2, which have higher expression of p55PIK than other cell lines (data not shown). The constructs (−839/+45)-p55PIK and (−651/+45)-p55PIK showed similar promoter activity compared with pGL3-Basic vector, whereas the (−1633/+45)-p55PIK, (−1243/+45)-p55PIK, and (−1064/+45)-p55PIK showed higher activities compared with control vector (Figures 1(c), 1(d)). Importantly, most remarkable changes of promoter activity were observed between constructs (−1243/+45)-p55PIK and (−839/+45)-p55PIK. These results suggested that p55PIK promoter activity is largely lost upon deletion of the sequence between −1243 and −839 of the full-length promoter.

The first set of experiments was designed to analyze the characteristics of p55PIK promoter, and to identify the most commonly activated promoter region of p55PIK in cancer cells, we performed luciferase-based reporter assays. The data demonstrate that the full length of p55PIK promoter located at −1243/+45 upstream of the translation start site (ATG)

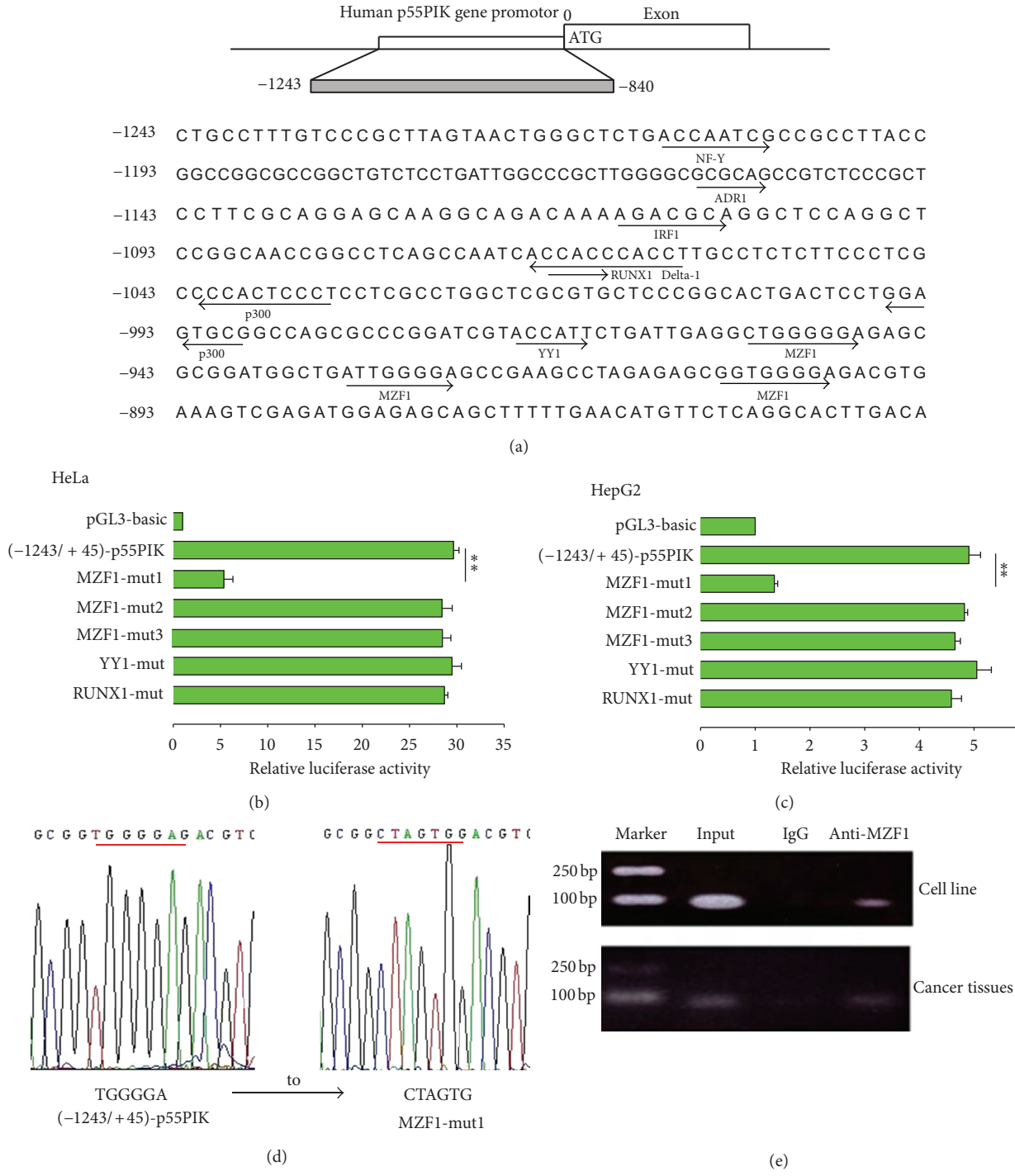

Figure 2: Transcription factor MZF1 binds on site of 5′ end of p55PIK, inducing p55PIK promoter activity. (a) Analysis of the −1243/−840 region, which affects main p55PIK promoter activity and transcription. Several transcription factors, including MZF1, YY1, Runx1, ADR1, IRF1, Delta1, or p300, bind on corresponding domains within p55PIK promoter. (b, c) Relative luciferase activity (RLA) at 24 h after-transfection of a series of mutant constructs of p55PIK reporter plasmids (−1243/+45)-p55PIK, named MZF1-mut1, MZF1-mut2, MZF1-mut3, YY1-mut, and RUNX1-mut are transfected into HepG2 or HeLa cell lines. Data are shown as mean ± SD ($n = 4$; $^{**}P < .01$, per Student's t-test). (Data of ADR1-mut, IRF1-mut, Delta1-mut, p300-mut1, and p300-mut2 are not shown). (d) Sequencing of mutant MZF1-mut1, showing mutagenesis from TGGGGA to CTAGTG at the −901/−896 site, of p55PIK reporter plasmids (−1243/+45)-p55PIK. Sequencing data show that associated binding site was mutated successfully on (−1243/+45)-p55PIK reporter plasmids (data not shown). (e) Transcription factors MZF1 bind to p55PIK promoter region. Chromatin immunoprecipitation (ChIP) assay was used to detect binding between MZF1 protein and TGGGGA sequence located at −901/−896 site of p55PIKpromoter in colon cancer cells and resected tissues.

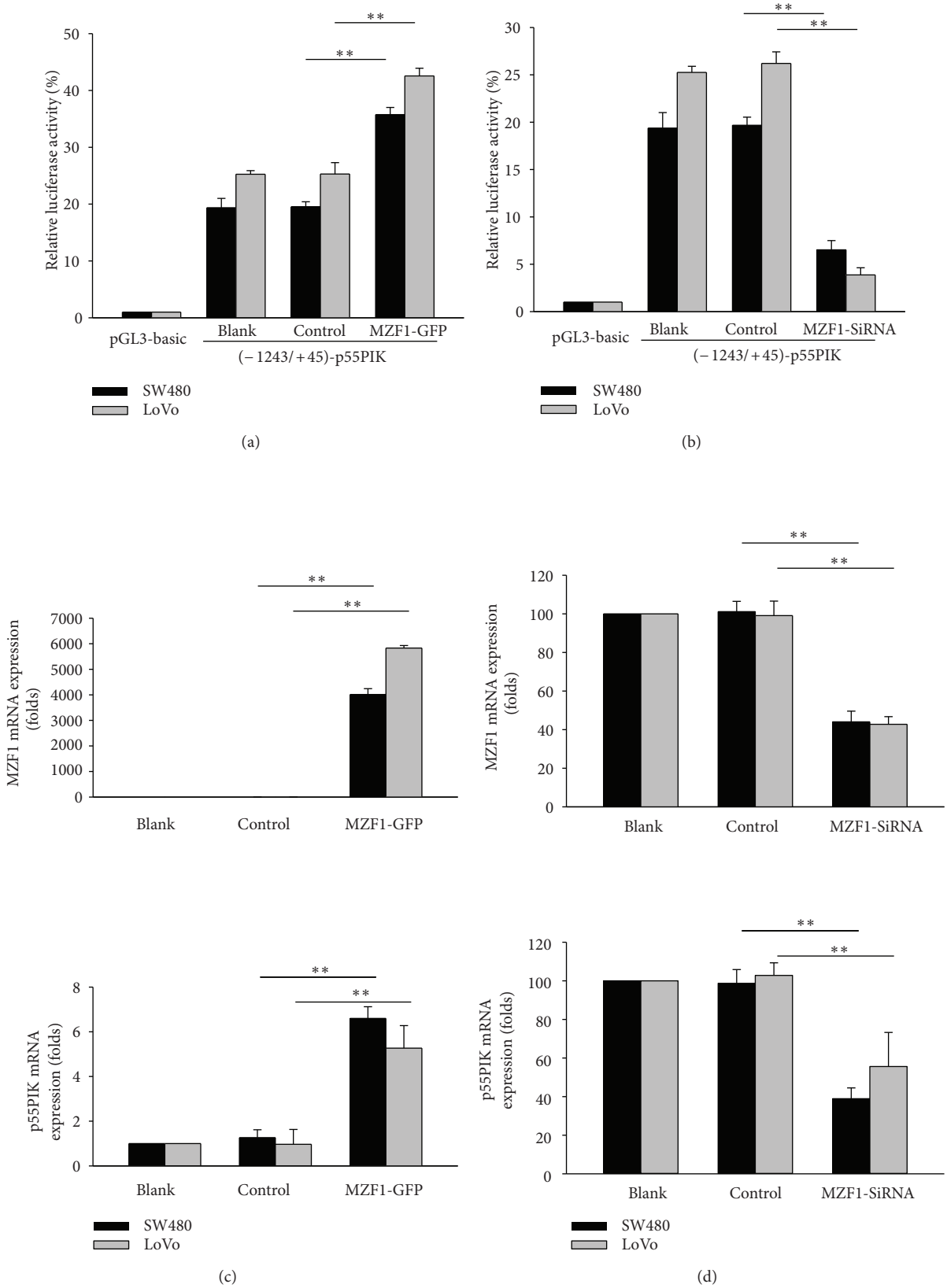

Figure 3: Continued.

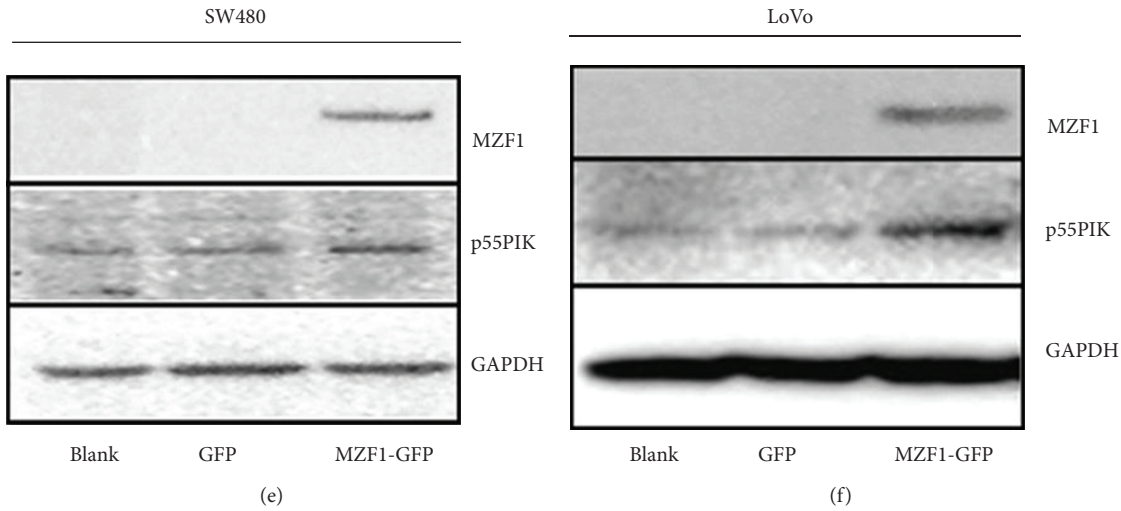

Figure 3: p55PIK expression is transcriptionally activated by MZF1 in human colon cancer cell lines SW480 and LoVo. Cells were transfected with a reporter plasmid for p55PIK promoter (−1243/+45)-p55PIK and cotransfected with or without MZF1-GFP expression plasmids or MZF1 SiRNA for 24 h. (a, b) Relative luciferase activity (RLA) was determined as described under "Materials and Methods"; (c), (d), mRNA expression of MZF1 or p55PIK was detected by real-time PCR; (e), (f) cell lysates were analyzed by MZF1, p55PIK, or GAPDH immunoblot. Data are shown as mean ± SD ($n = 3$; $^{**}P < 0.01$, per Student's t test).

and the −1243/−840 region were responsible for p55PIK gene transcription. We mapped the p55PIK promoter to find its most activated fragments. A series of 5′ flanking of p55PIK promoter DNA fragments (−1633/+45, −1243/+45, −1064/+45, −839/+45, and −651/+45) were cloned into luciferase-reporter construct and the relative luciferase activity was measured in cancer cells. The results show that −1243/+45 fragment confers highest promoter activity and −840/+45 fragment presents a significant decrease compared with −1243/+45 fragment. The current study indicate that the cis-elements were located at the −1243/−840 region of p55PIK promoter.

3.2. Identification of Cis-Acting Elements Controlling p55PIK Expression. To identify the critical cis-enhancing elements in the −1243/−840 region, we generated various mutant reporter based on the (−1243/+45)-p55PIK plasmid with substitution mutations by site-directed mutagenesis. As shown in Figure 2(a), the potential transcription factor binding sites of YY1, MZF1, Runx1, ADR1, IRF1, Delta1, and p300 were found in the −1243/−840 region based on motif analysis. The introduction of a TGGGGA site mutation (from TGGGGA to CTAGTG) which located at −901/−896 markedly reduced the luciferase activity of (−1243/+45)-p55PIK (Figure 2(d)), whereas mutation of YY1, RUNX1, or other MZF1 binding sites did not affect the promoter activity of (−1243/+45)-p55PIK (Figures 2(b), 2(c)). These results demonstrated that the putative MZF1 binding site TGGGGA located at −901/−896 region was crucial for functioning of the p55PIK promoter.

The focus of the second set of experiments was to identify the cis-element(s) of p55PIK promoter and corresponding transcription factor(s). The preliminary sequence analysis of the domain −1243/−840 reveals the presence of several nonoverlapping cis-elements and corresponding transcription factors. It was reported that MZF1 binds to the 5′-AGTGGGGA-3′ or 5′-CGGGnGAGGGGGAA-3′ sequence of gene promoters to regulate the expression of a target gene [19]. YY1, which may bind to the 5′-ACCATTC-3′ site of the p55PIK promoter, is a ubiquitously distributed zinc-finger-type transcription factor, involved in regulating a variety of promoters [16–18]. Runx1, which may bind to the 5′-CACCACCC-3′ sequence of the p55PIK promoter, is essential for hematopoietic development [19, 20]. Interferon regulatory factor 1 (IRF1), which may interact with the 5′-AGACGC-3′ DNA binding site, was initially described as a transcription factor able to activate expression of the cytokine interferon beta. IRF-1 plays important roles in immune response [21, 22], apoptosis [23, 24], and tumor suppression [25]. The p300/CBP coactivator family interacts with transcription factors p53 [26] and STAT3 [27] to transcriptionally activate the expression of their target genes. Only the mutant MZF1-mut1 shows decreased luciferase activity compared with the wildtype promoter plasmids.

3.3. MZF1 Binding on the TGGGGA Site Located at −901/−896 Region of the p55PIK Promoter in Colon Cancer Cell and Tissues. Next, to further verify whether MZF1 is involved in p55PIK transcription, we employed primers spanning the putative MZF1-binding site of the p55PIK promoter to perform chromatin immunoprecipitation (ChIP) assays, confirming the presence of endogenous MZF1 bound to this region in CRC cell line SW480 or CRC tissues. In Figure 2(e), the specific sequence within p55PIK promoter was precipitated from cell lysates by anti-MZF1 antibody but not by control IgG in both CRC cell line SW480 and CRC tissues. Thus, the data strongly indicate that MZF1 binds to

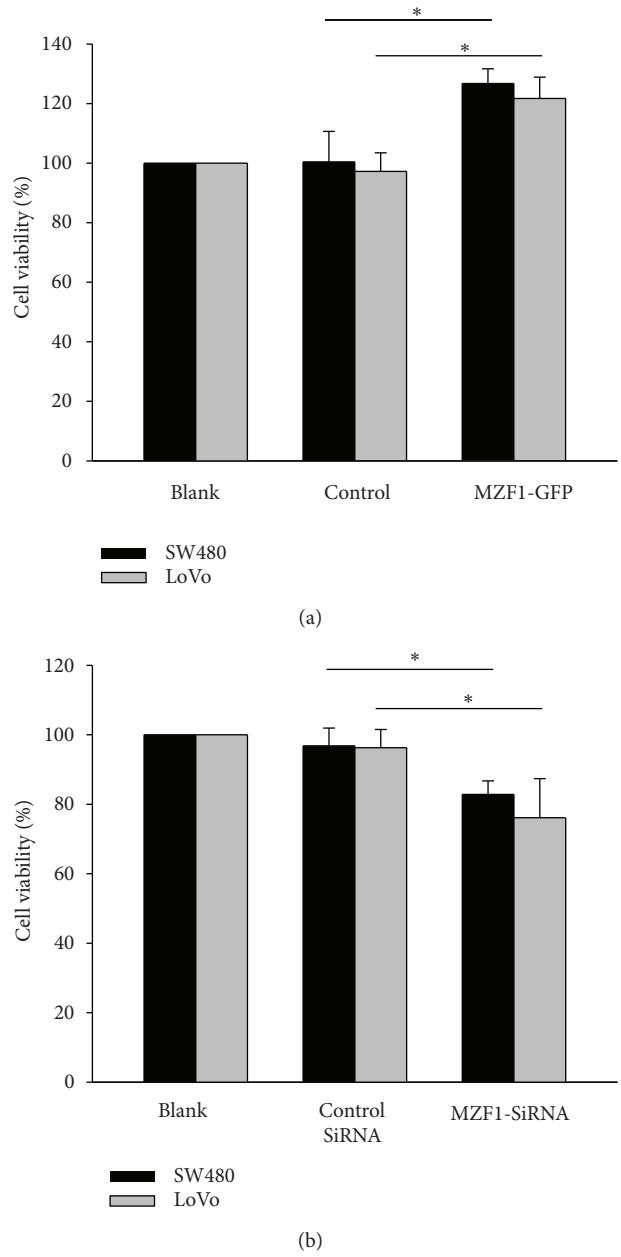

Figure 4: Transcriptional activation of p55PIK by MZF1 protein gives rise to cancer cell growth. Cells were transfected with a reporter plasmid for p55PIK promoter (−1243/+45)-p55PIK and cotransfected with or without MZF1-GFP expression plasmids or MZF1 SiRNA for 72 h to 96 h (a, b) Cell viability was detected with MTT assay as described under "Materials and Methods." Data are shown as mean ± SD ($n = 3$; $^{*}P < 0.05$, per Student's t test).

TGGGGA domain in the proximal promoter of p55PIK in CRC cells or tissues.

3.4. p55PIK Is Transcriptionally Activated by MZF1. To assess the role of MZF1 in transcriptional activity of p55PIK, we measured the luciferase activity of the p55PIK promoter construct after transfection of MZF1 expression plasmids or MZF1-SiRNA in CRC cell SW480 and LoVo. Increased luciferase activity was observed in MZF1 overexpressed cells (Figure 3(a)). Figure 3(b) shows decreased luciferase activity after MZF1 SiRNA transfection. p55PIK mRNA expression was evaluated in MZF1 over-expressing or MZF1-silencing CRC cells. As shown in Figures 3(c) and 3(d), p55PIK mRNA increased after MZF1 was overexpressed and decreased after MZF1 was silenced, respectively. By Western Blot analysis, MZF1 over-expressing CRC cell SW480 and LoVo showed increased p55PIK expression (Figures 3(e), 3(f)). Altogether, these findings indicate that MZF1 functions at least in part as a transcriptional regulator of p55PIK.

3.5. Transcriptional Activation of p55PIK by MZF1 Resulting in Accelerated Cell Proliferation in CRC Cell Lines. Myeloid zinc finger 1 (MZF1), a transcription factor belonging to the Krüppel zinc finger protein family, was previously reported as an important factor whose aberrant expression disturbed hematopoietic cell proliferation and cell tumorigenesis [19, 28, 29]. Transcription factor MZF1, binding on the DNA-binding consensus sequence of 5′-AGTGGGGA-3′ or 5′-CGGGnGAGGGGGAA-3′ [19], regulated several genes' expression which play important role in cancer migration, invasion, or cancer differentiation. Human liver cancer cell line treated with MZF1 antisense oligonucleotide showed repressed protein kinase C α expression and inhibited subcutaneous tumor growth in nude mice [30]. MZF1 transcriptionally regulates Axl receptor tyrosine kinase gene in human colon cancer or cervical cancer, which induced migration and metastasis of colon cancer *in vitro* and *in vivo* [31]. mRNA expression of MZF1 and AXL, with significant correlation, were both upregulated in colorectal cancer [31]. Raised cell cycling and loss of contact inhibition were detected in MZF-1 overexpressed NIH 3T3 cells [19]. Therefore, MZF1 may function as an oncogene in solid cancer.

Next, to determine the effects of the MZF1 induced p55PIK transcriptional activation on the growth, the CRC cell lines were examined with the MTT assay. We found that MZF1-GFP could induce acceleration of the proliferation of CRC (Figure 4(a)) and that MZF1-SiRNA could induce inhibition of growth of CRC (Figure 4(b)) as well.

3.6. Relationship between Expression of MZF1 and p55PIK in CRC Tissues. Finally, to demonstrate the relationship between MZF1 and p55PIK expression in human CRC, we examined endogenous expression of MZF1 and p55PIK in 10 resected CRC tissue samples and corresponding normal mucosal tissues from the same patient received therapeutic surgery. Tumors from 7 of 10 patients showed significant increased expression of MZF1 and p55PIK compared with normal tissues ($P = 0.046$ and $P = 0.047$, resp.); MZF1 gene expression was positively and significant correlated with p55PIK expression in the resected tumor tissues ($Rs = 0.94$; $P < .05$), indicating that MZF1 and p55PIK are involved in tumorigenesis (Figure 5).

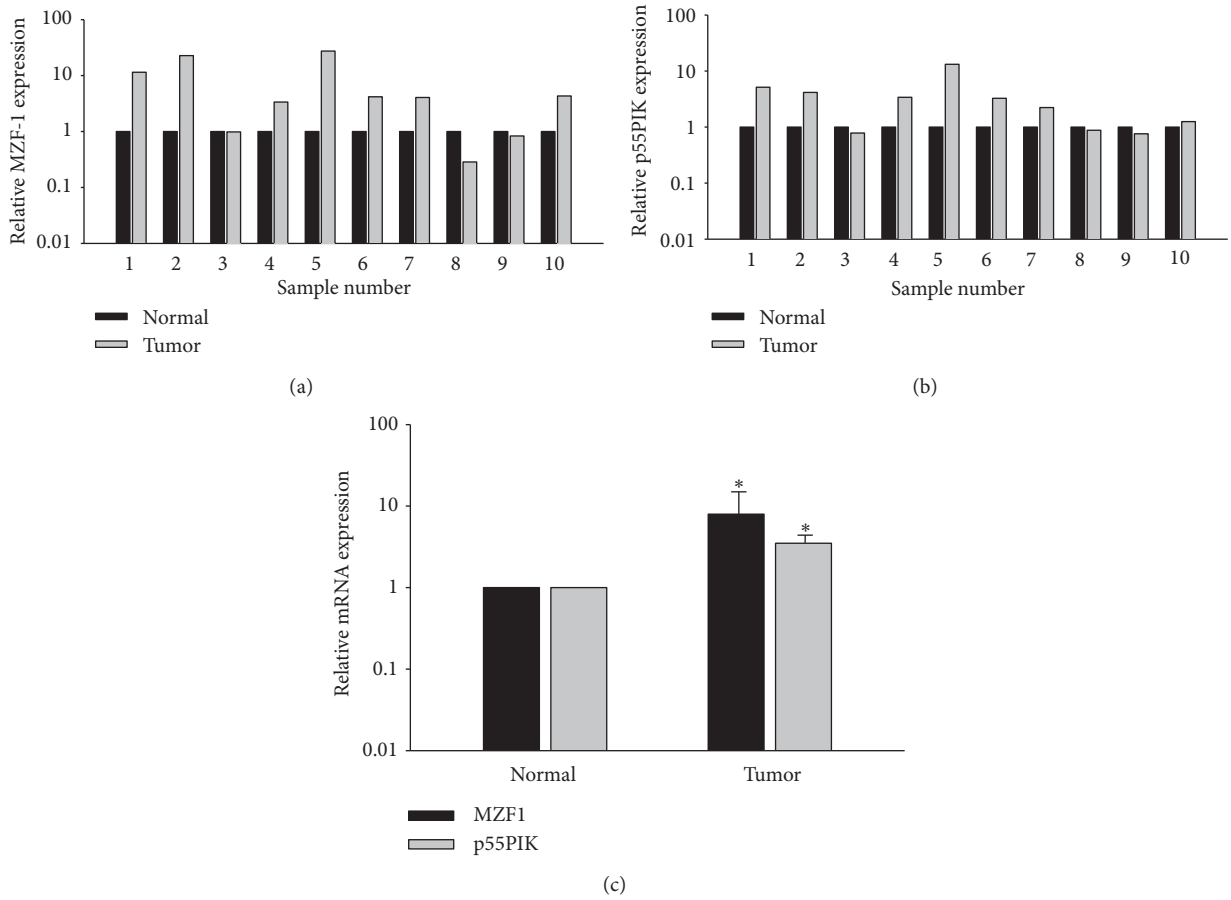

Figure 5: MZF1 and p55PIK expression are significant correlated in resected colorectal tissues.Total RNA was extracted from fresh-frozen human colorectal cancer samples. (a, b) Real-time PCR results comparing MZF1 and p55PIK expression in tumors and corresponding normal tissues. (c) Expression of MZF1 and p55PIK in normal tissues were normalized, and differences between normal and tumor tissues in all 10 patients were analyzed for average MZF1 or p55PIK expression ($^*P \leq .05$, per Student's t -test).

4. Conclusion

In summary, we have shown that the transcription factor MZF1, which directly binds to its cis-element within the p55PIK promoter, activates p55PIK expression and acts as a growth accelerator in CRC cells. We also demonstrate that the expression of MZF1 and p55PIK is significant correlated, and they are both overexpressed in resected CRC tissues. This investigation may suggest a strategy for development of therapies on p55PIK-associated cancer especially mitochondrion associated cancer.

Authors' Contributions

J. Wang, Y. Deng, G. Wang, Y. Jin, and X. Luo performed experiments; J. Wang, Y. Deng, G. Wang, and J. Hu analyzed results and made the figures; J. Hu and J. P. Gong designed the research and wrote the paper.

Conflict of Interests

The authors declare that there are no conflicts of interests.

Acknowledgments

The authors thank Dr. J. W. Zhou for providing materials. The study was supported by grants of the special Fund for Central University Basic Scientific Research (nos. 2011JC063, 2011JC062) and Foundation of 973 Program (no. 2009CB521802). The funders had no role in study design, data collection and analysis, decision to publish, or preparation of the paper.

References

[1] B. D. Manning and L. C. Cantley, "AKT/PKB signaling: navigating downstream," *Cell*, vol. 129, no. 7, pp. 1261–1274, 2007.

[2] J. A. Engelman, J. Luo, and L. C. Cantley, "The evolution of phosphatidylinositol 3-kinases as regulators of growth and metabolism," *Nature Reviews Genetics*, vol. 7, no. 8, pp. 606–619, 2006.

[3] I. Vivanco and C. L. Sawyers, "The phosphatidylinositol 3-kinaseAKT pathway in human cancer," *Nature Reviews Cancer*, vol. 2, no. 7, pp. 489–501, 2002.

[4] L. C. Cantley, "The phosphoinositide 3-kinase pathway," *Science*, vol. 296, no. 5573, pp. 1655–1657, 2002.

[5] L. C. Foukas, I. M. Berenjeno, A. Gray, A. Khwaja, and B. Vanhaesebroeck, "Activity of any class IA PI3K isoform can sustain cell proliferation and survival," *Proceedings of the National Academy of Sciences of the United States of America*, vol. 107, no. 25, pp. 11381–11386, 2010.

[6] L. Zhao and P. K. Vogt, "Class I PI3K in oncogenic cellular transformation," *Oncogene*, vol. 27, no. 41, pp. 5486–5496, 2008.

[7] D. A. Fruman, "Regulatory subunits of class IA PI3K," *Current Topics in Microbiology and Immunology*, vol. 346, pp. 225–244, 2010.

[8] S. Pons, T. Asano, E. Glasheen et al., "The structure and function of p55(PIK) reveal a new regulatory subunit for phosphatidylinositol 3-kinase," *Molecular and Cellular Biology*, vol. 15, no. 8, pp. 4453–4465, 1995.

[9] X. Xia, A. Cheng, D. Akinmade, and A. W. Hamburger, "The N-terminal 24 amino acids of the p55 gamma regulatory subunit of phosphoinositide 3-kinase binds Rb and induces cell cycle arrest," *Molecular and Cellular Biology*, vol. 23, no. 5, pp. 1717–1725, 2003.

[10] J. Hu, X. Xia, A. Cheng et al., "A peptide inhibitor derived from p55PIK phosphatidylinositol 3-kinase regulatory subunit: a novel cancer therapy," *Molecular Cancer Therapeutics*, vol. 7, no. 12, pp. 3719–3728, 2008.

[11] I. Ferecatu, N. Le Floch, M. Bergeaud et al., "Evidence for a mitochondrial localization of the retinoblastoma protein," *BMC Cell Biology*, vol. 10, article 50, 2009.

[12] L. Zhang, J. Huang, N. Yang et al., "Integrative genomic analysis of phosphatidylinositol 3′-kinase family identifies PIK3R3 as a potential therapeutic target in epithelial ovarian cancer," *Clinical Cancer Research*, vol. 13, no. 18, pp. 5314–5321, 2007.

[13] L. Soroceanu, S. Kharbanda, R. Chen et al., "Identification of IGF2 signaling through phosphoinositide-3-kinase regulatory subunit 3 as a growth-promoting axis in glioblastoma," *Proceedings of the National Academy of Sciences of the United States of America*, vol. 104, no. 9, pp. 3466–3471, 2007.

[14] J. C. Mallory, G. Crudden, A. Oliva, C. Saunders, A. Stromberg, and R. J. Craven, "A novel group of genes regulates susceptibility to antineoplastic drugs in highly tumorigenic breast cancer cells," *Molecular Pharmacology*, vol. 68, no. 6, pp. 1747–1756, 2005.

[15] J. Hu, Y. Chai, Y. Wang et al., "PI3K p55γ promoter activity enhancement is involved in the anti-apoptotic effect of berberine against cerebral ischemia-reperfusion," *European Journal of Pharmacology*, vol. 674, no. 2-3, pp. 132–142, 2012.

[16] A. Kallin, L. E. Johannessen, P. D. Cani et al., "SREBP-1 regulates the expression of heme oxygenase 1 and the phosphatidylinositol-3 kinase regulatory subunit p55γ," *Journal of Lipid Research*, vol. 48, no. 7, pp. 1628–1636, 2007.

[17] K. N. Tsai, E. C. Chan, T. Y. Tsai, K. T. Chen, C. Y. Chen, and K. Hung, "Cytotoxic effect of recombinant mycobacterium tuberculosis CFP-10/ESAT-6 protein on the crucial pathways of WI-38 cells," *Journal of Biomedicine and Biotechnology*, vol. 2009, Article ID 917084, 2009.

[18] X. Luo, X. Zhang, W. Shao, Y. Yin, and J. Zhou, "Crucial roles of MZF-1 in the transcriptional regulation of apomorphine-induced modulation of FGF-2 expression in astrocytic cultures," *Journal of Neurochemistry*, vol. 108, no. 4, pp. 952–961, 2009.

[19] J. F. Morris, R. Hromas, and F. J. Rauscher, "Characterization of the DNA-binding properties of the myeloid zinc finger protein MZF1: two independent DNA-binding domains recognize two DNA consensus sequences with a common G-rich core," *Molecular and Cellular Biology*, vol. 14, no. 3, pp. 1786–1795, 1994.

[20] T. Aoyama, T. Okamoto, K. Fukiage et al., "Histone modifiers, YY1 and p300, regulate the expression of cartilage-specific gene, chondromodulin-I, in mesenchymal stem cells," *Journal of Biological Chemistry*, vol. 285, no. 39, pp. 29842–29850, 2010.

[21] J. R. Li, J. G. Li, G. H. Deng et al., "A common promoter variant of TBX21 is associated with allele specific binding to Yin-Yang 1 and reduced gene expression," *Scandinavian Journal of Immunology*, vol. 73, no. 5, pp. 449–458, 2011.

[22] M. Ratajewski and L. Pulaski, "YY1-dependent transcriptional regulation of the human GDAP1 gene," *Genomics*, vol. 94, no. 6, pp. 407–413, 2009.

[23] G. Lacaud, L. Gore, M. Kennedy et al., "Runx1 is essential for hematopoietic commitment at the hemangioblast stage of development in vitro," *Blood*, vol. 100, no. 2, pp. 458–466, 2002.

[24] K. E. Elagib, F. K. Racke, M. Mogass, R. Khetawat, L. L. Delehanty, and A. N. Goldfarb, "RUNX1 and GATA-1 coexpression and cooperation in megakaryocytic differentiation," *Blood*, vol. 101, no. 11, pp. 4333–4341, 2003.

[25] R. Pine, "Constitutive expression of an ISGF2/IRF1 transgene leads to interferon- independent activation of interferon-inducible genes and resistance to virus infection," *Journal of Virology*, vol. 66, no. 7, pp. 4470–4478, 1992.

[26] A. Yarilina, K. H. Park-Min, T. Antoniv, X. Hu, and L. B. Ivashkiv, "TNF activates an IRF1-dependent autocrine loop leading to sustained expression of chemokines and STAT1-dependent type I interferon-response genes," *Nature Immunology*, vol. 9, no. 4, pp. 378–387, 2008.

[27] R. S. Chapman, E. K. Duff, P. C. Lourenco et al., "A novel role for IRF-1 as a suppressor of apoptosis," *Oncogene*, vol. 19, no. 54, pp. 6386–6391, 2000.

[28] R. Hromas, J. Morris, K. Cornetta et al., "Aberrant expression of the myeloid zinc finger gene, MZF-1, is oncogenic," *Cancer Research*, vol. 55, no. 16, pp. 3610–3614, 1995.

[29] R. Hromas, B. Davis, F. J. Rauscher et al., "Hematopoietic transcriptional regulation by the myeloid zinc finger gene, MZF-1," *Current Topics in Microbiology and Immunology*, vol. 211, pp. 158–164, 1996.

[30] Y. H. Hsieh, T. T. Wu, C. Y. Huang, Y. S. Hsieh, and J. Y. Liu, "Suppression of tumorigenicity of human hepatocellular carcinoma cells by antisense oligonucleotide MZF-1," *Chinese Journal of Physiology*, vol. 50, no. 1, pp. 9–15, 2007.

[31] G. Mudduluru, P. Vajkoczy, and H. Allgayer, "Myeloid zinc finger 1 induces migration, invasion, and in vivo metastasis through Axl gene expression in solid cancer," *Molecular Cancer Research*, vol. 8, no. 2, pp. 159–169, 2010.